Quarterly Progress Report

April 1 – June 30, 2014

Cooperative Agreement DE-PI0000017

West Virginia University Research Corporation

US-China Clean Energy Research Center
Advanced Coal Technology Collaboration

Project Director & Principal Investigator: Jerald J. Fletcher

Phone: 304-293-5499

Fax: 304-293-3752

Email: JJFletcher@mail.wvu.edu

Quarterly Progress Report

April 1 – June 30, 2014

Executive Summary

The project supports collaborative activities of the US Advanced Coal Technology Consortium (ACTC) as part of the US-China Clean Energy Research Center (CERC) during the third quarter of the fourth project year – April 1, 2014 through June 30, 2014.

During the current reporting quarter, the CERC-ACTC team worked to synchronize and implement recommendations from the China ACTC leadership meeting, Wuhan, March 1, 2014, to develop the Guidelines for Joint Research Projects for a Potential Phase II Renewal Application, and to respond to US Department of Energy (DOE) inquiries in support of the CERC 2.0 continuation request.

Other activities included the finalization and submission of the Joint U.S.-China CERC-ACTC annual technical report to DOE. The team has begun to co-organize the next US-China Joint meeting, scheduled for Hangzhou, China, on September 18-19, 2014.

James Wood, former deputy assistant secretary for clean coal in the U.S. Department of Energy, has joined West Virginia University Research Corporation as Director of the U.S.-ACTC of the CERC, effective May 15, while Dr. Jerald Fletcher has maintained the role of Founding Director and continues as the Principal Investigator for the U.S.-ACTC activities. Mr. Wood will focus his effort on building stronger ties between industry and academia to advance global clean coal technologies.

Quarterly Progress Report

April 1 – June 30, 2014

Project Performance

This report summarizes the collaborative activities of the US Advanced Coal Technology Consortium (US ACTC) as part of the US-China Clean Energy Research Center (CERC) supported by the US Department of Energy (DOE) under Cooperative Agreement DE-PI0000017 (US-China Clean Energy Research Center, Advanced Coal Technology Collaboration) with the West Virginia University Research Corporation (WVURC) during the third quarter of the fourth year of the project (April 1 through June 30, 2014).

The project is composed of a project management theme, eight research themes and an international integration, communication and intellectual property theme:

Theme 1—Advanced Power Generation
Theme 2—Clean Coal Conversion Technology
Theme 3—Pre-Combustion CO_2 Capture
Theme 4—Post-Combustion CO_2 Capture
Theme 5—Oxy-Combustion CO_2 Capture
Theme 6—CO_2 Sequestration Capacity and Near-Term Opportunities
Theme 7—CO_2 Algae Biofixation and Use
Theme 8—Integrated Industrial Process Modeling and Additional Topics
Theme 9—Communication, Integration and Intellectual Property Rights Management
Theme 0—Project Management Activities

This report outlines the approach taken, including specific actions by subtask. If there was no identified activity during the reporting period, the appropriate section is included but without additional information.

Theme 1 – Advanced Power Generation

Subtask 1.1. – Increase efficiency and availability of Existing Coal-Fired Power Plants

Approach

1. Survey existing population of coal-fired power plant sizes and types that offer the greatest opportunity for improvement in China and the US.
2. Identify specific units in both China and the US, with similar characteristics, and conduct a bench-marking study on best operating practices and designs.
3. Investigate specific needs due to cycling.
4. Evaluate other potential improvements based on the state of the art designs being deployed today.
5. Provide final toolbox of improvements that can be used by either China or the US to improve operations.
6. Conduct a workshop to present results and get additional feedback.

Results and Discussion

Task is complete at this time.

Plans for Upcoming Quarter

There are no joint plans for the upcoming quarter. Tsinghua and Shanghai Jiaotong are independently pursuing continued work on the following topics:

1. Use online monitoring and operation data to improve performance
2. Reduce power consumption of the balanced draft system

Subtask 1.2. – Advanced Ultra-Supercritical Boiler (A-USC) Development

Approach

Research on 600MW USC boiler of 700℃ main steam temperature combusting Xinjiang coal from Houxun coal field, provide technical support for power generation using Houxun coal efficiently with low pollution.

1. Research on thermodynamic system of 700℃ USC units combusting Xinjiang coal.
2. Design scheme of 700℃ USC boilers combusting Xinjiang coal.
3. Research on coupling characteristics of combusting and hydrodynamics of 700℃ USC boilers.
4. Research on fouling and slagging characteristics of 700℃ USC boilers.

Results and Discussion

Task is complete at this time.

Plans for Upcoming Quarter

There are no joint plans for the upcoming quarter.

Subtask 1.3 – Optimize pulverizing system for subcritical power plants with a focus on NOx control

Approach

The technical approach to determining the impact of such retrofit efficiency technologies as the LP Amina static classifier is as follows:

1. Evaluate the current state of installed coal-fired plants in China and the US with regards to pulverizer upgrades and the potential for efficiency and performance improvements. This study should include evaluating different types of pulverizers and milling systems to facilitate development of a target project strategy.
2. Collect and analyze data on classifier installations (LP Amina's A-type)
3. Model effect of staged fineness on NOx reduction, soot formation, ash fouling, slag, etc. (incl. China Zhundong coal)
4. Develop validated models for prediction of particle segregation / separation in cyclone separators.

Based on items 2) & 3) above, develop a technical paper that discusses how improved fineness can be used to improve boiler performance and lower NOx (may need to be staged, coupled with LNB + OFA system, etc).

Based on item 1) above, identify target projects in both China and the US where these new classifiers can be installed on all the mills on a large coal-fired unit so that the predicted benefits for UBC, NOx emissions, unit turndown, and fuel flexibility can be evaluated on a unit basis where all mill classifiers have been upgraded.

Results and Discussion

During the current reporting period, the research team conducted additional experiments using ground flaxseed as the solids material. Tests were conducted with solids loadings of 35, 42 and 51%, and were recorded with high speed video equipment. The mass flow rates of air and solids for these tests are shown in table 1.3.1. For these tests, two high speed cameras were synched together, allowing for simultaneous recording. Two sets of experimental runs were conducted for each test condition. For one of these sets, the cameras were positioned to allow video recording of side and bottom views of the horizontal glass pipe (following the elbow section). For the second set of experimental runs, the cameras were oriented to provide the side view of the horizontal pipe as well as the back side of the elbow (looking into the horizontal glass pipe). Still image samples from these videos are provided in figure 1.3.1.

Table 1.3.1: Test Conditions

Solids Loading (%)	Solids Mass Flow rate (kg/min)	Air Mass Flow rate (kg/min)	Superficial Gas Velocity (m/s)
35	1.1	3.14	9.4
42	1.1	2.62	8.0
51	1.1	2.16	6.6

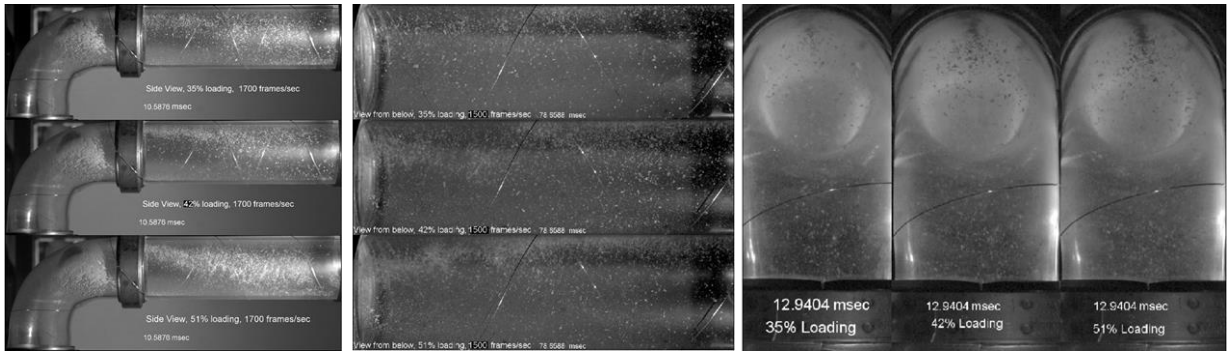

Figure 1.3.1: Still images taken from high speed video. Left: side view. Center: Bottom View. Right: Looking into elbow.

From the images provided in figure 1.3.1, the roping phenomena can easily be seen. In addition, the bottom view shows that the rope exhibits a preferential direction away from the centerline of the horizontal pipe, migrating towards the outer walls. Finally, the view looking into the elbow (the right-most picture in figure 1.3.1) shows how the solids particles become concentrated within the elbow, thus forming the rope.

The collected high speed video data is currently being analyzed via particle tracking. This analysis will calculate individual particle velocities and overlay particle trajectories onto the video. An example of the preliminary results of this analysis is shown in figure 1.3.2.

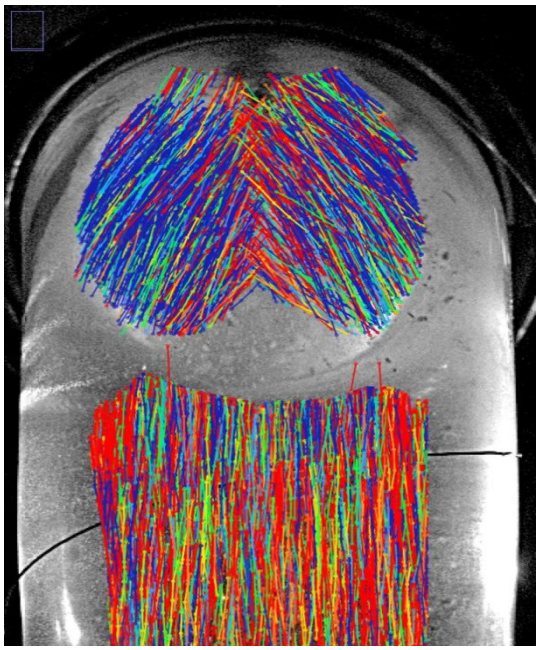

Figure 1.3.2: Overlay of particle velocity vectors (colored by velocity) for 50 ms of high speed video for 42% solids loading case (flaxseed).

Plans for Upcoming Quarter

Over the next reporting period, the particle tracking analysis, as well as estimation of local solids concentration, will be completed for the tests discussed above. The data resulting from this analysis will be used for CFD simulation verification and validation. Additional high speed video testing will be conducted as equipment and personnel availability allows.

Theme 2 – Clean Coal Conversion Technology

Subtask 2.1. – Co-Generation System with Combined Pyrolysis, Gasification, and Combustion

Approach

There has been significant progress in all different fronts: reactor model, experiments, and simulations. Concerning the reactor model, a literature review was performed to understand the formation of calcium carbide from burnt lime in multiphase reactions. The models and experiments performed by several authors were carefully studied. The intermediate reactions required to form calcium carbide from burn lime were investigated and used to formulate our own model. The kinetics of the overall reaction was also studied and a method to obtain the parameters of Arrhenius reaction rates from these experimental results was developed. Some preliminary calculations were done using some of the Arrhenius parameters found in the literature with a perfectly stirred reactor model, and the results compared to experimental data. The energy equations for the overall batch reactor to produce calcium carbide, as well as for each phase present in this reactor, were derived.

The melting temperatures of the main species in the calcium carbide reactor, and in the flue gas and ash/slag of the heat provider oxy-coal combustor were investigated. Their combination in binary, ternary and quaternary phase diagrams was also researched to study ways of decreasing the temperature and time required in the calcium carbide reactor. A combined model of the oxy-coal combustor and calcium carbide reactor is under development.

In the experimental work, cylindrical shape pellets were made from calcium oxide and carbon graphite to study initial reactions in a 4 ft long tube furnace. These experiments were run for a duration of 60 min at 1000 and 1500ºC. Additionally, the microwave furnace power is being increased to 12kW in order to reach the desired temperature levels.

Numerical simulations of the 100kW oxy-coal combustor have been continued and the effect of the percentage of oxygen in air and the swirl profile in the primary inlet on the flame and the temperature profiles near the burner has been investigated.

Results and Discussion

Reactor Design

The preliminary design of the WVU Very High Temperature Entrained Reactor (VHTER) has been completed. Efforts are currently underway to complete a thermal stress analysis of the reactor, as well as to generate engineering drawings for use in manufacturing. These efforts should be complete within the next 2-3 weeks, and will be included in the next reporting period.

CFD Simulations

Additional computational fluid dynamics (CFD) simulations have been conducted using the WVU-designed Very High Temperature Entrained Reactor (VHTER) and the L P Amina CTC horizontal reactor. These simulations were carried out using a set of "base case" operating conditions provided by L P Amina engineers. The purpose of the simulations was to (1) provide additional test cases against which the Reduced Order Model (ROM) could be validated and (2) address concerns raised by the L P Amina technical team. For these cases, the average outlet gas temperature predicted by the reduced order model (ROM) provides good agreement with the corresponding Fluent simulation results (differences of ~1% and ~8% for the VHTER and CTC reactors, respectively). Additionally, figure 2.1.1 shows that the reactor outlet gas composition

(in terms of elemental balances) is consistent between the fluent simulations and the reduced order model for both reactors. A journal paper, as well as a conference paper, is currently being prepared based upon this effort, and will be submitted for publication during the next reporting period.

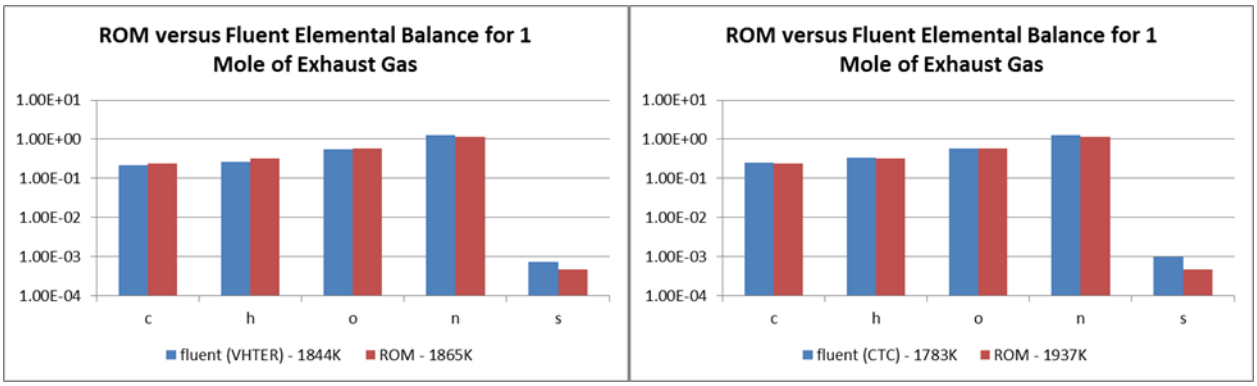

Figure 2.1.3: Reactor outlet gas elemental composition comparison between fluent (CFD) and reduced order model (ROM) simulations. Left: VHTER reactor. Right: CTC reactor

Furnace Experiments for Determining Kinetic Rates

As discussed in the previous report, a postdoctoral fellow was hired to continue the earlier high temperature furnace experimental work carried out by a recently graduated (and now former) student. The first task assigned to the new researcher was to repeat some of the previously-conducted experiments. For this, pellets consisting of a stoichiometric mixture of carbon and calcium oxide were heated at furnace temperatures of 1500 and 1700˚C for exposure times (at the desired temperature) of 0, 15, 30, 45 and 60 minutes. Additionally, stoichiometric mixtures of loose powder (instead of pellets) were also tested.

The preliminary analysis from these tests shows that, for the 1500˚C cases, no calcium carbide is present in the samples after being heated. This suggests that either (a) no calcium carbide was formed at this temperature, or (b) the rate of disassociation of calcium carbide is either equal to or greater than the rate of calcium carbide formation at this temperature. Further analysis is required to determine which of these the case is. For the tests conducted at 1700˚C, calcium carbide is present after heating for each of the exposure times tested. It can also be observed that the weight percentage of CaC_2 is systematically greater for the tests involving the use of pellets as opposed to loose powders. This is most probably due to the fact that the carbon and calcium oxide will have improved surface contact when compacted into pellets, thus allowing for better molecular diffusion and resulting in higher effective reaction rates.

It should be noted that the listed temperatures at which these tests were conducted are the temperature settings on the furnace temperature controls. Inserting a thermocouple directly into the furnace's alumina tube where the crucibles containing the graphite/CaO charge provided internal temperature readings of 1630 and 1420˚ for the 1700 and 1500 degree cases, respectively. These actual temperatures will be used when determining kinetic rate data.

Finally, the conventional nabertherm tube furnace has been relocated to another lab facility with an available fume hood so that it can be used to test the effects of varying levels of CO partial pressure on the reaction kinetics.

Plans for Upcoming Quarter

Over the course of the upcoming reporting period, additional testing will be conducted using both the conventional tube furnace, and the microwave furnace. These tests will include additional temperatures and varying partial pressures of CO using different mixtures of Ar/CO as the purge gas inside the furnace.

Subtask 2.2. – Chemical Looping Gasification With CO_2 Capture.

Approach

The proposed chemical looping gasification process using CaO as a CO_2 acceptor may obtain high hydrogen content gas from the gasifier while the CO_2 rich gas will be produced using a little pure oxygen in the combustor.

Results and Discussion

No activity this quarter.

Plans for Upcoming Quarter

No input.

Subtask 2.3. – Direct SNG Production from Coal

Approach

China Supported Task Only. Does not include DOE or Cost Shared Support. Any technical data or results provided to the US CERC-ACTC Team will be included in project reporting. Task is included for completeness and clarity.

Results and Discussion

No input.

Plans for Upcoming Quarter

No input.

Subtask 2.4. – Coal to SNG by Catalytic Gasification

Approach

China Supported Task Only. Does not include DOE or Cost Shared Support. Any technical data or results provided to the US CERC-ACTC Team will be included in project reporting. Task is included for completeness and clarity.

Results and Discussion

No input.

Plans for Upcoming Quarter

No input.

Subtask 2.5. – Gasification Properties of Coal DTL Residue

Approach

The Shenhua Direct Coal Liquefaction (DCL) process produces petroleum-like fuels by direct hydrogenation of coal. The unconverted coal fraction (residue) can be gasified to produce hydrogen for the process or syngas for conversion to additional products. Coal can be added to the gasifier feed to increase the quantity of hydrogen or syngas.

If this process were to be built in the U.S., there is a high probability that it would use Powder River Basin (PRB) coal. To identify appropriate gasifier technology for the residue derived from PRB coal, we are pursuing a two part experimental strategy. The first part is to measure the gasification kinetics of PRB coal under conditions that simulate a fluidized bed gasifier. The second part is to solvent extract PRB coal with tetralin under elevated temperature and pressure. We will carry out additional gasification kinetics experiments with the residue of this extraction, which should be similar to the DCL residue.

PRB coal is a benchmark coal for gasification technology. PRB coal, and more reactive feedstocks such as lignites and biomass, give good yields in fluidized bed gasfiers. Coals with lower reactivities do not give good yields in fluidized bed gasifiers, and higher temperature, entrained flow gasifiers are recommended for these coals.

If the residue is more reactive than PRB coal, then a fluidized bed gasifier will be recommended. The residue will have a high mineral content due to the disposable liquefaction catalyst and due to the concentration of ash. Since fluidized bed gasifiers operate under non-slagging conditions, the heat of melting this mineral content can be avoided. There is also the possibility that the catalyst can be separated from the ash and recycled. If the residue is less reactive than the parent PRB coal, then an entrained flow gasifier will be recommended.

Results and Discussion

PRB coal gasification measurements in CO_2 are complete. We found that the rate of gasification is nearly zero order with respect to CO_2 partial pressure, a surprising result. We also found a significant annealing effect, meaning that chars held at elevated temperature for about an hour are only about half as reactive as a freshly formed char. A paper describing this work is nearly complete and will be submitted for publication.

Construction of the coal extraction apparatus is nearly complete.

Plans for Upcoming Quarter

PRB gasification rate measurements in steam are underway. We intend to complete the coal extraction apparatus and initiate coal extraction experiments.

Subtask 2.6. – Measurement, Modeling and Environmental Technologies for Unconventional Coal Gasification

Approach

China Supported Task Only. Does not include DOE or Cost Shared Support. Any technical data or results provided to the US CERC-ACTC Team will be included in project reporting. Task is included for completeness and clarity.

Results and Discussion

No input.

Plans for Upcoming Quarter

No input.

Subtask 2.7. – Coal/Biomass Co-Conversion Processes

Approach

Gas chromatographic analysis was done for two purge gas feed rates (i.e., nitrogen 100 and 200 sccm) in WVU pyrolysis unit. Additionally, two types of tests have been conducted using the Enerac exhaust analyzer. The first type is to heat the reactor chamber to a given temperature and taking a sample with the analyzer. The second type is to sample with the analyzer every 100ºC. Both tests were done for 10 g. of coal with a purge gas flow rate of 200 sccm. The product yields are being monitored and analyzed.

Results and Discussion

No Activity this Quarter.

Plans for Upcoming Quarter

No input.

Subtask 2.8. – Coal to Chemical Production of Ethylene Glycol

Part I: Synthesis of diethyl oxalate (DEO) with syngas

Approach

Syngas to ethylene glycol contains two main steps: (1) reaction of CO with ethyl nitrite (EN) to form diethyl oxalate (DEO) and (2) hydrogenation of DMO to ethylene glycol. To achieve the first step, the experimental set-up used for synthesis of EN was built and its schematic drawing is shown in Figure 2.8.1. Three-necked bottled was fixed on an iron stand with a flask clamp. Water bath container and stirrer were put under the bottle. Thermometer, constant pressure funnel and condenser were connected with the bottle. All the connectors were sealed with wax followed by Parafilm. Vacuum tubing was used to connect the condenser with the filtering flask (#7) which was filled with DI water to remove the methanol from the gas. Flask (#7) was then connected with the buffer flask (#8) by vacuum tubing and flask (#9) was connected orderly. Flask (#9) was filled

with concentrated sulfuric acid (98%) to remove the moisture from the gas. All the flasks were fixed with clamps and sealed with rubber stoppers. Rubber stops were further sealed with wax followed by Parafilm. Flask (#9) was then connected with two drying tubes (#10) which were filled with anhydrous calcium sulfate to further remove the moisture from the gas. The heads of drying tube were further sealed with wax followed by Parafilm. Drying tubes (#11) were then connected the regulator (#17) of methyl nitrite cylinder via vacuum tubing and a three-way valve (#12). One head of the valve was connected to either oil pump (#13) or the regulator (#14) of the nitrogen cylinder. Oil pump (#13) and the regulator of nitrogen (#14) cylinder were connected with the three-way valve (#12).

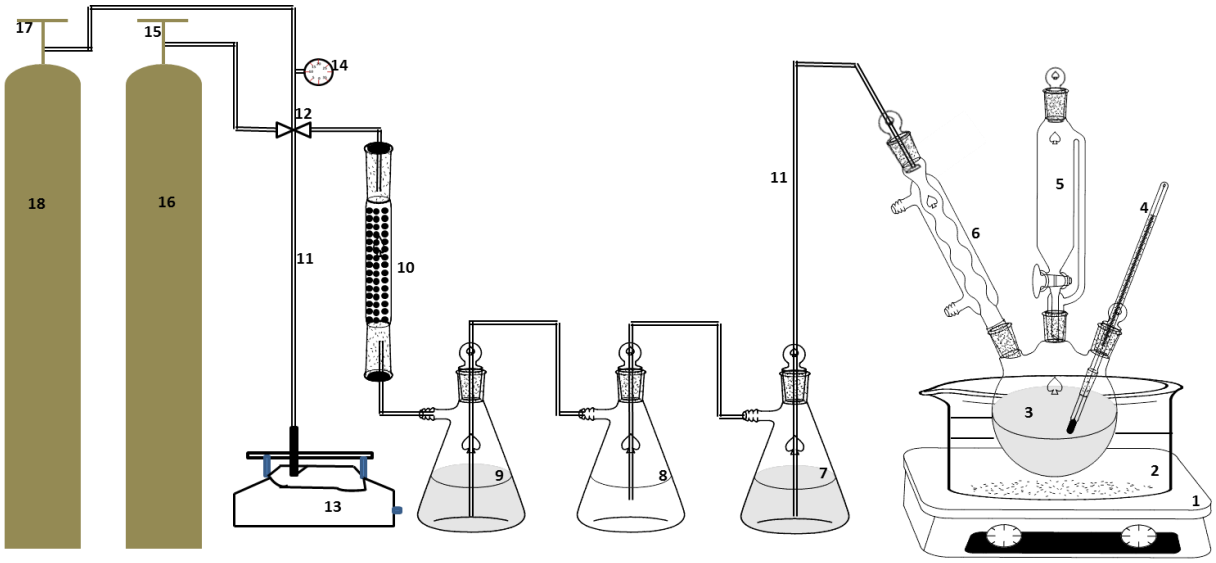

Figure 2.8.1. The experimental set-up of ethyl nitrite production. 1. Stirrer; 2. Water bath container; 3. Three-necked bottle; 4.Thermometer; 5. Constant pressure funnel; 6. Condenser; 7. Filtering flask; 8. Buffer flask; 9. Filtering flask; 10. Drying tube; 11. Vacuum tubing; 12. Three-way connector; 13. Oil pump; 14. Vacuum Gauge; 15. Nitrogen regulator; 16. Nitrogen cylinder; 17. Methyl nitrite regulator; 18.Methyl nitrite cylinder.

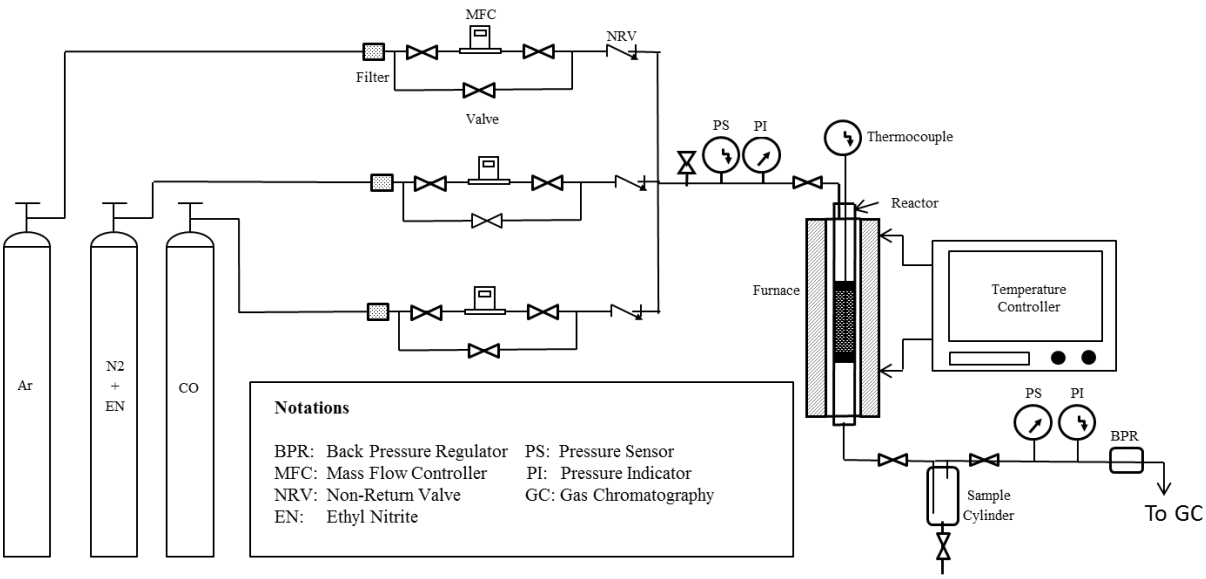

Figure 2.8.2. Schematic diagram of the EN to DEO installation.

The experimental set-up used for synthesis of DEO from EN was built and its schematic drawing is shown in Figure 2.8-2. CO and N2 + EN cylinders (US Welding) were connected with two mass flow controllers (Porter Instruments) separately with stainless tubing (Swagelok). High pressure valves (Swagelok) were used before and after the mass flow controllers to protect them. Before the gases came into the reactor, check valves (Swagelok) were used to make sure no gas could go reversely into the mass flow controller. The mixture gas went into the reactor through stainless tubing (Swagelok) while a thermal couple was inserted into the reactor to control the temperature. A cold trap (Swagelok) was connected after the reactor to collect the product while all the tubing between reactor and cold trap was wrapped with heating taps. GC (SRI) was connected with the cold trap and a back pressure regulator (Swagelok) was used between them to adjust the temperature. All the exhausts came out from the GC will be released into the hood via stainless tubing. The reaction system is controlled by a National Instruments DAQ system and all the reaction parameters are recorded automatically. Security measures will be implemented for 24/7 unattended operation.

Results and Discussion

The whole set-up must be leak tested (nitrogen) before attempting to start the reaction. Any leak must be fixed before starting experiment. Check the methyl nitrite regulator for leaks first. Use a tubing (Swagelok, SS-T2-S-028-20, 1/8" OD X .028 WALL) to connect nitrogen cylinder to the methyl nitrite regulator. Set the nitrogen regulator at a pressure of 200 psi (maximum test pressure will be 100 psi). Open the on-off valve (#16, Fig. 2.8-1) downstream to the gas-in quick-connect at methyl nitrite regulator (#18, Fig. 2.8-1) first while keeping close the on-off valve (#19, Fig. 2.8-1) downstream to the regulator. Turn the knob of the regulator (#18, Fig. 2.8-1) to allow gas to flow downstream to the regulator. Use snoop to check the leaks at all connections. If the pressure (200 psi) can keep 24 h without any decrease, the whole system has no leak.

The reaction can be carried out after all the leak tests completed. At room temperature, 600 mL of sodium nitrite solution in DI water (4 mol/L) and 120 mL of ethanol (200 pf) were added into

the three-necked bottle (#2, Fig. 2.8-1). A stirring bar was put in the bottle and the thermometer was put into the solution. Sulfuric acid (250 mL, 50 vol%) was added into the constant pressure funnel (#5, Fig. 2.8-1). The funnel is sealed with a glass stopper. Vacuum grease, wax and Parafilm are used to make the seal better. The EN cylinder is vacuumed thoroughly with the oil pump (#13, Fig. 2.8-1). Adjust the valve to connect the regulator (#17, Fig. 2.8-1) of the EN cylinder and the oil pump. Turn on the oil pump to vacuum the cylinder until the pressure is less than 0.1 bar from the vacuum gauge. Close the regulator valve (#19, Fig. 1) and turn off the pump. Before the reaction, the whole set-up was vacuumed and refilled with UHP nitrogen for three times. The three-way valve (#12, Fig. 2.8-1) was connected with the nitrogen cylinder, oil pump and the drying tube (#11, Fig. 2.8-1) respectively. Adjust the valve (#12, Fig. 2.8-1) to connect oil pump with the drying tube and turn on the pump to vacuum the set-up.

Sulfuric acid is added in the sodium nitrite solution dropwise [one drop every 3 seconds, adjust the valve (#3, Fig. 2.8-1) of the constant pressure funnel] while temperature is controlled at around room temperature (22 ±5 °C) via the water both (#1, Fig. 2.8-1). The temperature of the condenser is kept at -5 °C (chiller is used here) to cool down water and methanol. Once the gas comes out, the vacuumed EN cylinder is connected with the set up via the three-way valve. The EN gas will go into the cylinder due to the pressure difference while the water and ethanol will be removed by the condenser and the gas-washing bottles. When the pressure of the EN cylinder got to 1 atmosphere pressure, the reaction was stopped by closing the valve (#3, Fig. 2.8-1). The cylinder was refilled with UHP N_2 until the final pressure got to 5 bars. Figure 2.8-3 shows the EN characterized with GC. The concentration of EN in the N_2 + EN can be calculated by using the standard curve.

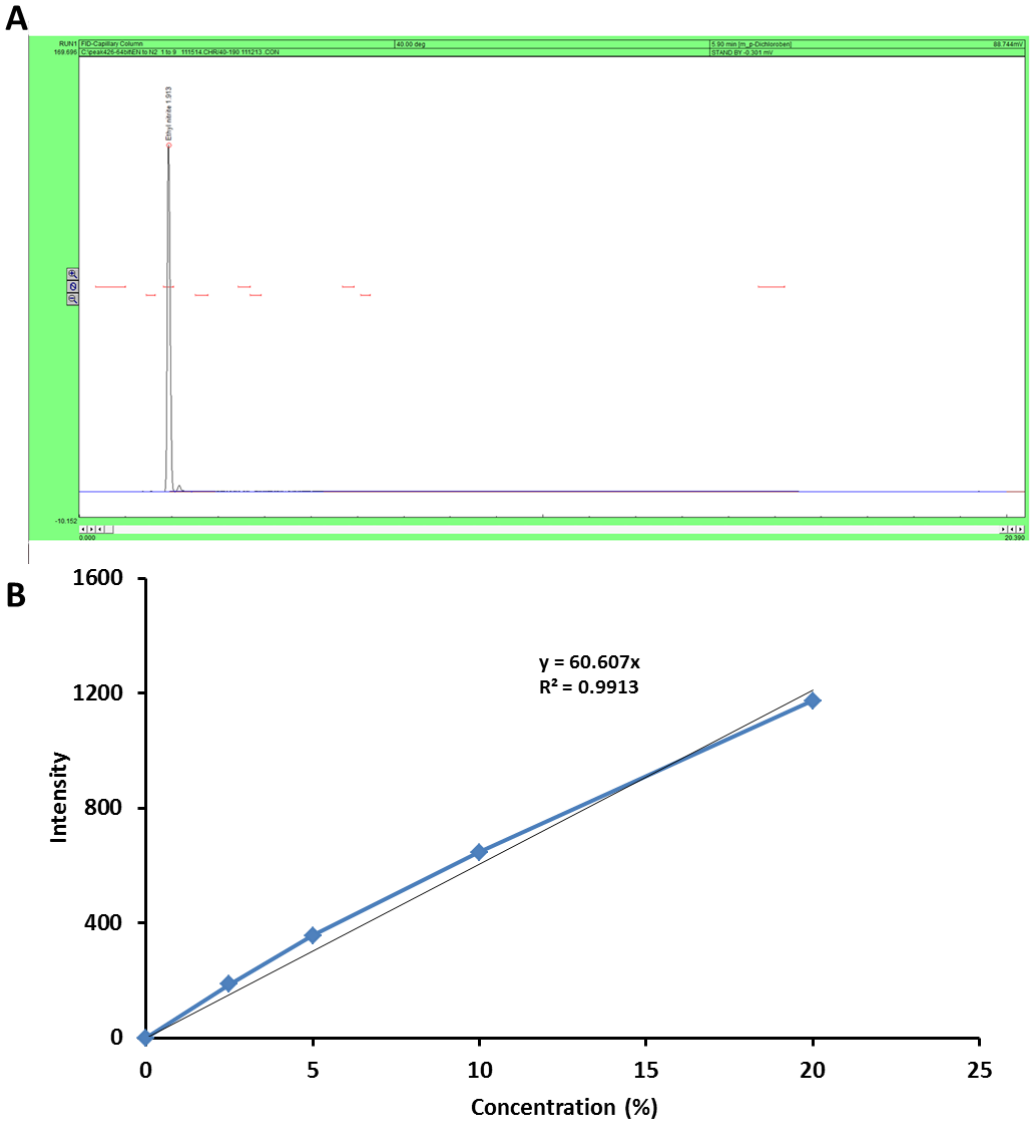

Figure 2.8-3. The pure EN characterized with GC (A) and the standard curve of EN with different concentrations .

Preparation of new EN to DEO catalysts

A variety of catalyst supports have been reported for the dialkyl oxalate, especially for DEO synthesis, such as activated carbon, silica, activated alumina, α-Al_2O_3, silica alumina and so on. Pd/α-Al_2O_3 has been proven to be the best catalytic system, with good activity, selectivity and stability. Therefore, the catalyst structure, support, operating conditions and process, kinetics and mechanism of Pd/α-Al_2O_3 catalytic system have been widely studied. [1-4] Here, we used a new method to synthesize nano-sized Pd particles while CeO_2 was chosen as a promoter.

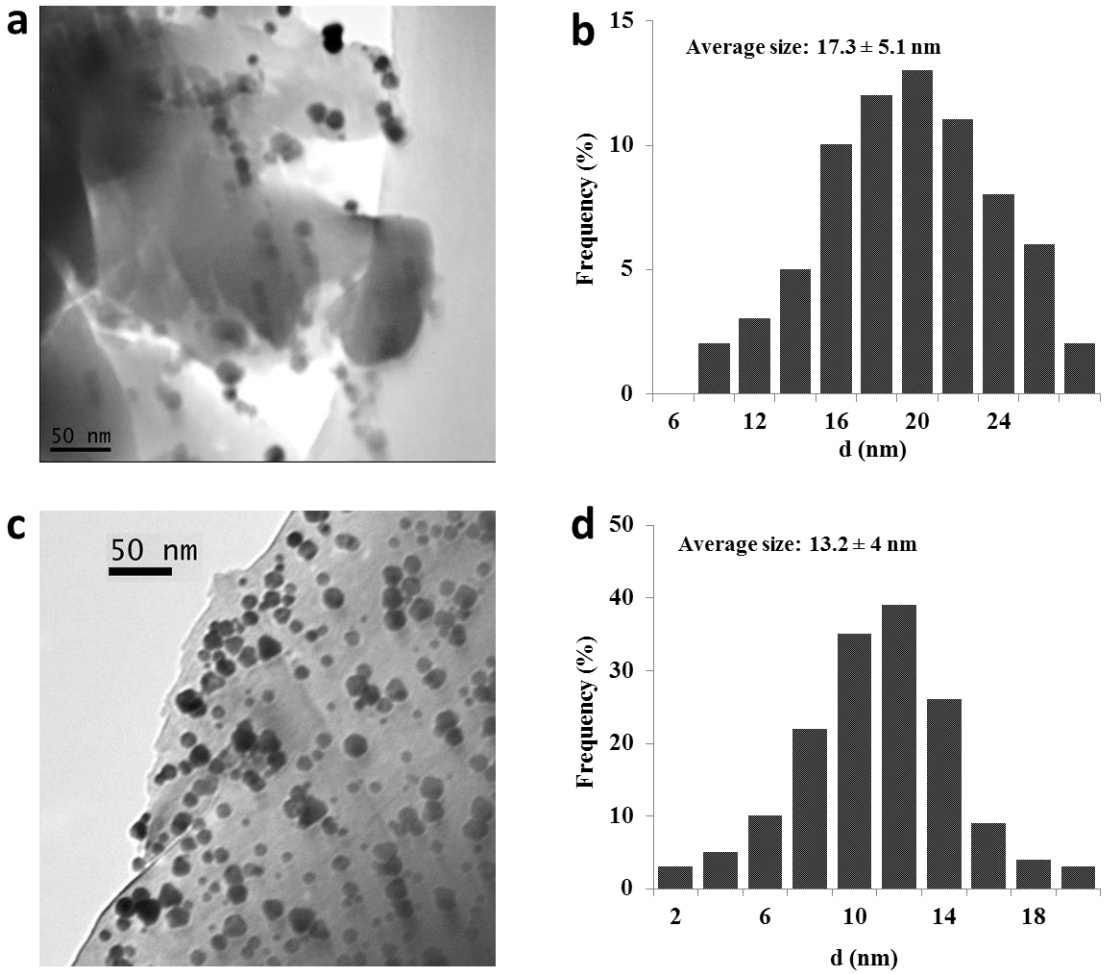

Figure 2.8-4. TEM (a) and size distribution (b) of catalyst Pd/α-Al2O3; TEM (c) and size distribution (d) of catalyst Pd-CeO2/α-Al2O3.

In a typical synthesis, K2PdCl6 (0.05 mmol), $PdCl_2$ (0.05 mmol), KCl (1.5 mmol), L-ascorbic acid (0.2 mmol) and PVP (2 mmol) were dissolved in 20 mL of water . The mixed solution was refluxed at 100 °C for 3 h, and then stirred at 60 °C until all the solvents evaporated. The product was washed with acetone/water and acetone/ethanol for several times and vacuum dried at 60 °C overnight. Pd-CeO_2/α-Al_2O_3 was synthesized with similar method. Ce was loaded on α-Al_2O_3 first at the weight percentage of 0.8%. The mixture was calcined at 500 °C for 5 h to get CeO_2/α-Al_2O_3. Pd was then loaded using the above method. Figure 2.8-4 shows the Pd nanoparticles detected with dynamic light scattering. XRD was also used to characterize the new catalysts (Fig. 2.8-5---2.8-8).

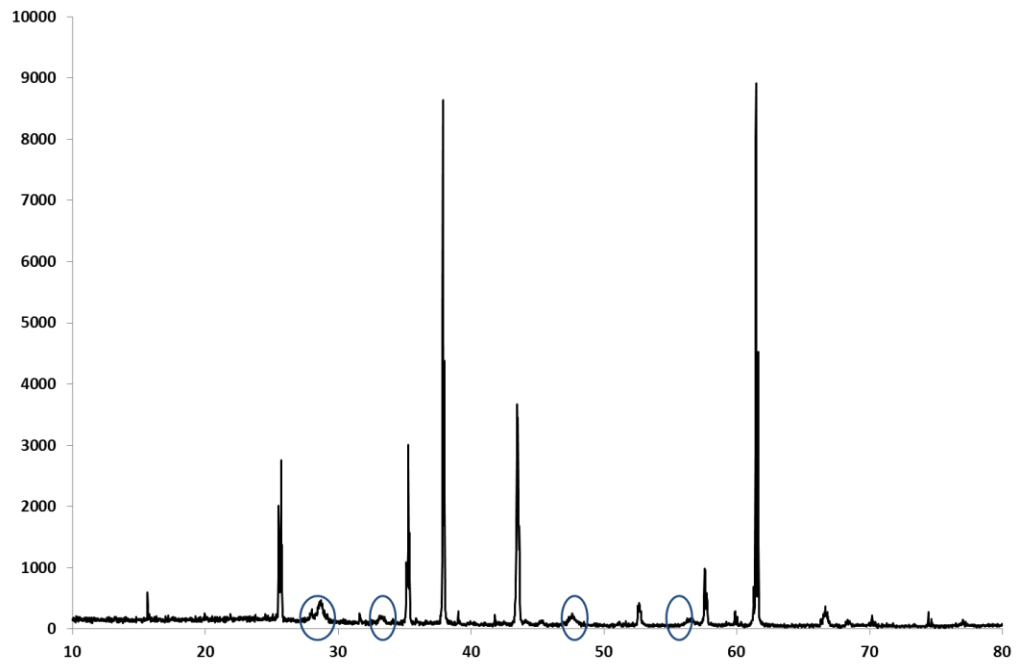

Figure 2.8-5. X-ray powder diffraction of CeO2/α-Al2O3. CeO2 peaks were highlighted with blue cicrcles.

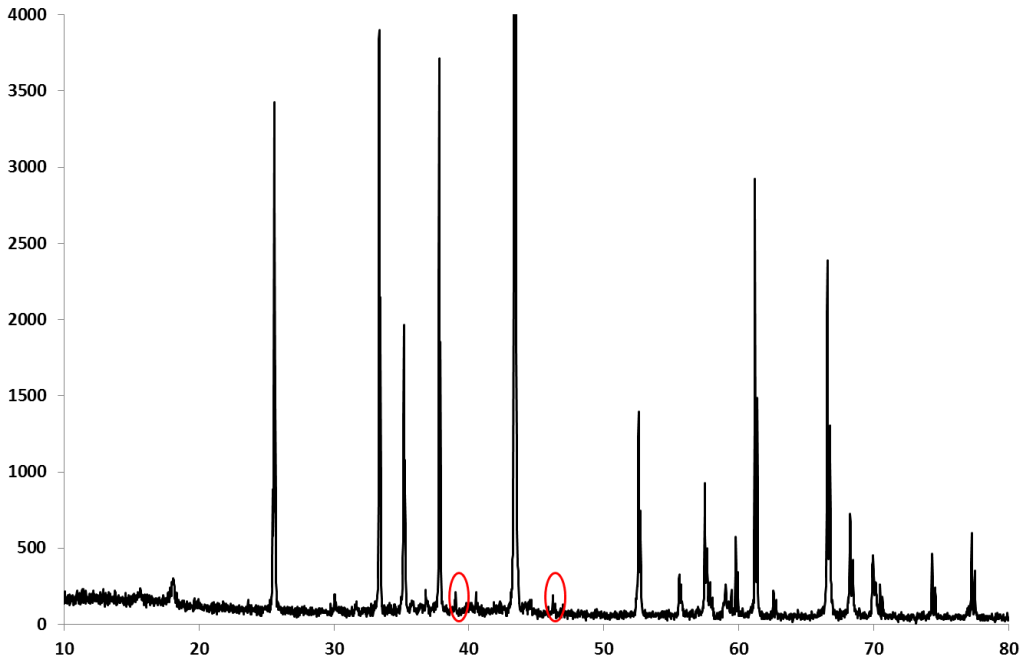

Figure 2.8-6. X-ray powder diffraction of Pd/α-Al2O3. Pd peaks were highlighted with red cicrcles.

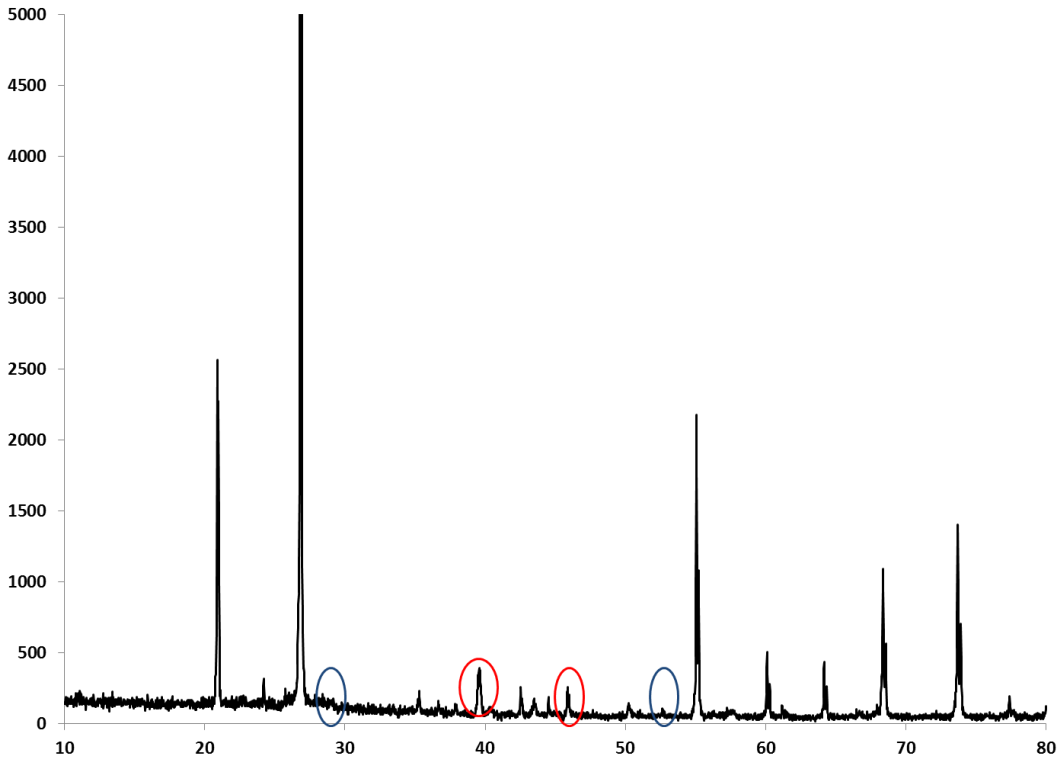

Figure 2.8-7. X-ray powder diffraction of Pd-CeO2/α-Al2O3. CeO2 peaks were highlighted with blue cicrcles. Pd peaks were highlighted with red cicrcles.

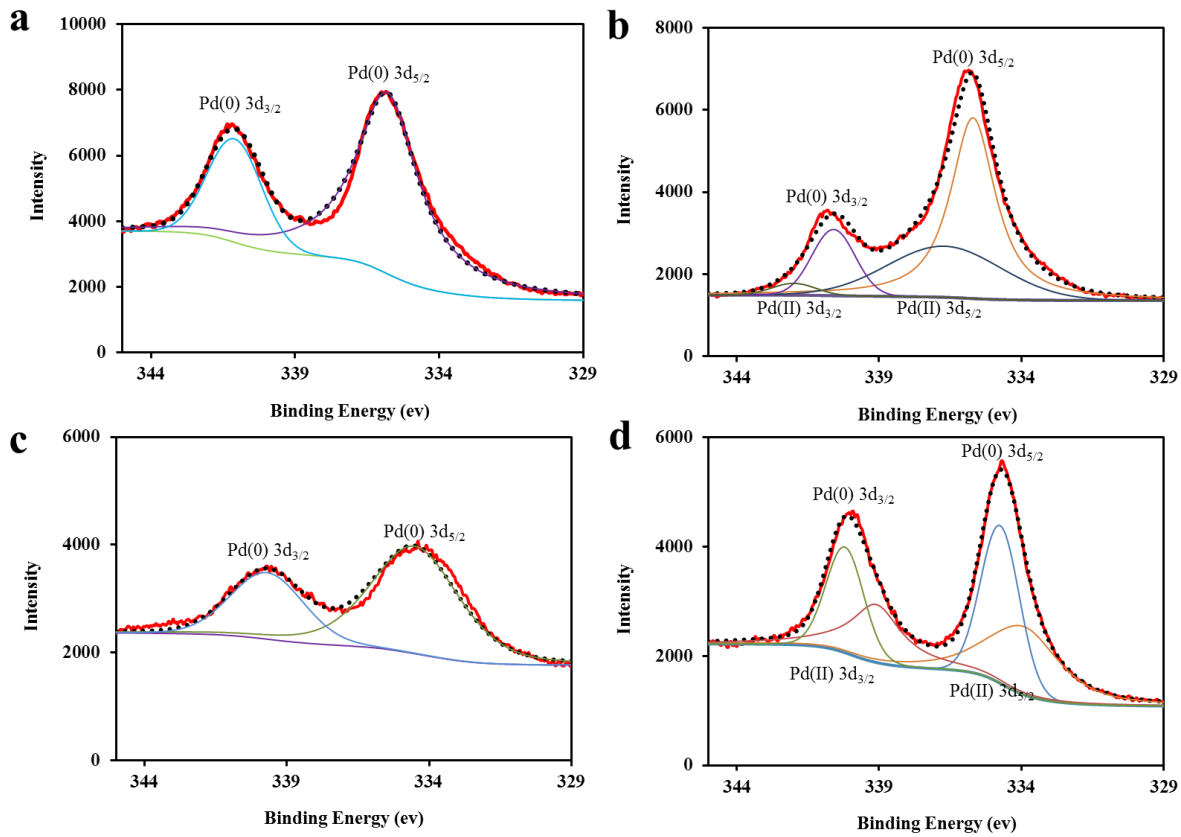

Figure 2.8-8. Pd 3d XPS spectra of catalysts Pd/α-Al2O3 (a before reaction and b after reaction) and Pd-CeO2/α-Al2O3 (c before reaction and d after reaction).

The two catalysts, Pd/α-Al_2O_3 and Pd-CeO_2/α-Al_2O_3, were detected with XPS (Pd 3d) before and after the reaction with CO and EN at 140 °C (Fig 2.8-8). Although there were small differences between Pd/α-Al_2O_3 and Pd-CeO_2/α-Al_2O_3, the obtained Pd $3d_{3/2}$ and pd $3d_{5/2}$ values for both Pd (0) and Pd (II) were consistent with the published literatures. [5-7] In Fig. 2.8-8a and c, both the Pd $3d_{5/2}$ and Pd $3d_{3/2}$ of catalysts Pd/α-Al_2O_3 and Pd-CeO_2/α-Al_2O_3 are around 335 and 340 eV, respectively, which indicates that the oxidation state of Pd in the catalysts is Pd(0). However, after reaction, two new peaks appeared in both the two catalysts (Fig. 2.8-8c and d), which are assigned to Pd(II),[7] indicating that some Pd(0) in the two catalysts was oxidized to Pd(II) by methyl nitrite to form an intermediate, CH3O− Pd(II)−OCH3.[8] The peaks area of the Pd(II) in Fig. 2.8-8d is much bigger than the peaks area in Fig. 2.8-8b, which indicates that more intermediate were generated on the surface of Pd-CeO_2/α-Al_2O_3 catalyst, and therefore Pd-CeO_2/α-Al_2O_3 may have higher catalytic activity with the addition of CeO_2. Furthermore, the percentage of the Pd on both catalysts was calculated using the peaks area of the XPS, the Pd-CeO_2/α-Al_2O_3 catalyst showed higher Pd concentration (0.92%) than that of the Pd /α-Al_2O_3 catalyst (0.81%) , which strongly suggests that the promoter CeO_2 can also enhance the Pd loading concentration on the support.

<u>Evaluation of the EN to DEO set-up</u>

The whole set-up must be leak tested before attempting to start the reaction. Any leak must be fixed before starting experiment. Check the nitrogen regulator for leaks. Set the nitrogen

regulator at a pressure of 50 psi (maximum test pressure will be 20 psi). Use snoop to check the leaks at all connections. If the pressure (50 psi) can keep 24 h without any decrease, the whole system has no leak. Check the CO regulator for leaks. Set the CO regulator at a pressure of 50 psi (maximum test pressure will be 20 psi). Use snoop to check the leaks at all connections. If the pressure (50 psi) can keep 24 h without any decrease, the whole system has no leak.

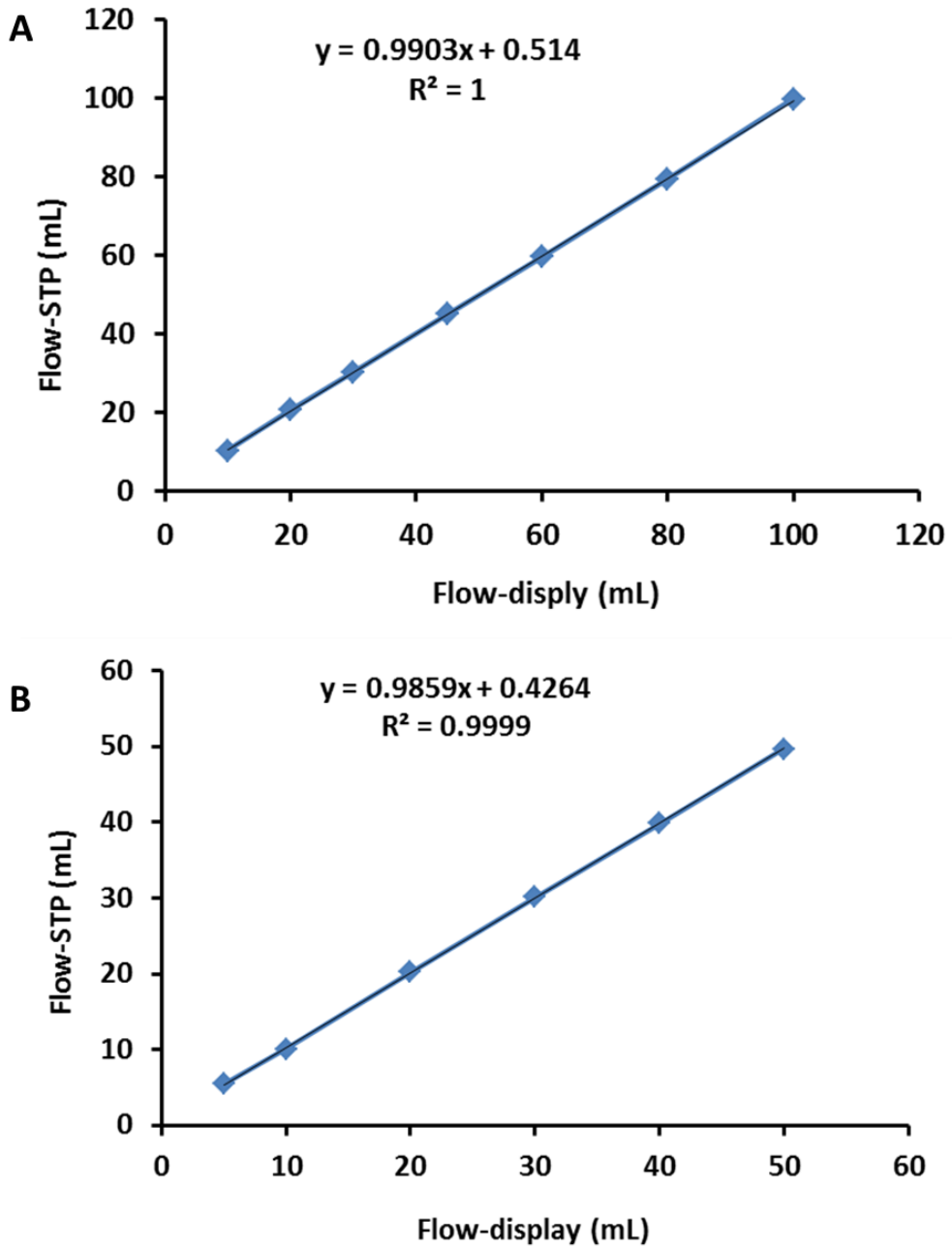

Figure 2.8-9. The mass flow controller N_2 + EN (A) and CO (B) were calibrated with bubble flow gas meter.

All the mass flow controllers were calibrated before the reaction started (Fig 2.8-9). The reactant gases were 20 vol% CO, 15 vol% C_2H_5ONO, and 65 vol% N2 with a space velocity ranging from 600 to 3600 h-1. Liquid-phase ethyl nitrite introduced using a pump entered the reactor

together with carbon monoxide and nitrogen. Flow rates of carbon monoxide and nitrogen were controlled by a mass flow controller. Temperature of catalyst bed in the reactor was monitored by a thermocouple (no higher than 200 °C). Reaction pressure was maintained constant by a back pressure regulator (no higher than 20 psi). Products are analyzed by online GC and liquid products are collected and analyzed by offline GC-MS. When the GC analysis results show that the reaction is in steady state, the sample cylinder vessel is emptied and the start time of the reaction is recorded. Samples from the sample cylinder vessel are collected in specified intervals. Figure 2.8-10 shows the GC result of EN converting to DEO with Pd/α-Al2O3 catalyst with reaction time of 36 h. The main product is DEO with the retention time around 14 min. Figure 2.8-11 shows the conversion of EN with Pd /α-Al_2O_3 and Pd-CeO_2/α-Al_2O_3. Pd-CeO_2 /α-Al_2O_3 shows higher EN conversion (around 83%) compared to Pd/α-Al_2O_3 (around 63%). Both of this two catalysts have high DEO selectivity.

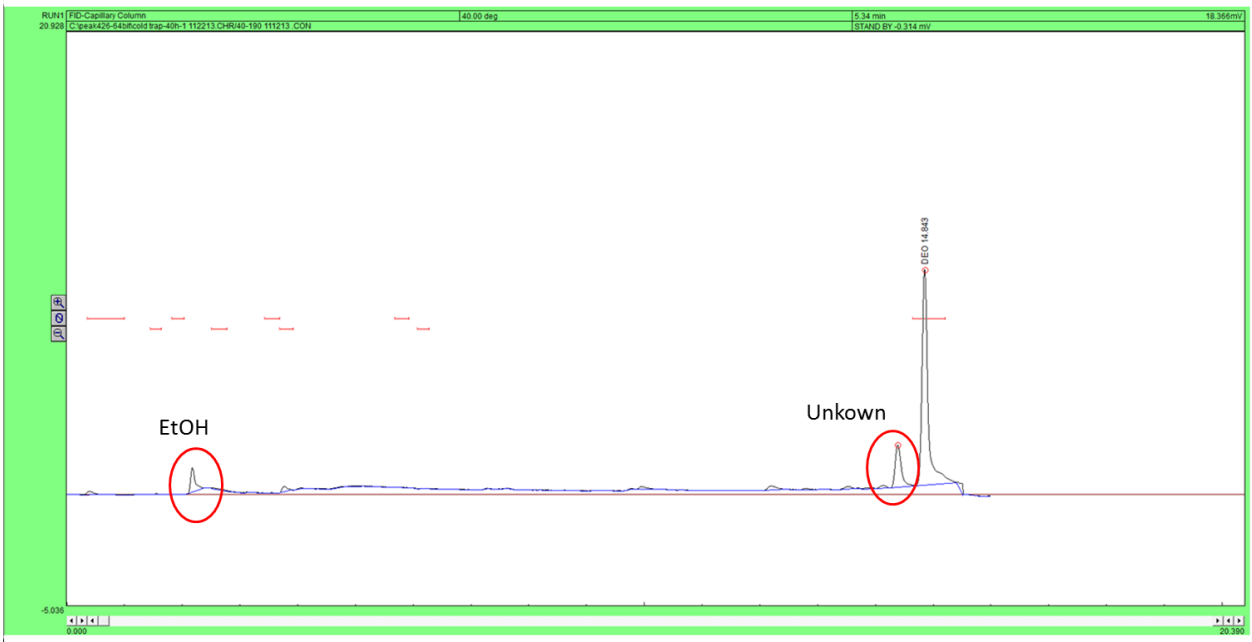

Figure 2.8-10. The GC result of EN to DEO with Pd/α-Al2O3 catalyst (36 h). The main product is DEO with retention time around 14 min.

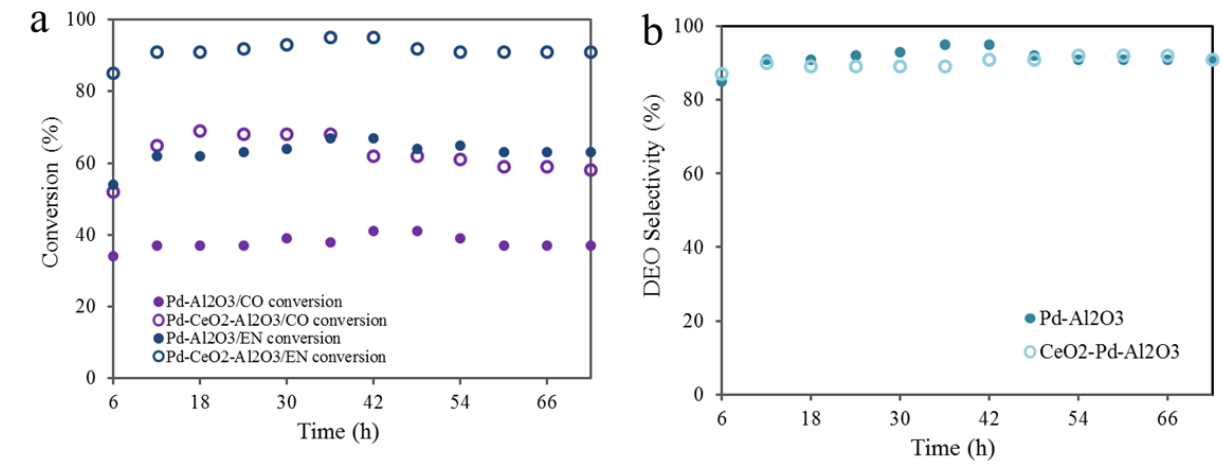

Figure 2.8-11. (a) Conversion of CO (blue lines) and EN (red lines) of CO oxidative coupling to DEO with different catalysts within 72 h. (b) DEO selectivity of CO oxidative coupling to DEO with different catalysts within 72 h.

Table 2.8-1. CO oxidative coupling to DEO with different catalysts.[a]

Catalysts	Pd content (wt%)	Ce content (wt%)	Conversion[b] (%)	Selectivity (%)	STY (g L^{-1} h^{-1})
Pd/α-Al_2O_3	0.8	_	39	95	195
Pd-CeO_2/α-Al_2O_3	0.8	0.15	65	93	318
CeO_2/α-Al_2O_3	_	0.2	_	_	_

[a] Reaction conditions: 3.5 g of catalyst, 1200 h^{-1} of gas hourly space velocity (GHSV), reactants volume ratio CO/EN is 1.2. 0.1 Mpa, 140 °C. [b] Conversion of CO.

The catalytic performances of the two catalysts were evaluated under the same conditions. With the addition of CeO_2, the conversion of CO and EN was increased from 39% to 65% and 64% to 92%, respectively (Fig. 2.8-12a). There is 50% more of conversion for both of the reactants. The STY of DEO with Pd-CeO_2/α-Al_2O_3 was also greatly increased, which is 60% higher than that of Pd/α-Al_2O_3 at 140 °C (Table 2.8-1). In the meanwhile, the selectivity of DEO with these two catalysts was almost the same (around 92%). Since there was no catalytic activity found for the catalyst CeO_2/α-Al_2O_3, the CeO_2 must play an important role as a promoter and the interaction of CeO_2 with Pd was responsible for the high activity and selectivity in CO oxidative coupling to DEO. Most of all, the catalytic activity of catalyst Pd-CeO_2/α-Al_2O_3 can be maintained for at least 72 h (Fig. 2.8-12b), which lays a good foundation for further enlarging a long-term stability test.

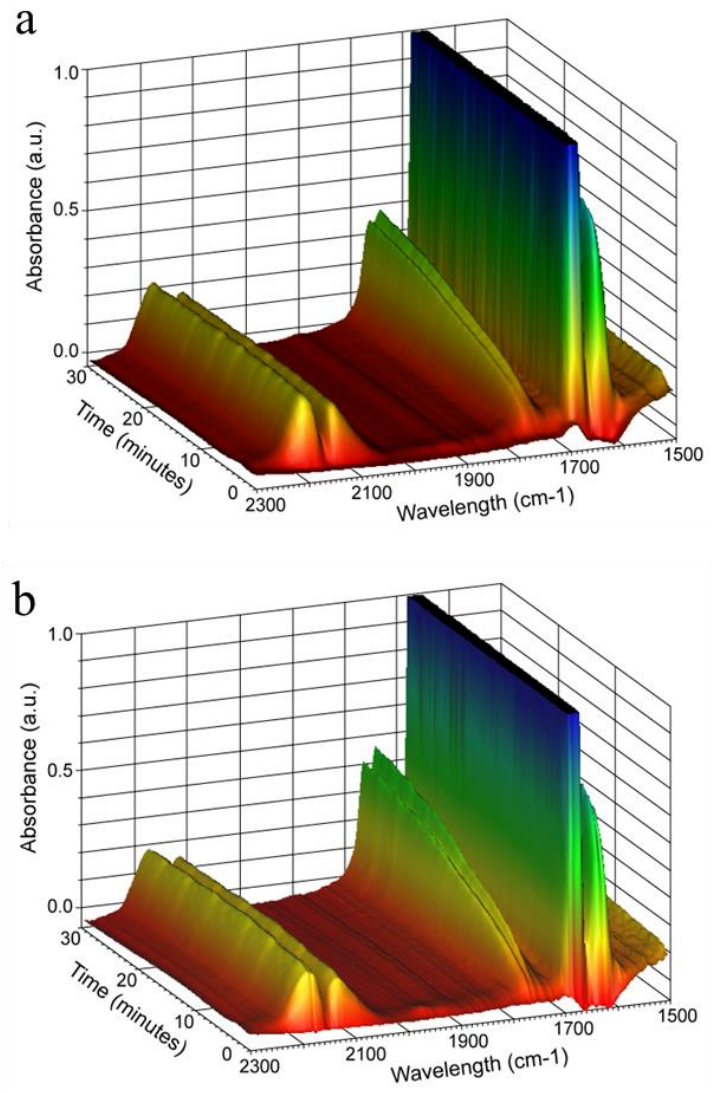

Figure 2.8-12. ***In situ*** **FTIR sepctra for the CO oxidative coupling to DEO reaction with Pd/α-Al_2O_3 (a) and Pd-CeO_2/α-Al2O_3 (b).**

Temperature

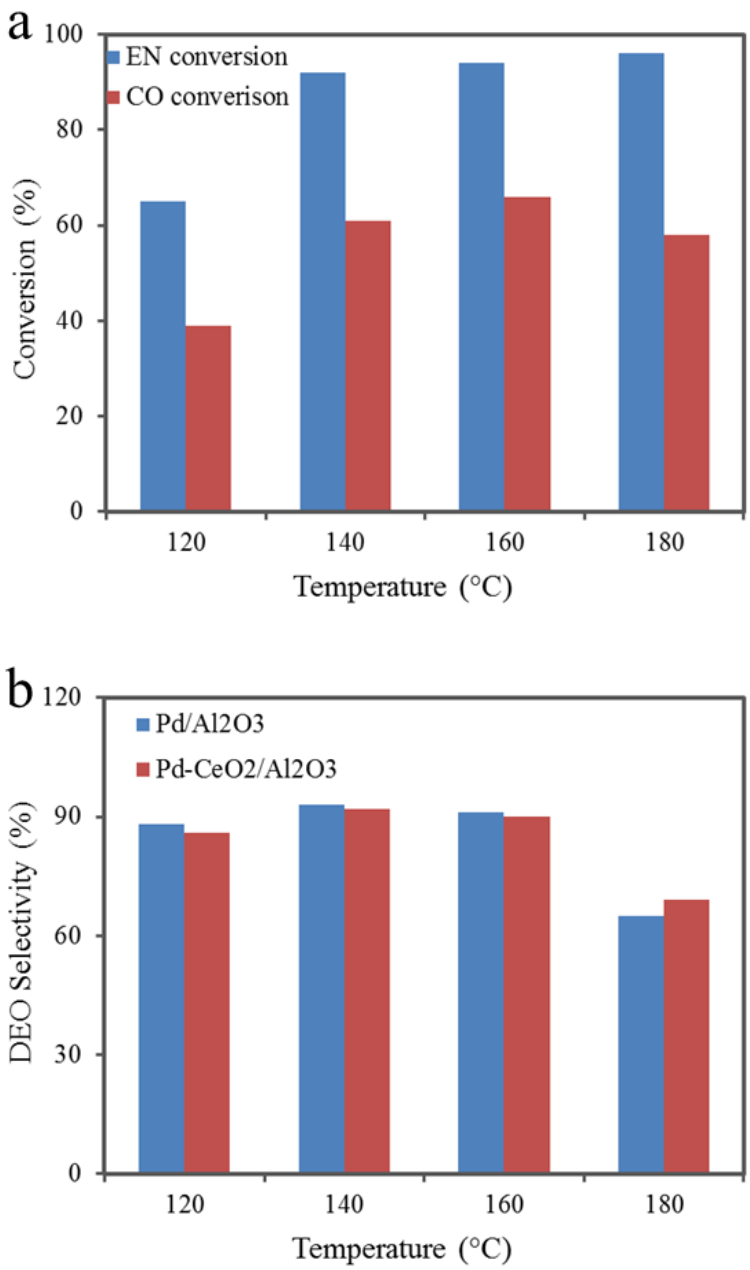

Figure 2.8-13 (a) Conversion of CO (blue lines) and EN (red lines) of CO oxidative coupling to DEO with different reaction temperatures. Reaction condition: 3.5 g of Pd-CeO_2/Al_2O_3 catalyst, 1200 h^{-1} of gas hourly space velocity (GHSV), reactants volume ratio CO/EN is 1.2, 0.1 Mpa. (b) DEO selectivity of CO oxidative coupling to DEO with different reaction temperatures.

Figure 2.8-13a shows the effect of temperature on both EN and CO conversion where Pd-CeO_2/Al_2O_3 was used as the catalyst for CO oxidative coupling to DEO reaction. The conversion of EN and CO became higher with the temperature increasing, especially when the temperature increased from 120 °C to 140 °C. Both EN and CO conversion increased 20% accordingly. However, with the temperature increasing, the selectivity of DEO had almost no change except

when the temperature reached to 180 °C. Both the CO conversion and DEO selectivity decreased at 180 °C due to the decomposition of the EN. Therefore, the future plan for this project is optimizing the Pd-CeO_2/Al_2O_3 catalyst to achieve a lower reaction temperature while with high DEO selectivity.

Plans for Upcoming Quarter

The activities will be focused on continuing the research on synthesis of stable catalysts needed for synthesizing DEO.

Part II : DEO/DMO hydrogenation for EG production

Approach

The schematic drawing the experimental set-up is shown in Figure 2.8-14 and a picture of the whole set-up including the GC-MS (left) is shown in Figure 2.8-15. The system has four main gas lines (H_2, N_2 , Ar and optional gas), shown at the top left corner of the drawing) whose flow rates are controlled by the corresponding mass flow controllers, and a liquid injection line whose flow rate was regulated with a high pressure pump. H_2 is the reaction gas, N_2 is the while He or Ar serves as an internal gas standard for calculating the conversions of H_2. The reaction gas mixture (H_2 +N_2 and He) is supplied pressurized from their gas cylinders by high pressure reducers, regulated by high pressure mass flow controllers (Parker-Porter) and then mixed with the vaporized liquid. The reactor is a fixed bed reactor and its temperature is set by a furnace regulated by a controller. Products are analyzed by online gas chromatographs and liquid products can be collected and analyzed by offline GC-MS. The reaction system is controlled by a DAQ system and all the reaction parameters are recorded automatically. After catalyst hydrogenation the pressure and temperature are set to the activity test. During test, the pressure was maintained at 300PSI (2.068 MPa) and the lowest test temperature was 170°C (above the vaporization temperature of DMO) and the maximum temperature was established as selectivity to EG and MG decreased to less than ~30%. The test conditions are: catalyst mass corresponding to 0.3 g Cu, 300PSI (2.068 MPa) pressure, temperature at least 170°C, weight hourly space velocity (WHSV) 0.8 (g DMO h/g cat), 92.6v.% H_2, 7.4v% N_2, H_2/DMO mol ratio 80/1, 10wt% DMO/methanol.

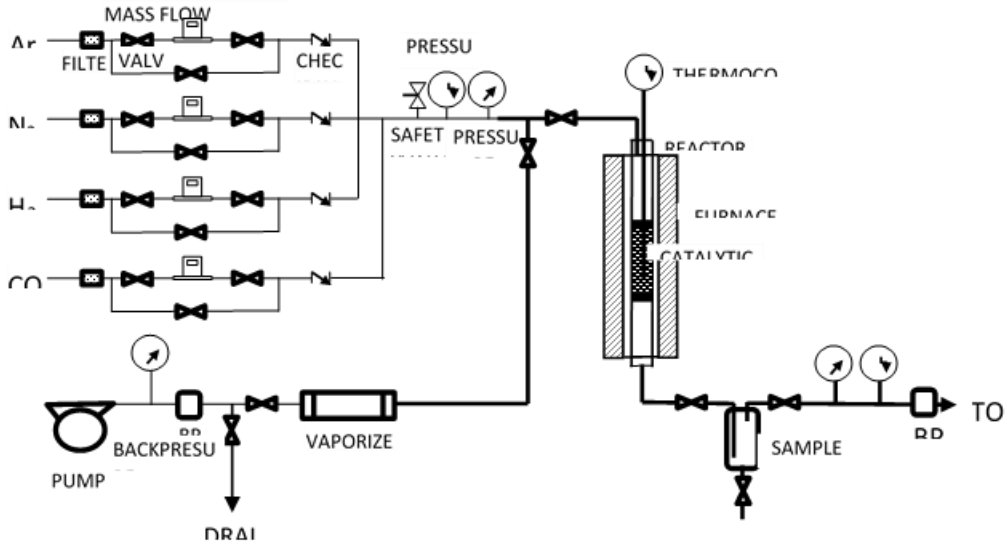

Figure 2.8-14 Schematic diagram of the DMO hydrogenation installation

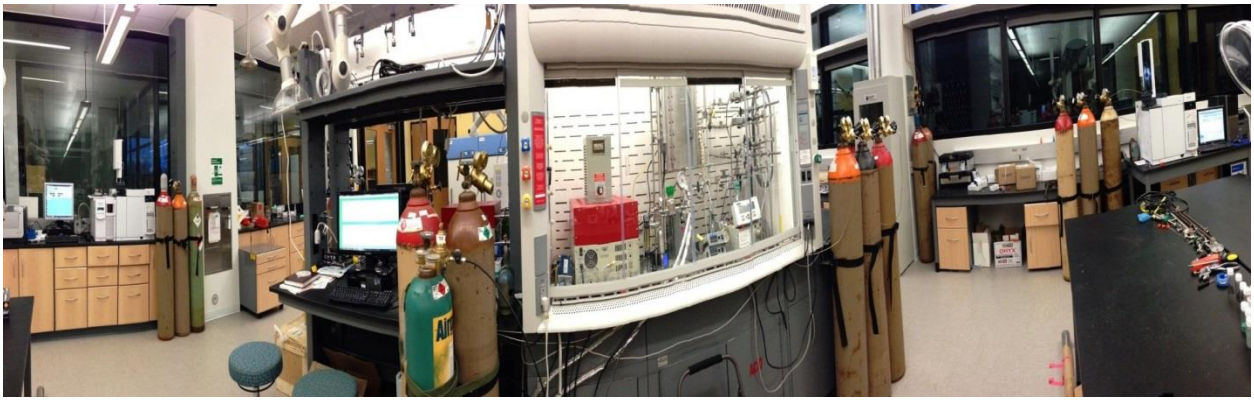

Figure 2.8-15 Picture of the DMO hydrogenation installation. From left to right-far left: GC-MS for testing liquid products; center: control computer and the fume hood containing the inline GC for gas phase (red) and the installation for DMO hydrogenation;

To accommodate the reaction requiring pressure at least 2MPa (~300psi) and minimize the stringent temperature control required, the installation and testing procedures were refined several times. After aiming to replicate the results from literature, catalysts' syntheses methods were redesigned having the goals of inherently safe, ease of scale-up procedures. DMO hydrogenation was chosen because the DMO is more corrosive to the catalyst due to nascent methanol compared with DEO, generating tetramethyl silane and eroding the catalyst support while using DEO is less aggressive in this aspect. Finding a stable catalytic material for more aggressive conditions ensures producing longer lasting catalysts suitable for industrial use in the case of using DEO. Furthermore, the products of DMO hydrogenation are ethylene glycol (EG) and methanol; the products of DEO hydrogenation are ethylene glycol and ethanol. In the case of over-hydrogenation the reaction product of H_2 with ethylene glycol is ethanol, if DEO is used, this ethanol produced from EG is indistinguishable from the ethanol generated from the ethoxy groups of DEO, unless marked carbon is used which would drastically increase the research costs.

<u>Catalyst preparation</u>

a) Deposition-precipitation using NH_3 as precipitation agent (ammonia evaporation-AE). The appropriate quantities of $Co(NO_3)_2*xH_2O$ (Puratronic®, 99.999% (metals basis), Alfa Aesar), were dissolved in water and stirred 30 minutes. Then ammonia solution 30% was added to pH=10-11 and stirred another 30 minutes. Silica generating substances (silica sol LUDOX® AS-30 colloidal silica 30% silica in water, Sigma-Aldrich) were added and stirred another 4 hours. Then the temperature was raised to 90°C for the evaporation of ammonia until pH~7. The precipitate was filtered, washed and dried at 89°C for 12 hours. The resulted material was calcined in air at 450°C for four hours.

b) Deposition-precipitation using $(NH_3)_2CO_3$ as precipitation agent (Deposition using Ammonium carbonate -AC): The appropriate quantities of $Co(NO_3)_2*xH_2O$ (Puratronic®, 99.999% (metals basis), Alfa Aesar), were dissolved in water and stirred 30 minutes. The appropriate quantities of silica generating substances (silica sol LUDOX® AS-30 or AM-30 colloidal silica 30% silica in water, TEOS (Tetraethoxysilane (TEOS- 99+% Alfa Aesar)) or zeolites (ZSM-5, zeolite Y- Zeolyst) were added and stirred 30 minutes. $(NH_3)_2CO_3$ (Ammonium carbonate, ACS reagent, NH3>30.0+%, Sigma Aldrich) saturated solution was added slowly to end pH 6-7. The precipitate continued stirring for crystals maturation, then filtered, washed and dried at 89°C for 12 hours. The resulted material was calcined in air at 450°C for four hours.

c) Sol-Gel precipitation (SG): The appropriate quantities of $Co(NO_3)_2*xH_2O$ (Puratronic®, 99.999% (metals basis), Alfa Aesar), were dissolved in water and stirred 30 minutes. In one case ammonia solution 30% was added to pH 10-11. Separately the appropriate quantity of TEOS Tetraethoxysilane (TEOS- 99+% Alfa Aesar) was mixed with ethanol 100% ratio 1/1. The mixture TEOS-Ethanol was added to the copper solution slowly and then left for gelation. In the above mentioned special case the mixture containing ammonia was boiled at 70°C to pH=8 when mass precipitation occurred, the precipitated was filtered and washed. The gels were dried/aged in oven at 89°C for 12 hours. The resulted materials were calcined in air at 450°C for four hours.

All resulted materials were crushed and sieved, the fractions 125-250 µm were used for catalytic testing.

<u>DMO hydrogenation procedure</u>

The catalysts after synthesis are in form of CuO/SiO_2 hence the test require the pre-reduction to $Cu(Cu_2O)/SiO_2$ in order to function as hydrogenation catalyst.

1.51g catalyst corresponding to 0.3 g Cu is loaded into the reactor. The prepared catalyst is loaded into the reactor with the thermocouple in the middle of the catalyst bed. The top and bottom of the catalyst bed are packed with inert materials (ceramic wool). In one test the catalyst was diluted with quartz sand for comparison purposes aiming for better temperature control. After leak check the system is pressurized with N_2 to the reaction pressure for additional leak check and the catalyst is reduced in 93v.% H_2 7%v. N_2 at 350°C for 4 hours. Then the temperature is reduced to reaction temperature and the DMO 10%wt./methanol is introduced.

Gas products are analyzed by online GC and liquid products are collected and analyzed by offline GC-MS. Samples from the sample cylinder vessel are collected in specified intervals (typically every hour).

During test, the pressure is maintained at 300PSI (2.068 MPa) and the lowest test temperature is 170°C (above the vaporization temperature of DMO) and the maximum temperature was established as selectivity to EG and MG decreased to less than ~30%. The test conditions are: catalyst mass corresponding to 0.3 g Cu, 300PSI (2.068 MPa) pressure, temperature at least

170°C, weight hourly space velocity (WHSV) 0.8 (g DMO h/g cat), 92.6v.% H_2, 7.4v% N_2, H_2/DMO mol ratio 80/1, 10wt% DMO/methanol.

Materials tests

Specific surface area (BET): The specific surface area, pore size and pore volume in zeolite support and catalyts, N_2 adsorption isotherms were performed on a volumetric system AutosorbIQ ASIQC0100-4 Quantachrome Instruments, using nitrogen. Degassing procedure: 4 hours, heating to 150°C. BET isotherm equation for macroporous and mesoporous solids and BJH method was used for the pore size distribution for mesopores and Horvath–Kawazoe method was used for micropores [17]. The analyses are on 0.1g catalysts.

XRD patterns for the crystalline phase and the average crystal sizes were collected using the powder on a Rigaku Smartlab XRD machine using Cu Kα X-ray source in thin layer powder configuration, 2Theta/Theta mode, 20-100° range, 0.02^{o} step, 1°/minute scanning speed

The reducibility of the material was generated using Temperature Programmed Reduction (TPR) executed in a quartz reactor containing 0.1 g sample, 5 mol%H_2 balance He, using for measurements a mass spectrometer HPR 20-Hiden Analytical. After one hour at 110°C in He for dehydration, the material was cooled at 50°C and after temperature stabilization the samples were heated 10°C/minute to above900^{o}C (typically to 1000C).

Transmission Electron Microscopy (TEM) is giving the particle dimension and coverage. Images were obtained at Materials Characterization Laboratory in University of Wyoming's Geology Department.

X-ray photoelectron spectroscopy (XPS): The data was collected using a Kratos Axis Ultra DLD X-ray Photoelectron Spectrometer (XPS). It uses a monochromated Al K-alpha source running at 150 W. Survey scans were acquired at 80 eV pass energy at 1 eV resolution. High resolution elemental scans were acquired at 40 eV pass energy at a resolution of 0.05 eV.

RESULTS AND DISCUSSION

The catalysts activity was analyzed as function of the DMO conversion and selectivity toward EG and MG at various temperatures.

Catalytic activity: All the samples were tested in the same conditions: catalyst mass corresponding to 0.3 g Cu, 300PSI (2.068 MPa) pressure, temperature at least 170°C, weight hourly space velocity (WHSV) 0.8 (g DMO h/g cat), initial gaseous phase 92.6v.% H_2, 7.4v% N_2, H_2/DMO mol ratio 80/1, initial liquid phase 10 wt% DMO/methanol.

Figure 2.8-16 shows the selectivity toward EG and MG of the catalysts prepared using various methods. As can be seen from this figure, all catalysts with the exception of the catalyst prepared by the gelation of $Cu(NO_3)_2$ in TEOS ("20 wt% Cu/SiO2-TEOS-Cu(NO3)2 sol-gel") show as products containing C-C bonds only EG and MG until 200°C. It can be seen that in this aspect the catalyst produced using AE on silica sol have a fast decrease of the selectivity above 190°C in our testing conditions. A test boiling slower ammonia (AE) to pH 6-7 resulted in longer range of selectivity to 210°C but at lower DMO conversion compared with the AE precipitated at pH 7-8, signifying that the reduction in end pH of the precipitation is beneficial. The catalysts prepared using ammonium carbonate fast gelification performed close to the catalysts prepared using ammonia fast gelification which was the next performer in term of selectivity. The catalyst prepared using slow boiling of ammonia to neutral pH on TEOS performed well (but at lower conversion). By comparison the catalysts using precipitation using ammonium carbonate had similar selectivity to 210°C.

Figure 2.8-17 shows the DMO conversion at the test temperatures. The maximum conversion was achieved by the gelation of $Cu(NO_3)_2$ in TEOS ("20 wt% Cu/SiO2-TEOS-Cu(NO3)2 sol-gel") although at lower selectivity, followed closely by the catalysts prepared using ammonium carbonate fast gelification. The catalysts prepared using slow boiling of ammonia to neutral pH on TEOS performed worst close, while the AE -slow boiling- Cu/silica sol catalysts performed also close to the least active catalyst. This shows that the catalyst prepared by ammonium carbonate fast gelification performed well in terms of both selectivity and DMO conversion.

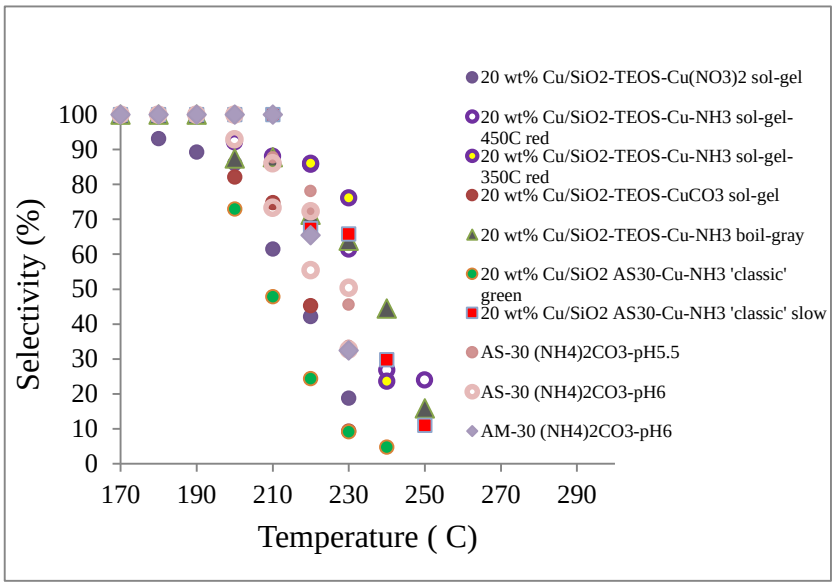

Figure 2.8-16: Selectivity to EG and MG of the 20wt% Cu/SiO2 catalysts (catalyst mass corresponding to 0.3 g Cu, 300PSI (2.068 MPa), WHSV 0.8 (g DMO h/g cat), 92.6v.% H_2, 7.4v% N_2, H_2/DMO mol ratio 80/1)

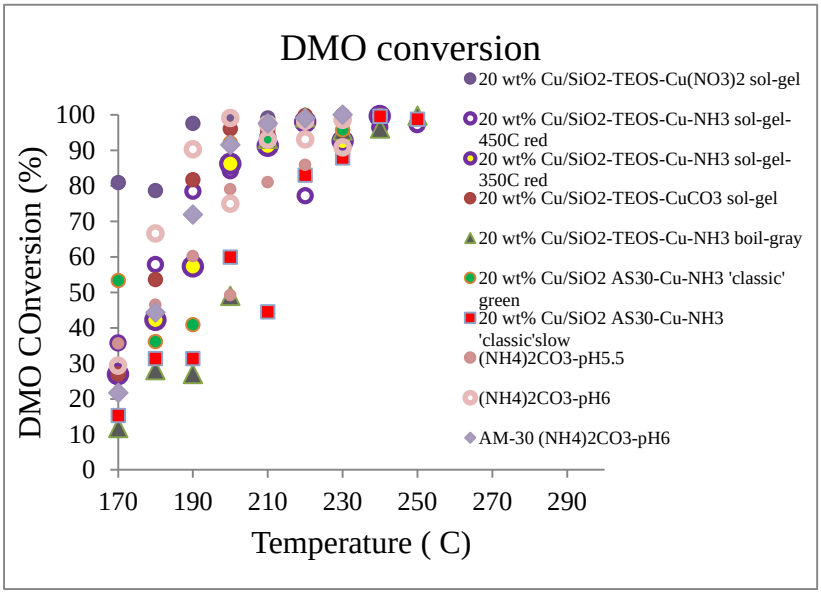

Figure 2.8-17: DMO conversion of the 20wt% Cu/SiO2 catalysts (catalyst mass corresponding to 0.3 g Cu, 300PSI (2.068 MPa), WHSV 0.8 (g DMO h/g cat), 92.6v.% H_2, 7.4v% N_2, H_2/DMO mol ratio 80/1)

The catalyst prepared using AS-30 silica sol ($NH4^+$ stabilizing cation) as support and precipitation using ammonium carbonate at end pH 5-6 were very active catalysts maintaining good activity also next day with a loss of only 25% DMO conversion and 8% selectivity to MG and EG (measured at 200°C) after 14 hours on stream while most of the unstabilized catalysts in literature loose almost all their activity after around 10 hours on stream [2, 4]. The catalyst prepared using AM-30 silica sol (Na^+ stabilizing cation) had by comparison around 7% smaller DMO conversion at similar temperature, pointing at the importance of having raw materials with low Na^+ for the support synthesis.

Cu-zeolites: Cu-zeolites were prepared using AC method and they were also reduced for 4 hours in in 93v.% H_2 7%v. N_2 at 350°C. The zeolites were type Y (Faujasite) CBV780, CBV400 and ZSM5 (Zeolyst). This type of catalysts, due to their variable SiO_2/Al_2O_3 ratios generate variable number of Bronsted and Lewis acid sites and due to dehydration reactions they promote were useful in generating etherated by-products due to the reaction with the methanol which was used as solvent.

Specific surface area: the results of the BET analyses are in Table 2.8-2. It shows that the catalyst obtained using ammonia evaporation has highest surface area for the fresh catalyst (375 m^2/g) but after ~ 16 h at high temperature (4 hours, 350°C reduction in H_2 then above 170°C in DMO-H2 stream) the catalyst loses 43.38% from the specific surface area, while in the case of the AC precipitation the catalyst 20Cu-AS30-AC loses 26.8% in the same conditions, while 20Cu-AM30-AC starts with the lowest specific surface area (152 m^2/g) and also loses 34.9% of the initial specific surface area.

Table 2.8-2: Specific surface area for the catalyst

Material	Specific surface area (m^2/g)
20Cu-AS30-AE fresh	375
20Cu-AS30-AC fresh	216.371
20Cu-AM30-AC fresh	152.387
20Cu-AS30-AE used	216.063
20Cu-AS30-AC used	158.337
20Cu-AM30-AC used	99.165

XRD patterns obtained for the unreduced (fresh), reduced and used catalysts are shown Figure 2.8-18. It shows the growth of crystalline phase for metal oxide phase for the used catalysts and confirms sintering as one of the deactivation mechanism.

Figure 2.8-18 shows the XRD patterns obtained for the unreduced (fresh) samples as they resulted after calcination in air for four hours at 450°C in the form Intensity vs. 2θ. As can be seen from Fgure 2.8-18, the sample obtained by ammonia evaporation technique using the ammonia stabilized silica sol (20Cu-AS30-AE-fresh) displays less evident peaks signifying less crystallinity compared with the other two samples. The large peak centered around 23° is hard to analyze due to the large signal/noise ratio but it can be assigned to poorly crystalized SiO_2 structures. If it would be assigned to quartz, there should be a large peak centered at 26.65^o (69.9% relative peak intensity) having a smaller peak at 20.87^o,which is possible but also by a small peak at 50.17^o which was not found. As tridymite, the largest peak should be centered at 20.53^o (100%), followed by a smaller signal at 20.66^o (45.33%), a large peak at 21.64^o (97.52%)

while next peaks to 23.46º are of 25-29% relative intensity (small). An interesting alternative would be to assign the peak to poorly crystalized cristobalite (tetragonal) having the largest peak at 22.01º (100%) and in that case it would be formed at the interface with Cu_2O cuprite (cubic) resulted by the decomposition of amminocupric complexes. In such case we can assign the crystallization order CuO/Cu_2O first and during calcination the silica gel crystalizes following the type of order present at the interface with copper oxides (Cu_2O cubic and CuO monoclinic). All three samples display this peak, while the rest of the larger peaks displayed by the samples can be assigned to CuO (tenorite).

As can be seen in the Figure 2.8-18 the crystallinity of the samples is in order from more crystalline to less crystalline 20Cu-AS30-AC-fresh > 20Cu-AM30-AC-fresh>20Cu-AS30-AE-fresh. Interestingly it correlates with the catalyst activity. In the case of the catalyst prepared using the Na^+ stabilized silica sol although Na was not found in the XPS tests, the XRD results suggests it depressed the proper crystallization of tenorite (CuO) during precipitation, statement strengthen by the TPR results showing only one peak corresponding to the reduction of CuO finely disseminated.

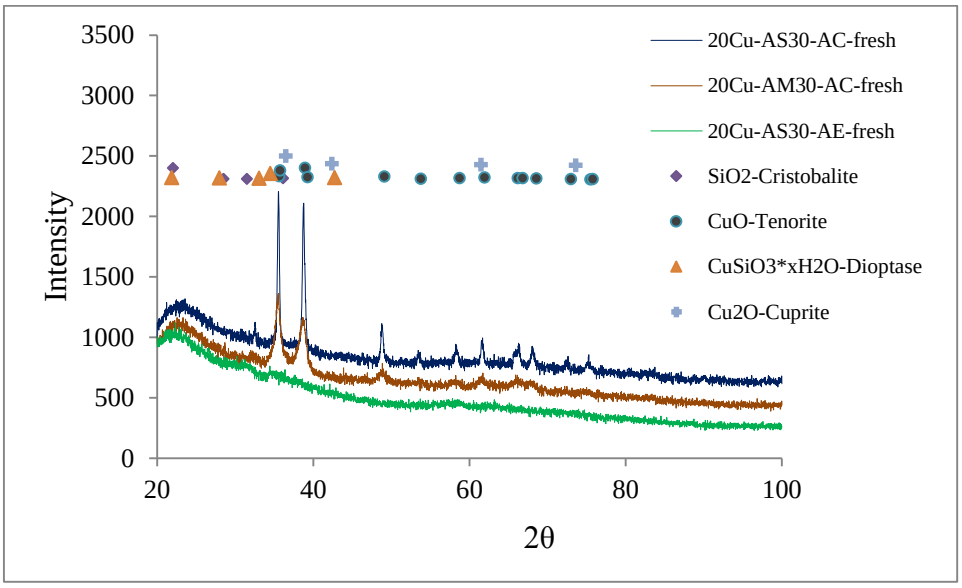

Figure 2.8-18: XRD results for the most active catalysts, fresh (unused and unreduced) samples

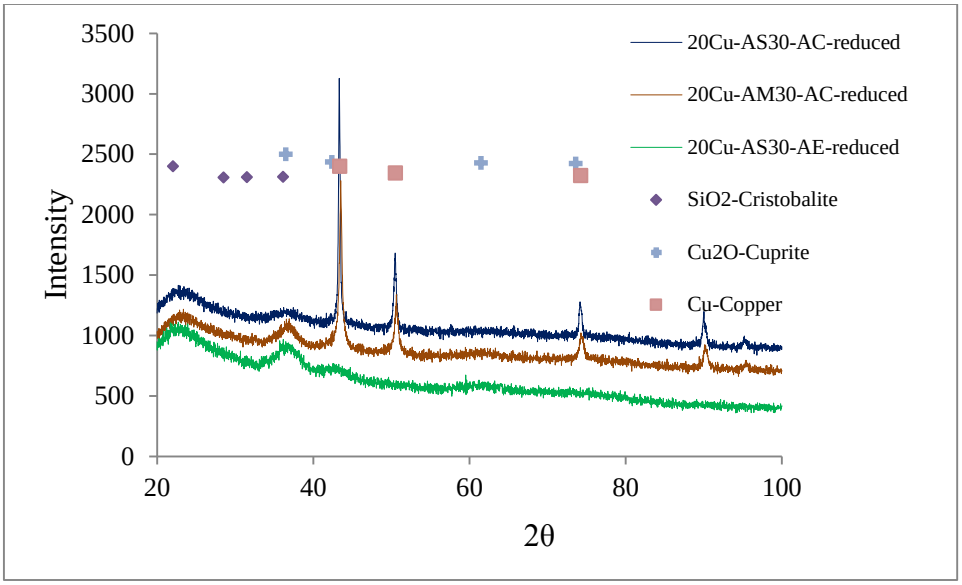

Figure 2.8-19: XRD results for the most active catalysts, reduced (but unused on DMO stream) samples

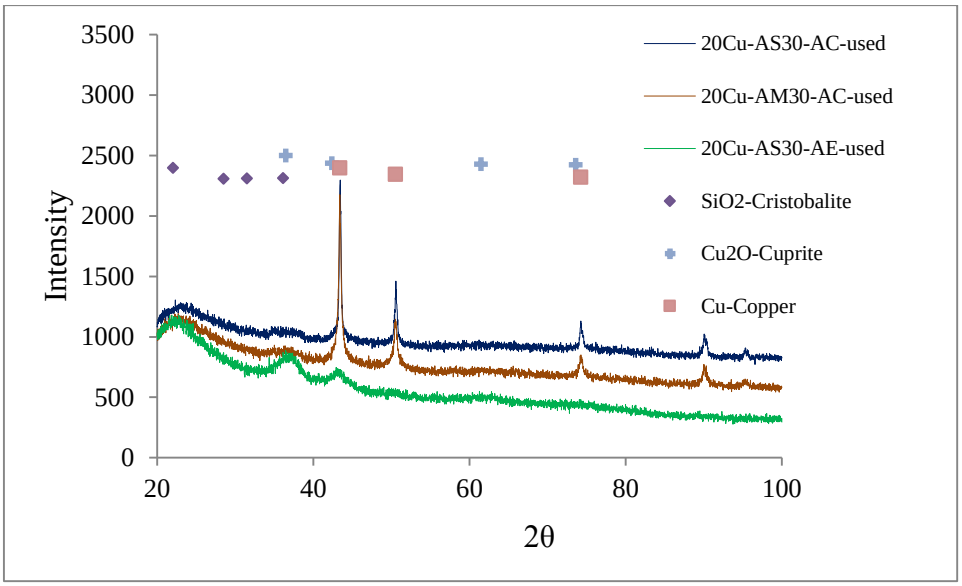

Figure 2.8-20: XRD results for the most active catalysts, used on DMO stream samples (~ 16 hours)

Figures 2.8-19 and 2-8-20 illustrate the results of the XRD test for the reduced and used catalysts. The large peaks at ~ 43.4, 50.6 and 74º can be assigned to metallic Cu (Cu^0) while the peak at 36.5º and the large peak centered around 61.5º can be assigned to cuprite (Cu_2O shows larger peaks at 36.46, 42.35, 61.44, 73.6º). Compared to the peaks generated by metallic Cu, the cuprite peaks are much wider signifying a poorly crystalline and small crystal domains phase. Comparing the catalysts it can be seen that in the case of the catalyst prepared using ammonia evaporation the peaks for Cu^0 are much smaller compared with the catalyst prepared using ammonium carbonate precipitations, while the peak assigned to cuprite tend to be much larger. The catalyst prepared using Na^+ stabilized silica sol (AM30) displays initially a larger cuprite wide peak at ~36.5º after reduction but after use it show a peak resembling the peak generated by the other catalyst prepared using ammonium carbonate precipitation.

Temperature Programmed Reduction (TPR) results for the samples are shown in Figure 2.8-21. For the sample 20Cu-AS30-AE it shows only one peak at 290°C corresponding to the reduction of the finely disseminated CuO to Cu. In the case of 20Cu-AS30-AC there are two peaks, one having a maximum of H_2 consumption at 270°C corresponding to the reduction of finely disseminated CuO and a second of smaller intensity showing maximum H_2 consumption at 320°C corresponding to the reduction of bulk CuO in the structure. The sample 20Cu-AM30-AC shows again only one peak centered at 300°C and larger width if compared with the 20Cu-AS30-

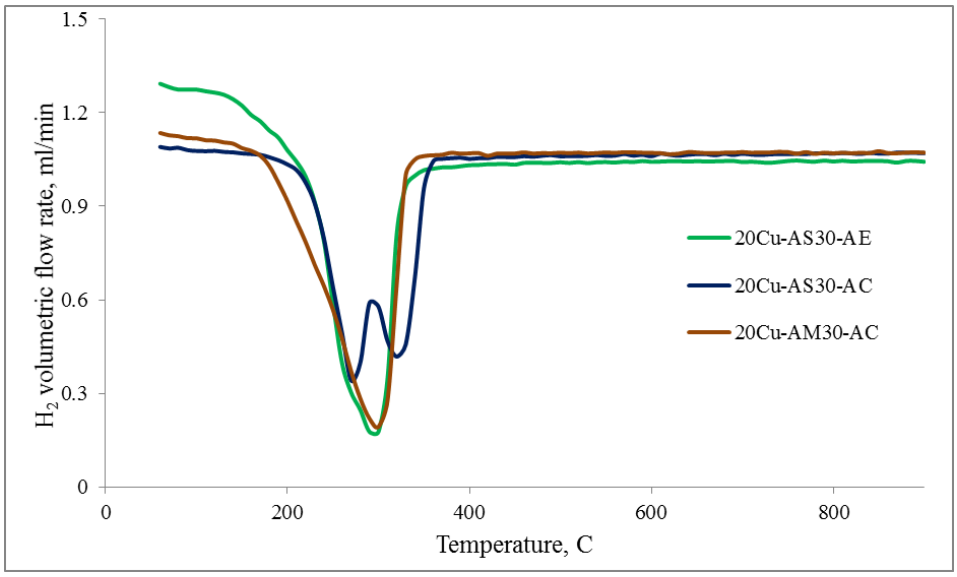

Figure 2.8-21. TPR results for the 20Cu-AS30-AE, 20Cu-AS30-AC and 20Cu-AM30-AC (0.1 g sample, in 5 mol%H_2 balance He, 10°C/min)

AE peak. Comparing the areas of the peaks it can be seen that the peak generated by 20Cu-AS30-AE appears to be narrower corresponding possibly to an incomplete release of Cu from SiO_2 matrix as suggested by the XRD also comparing the samples prepared by AC technique since the H_2 consumption is correlated with the size of the CuO_x crystallites, the result correlates with the XRD result showing a the presence of smaller CuO structures in the case of 20Cu-AM30-AC compared to 20Cu-AS30-AC. Comparing the onset of H_2 consumption it is debatable the start for 20Cu-AS30-AE due to the desorption of H2 during heating (20Cu-AS30-AE has also the largest specific surface area among the three catalysts) but it starts ~140°C for 20Cu-AS30-AE and 20Cu-AM30-AC and at ~170°C for 20Cu-AS30-AC which also correlates with the XRD results.

Plans for Upcoming Quarter

Materials tests were underway and their results have to be analyzed. XRD shows that the catalyst prepared using ammonia evaporation generates copper silicate mineral $CuSiO_3*H_2O$ (dioptase) which seems to be metastable at calcination temperature (450°C). Also the Cu/SiO_2 catalyst has to be stabilized by adding transitional metals as alloy of Cu, but since most of the transitional metals have precipitation in basic end-pH challenges will arise, besides the phase separation in mixed oxides, phase separation in Cu alloys and the reactivity of the transitional metals toward SiO_2 producing very stable silicates.

Theme 3 – Pre-Combustion CO_2 Capture

Subtask 3.1. – IGCC with CCS

Approach

Combining advanced gasification with CCS in the power sector remains a critical pathway towards low-carbon power generation. Industrial, research, and academic leaders from both countries will work with the major demonstrative projects and best in class technologies to provide the world with robust, transparent cost and performance estimates for the class of power plant. Pilot testing platform wil be constructed via this research work, based on which the technology of CO2 capture, utilization and storage based on IGCC will be developed and demonstrated.

Results and Discussion

Task is complete at this time.

Plans for Upcoming Quarter

Task is complete at this time.

Subtask 3.2. – IGCC Knowledge Transfer

Approach

Duke Energy and Huaneng are working to share start-up and operational lessons learned from Huaneng's GreenGen facility and Duke Energy's Edwardsport IGCC facilities. In addition, they will work with each other to expand knowledge and identify best practices.

Results and Discussion

Task is complete at this time.

Plans for Upcoming Quarter

Task is complete at this time.

Theme 4 – Post-Combustion CO_2 Capture, Utilization and Storage Technology

Subtask 4.1. – 1 MTons/Year Post Combustion CO_2 Capture at Duke Gibson Station

Approach

The activity of this task will be to perform a Pre-engineering Study of the 1 Million Tons/year Post-combustion CO_2 Capture systems, combined with a preliminary Techno-Economic Analysis and Budgetary Cost Estimate (±30%). Upon completion of these itms, a Sensitivity Study of Power Generation with Post-Combustion Carbon Capture System will be performed.

Results and Discussion

The final report of this task is attached as an appendix. Task is Complete

Plans for Upcoming Quarter

Task is Complete

Subtask 4.2. – Development of Solvent for CO_2 Separation from Utility Flue Gas

Approach

The project is set up to develop innovative solvent compositions to reduce the overall cost of CCS. The first step in the process it the establishment of a technical team and a performance matrix for solvent formulation and evaluation. The next step will be the formulation of the solvent. Finally, evaluation will occur at various levels of scale to determine the solvent's performance capabilities. In this quarter a joint working group was established and met to determine the performance matrix which is reported below.

Results and Discussion

Task is Complete

Plans for Upcoming Quarter

Task is Complete

Subtask 4.3. – Development of Catalyst to Enhance CO_2 Capture Kinetics In Scrubber

Approach

Previous works on the second generation catalyst containing ionic ligands were showed to obtain high CO_2 hydration activity. Using a salen analog containing an imidazolium or phosphonium salt functionality were found to increase the rate enhancement of CO_2 hydration by two orders (~10^5) in comparison to earlier reported Zinc(cyclen) systems using CAER pH-drop assay. The success of the salen analog discussed in the previous quarter will guide the design of future catalysts for CO_2 hydration. It was discovered that by using slight variation in the salen framework we can tune the activity of the catalysts to fit specific needs.

Results and Discussion

Through previous studies in the catalysis group, we have identified several key characteristics that need to be considered in the rational design of new catalysts. Thermal stability experiments have indicated that ligand flexibility is one factor that significantly impacts catalyst stability. Several Salen-type complexes have been made by our group that incorporate alkane "backbone" segments.

The added flexibility from an sp^3 (vs sp^2 hybridized) backbone has led to significant improvements in overall activity in recent complexes, however the use of linear alkanes allows for free rotation along the backbone, which in turn has led to the isolation of multinuclear (bis-Zn) complexes. With this information, we have been exploring the use of diaminocyclohexane as an alternative "backbone". This new catalyst, (C_6H_{10})-PSA Zn Salen, should allow for the best of both worlds, a sp^3 hybridized alkane backbone for added flexibility that is also locked in geometry by the cyclic nature of the linker to prevent rotation and the formation of bis-Zn complexes.

Preliminary activity studies have been conducted with (C_6H_{10})-PSA Zn Salen, and this catalyst shows significant enhancement for CO_2 hydration in 30% MEA (wt/wt) by pH-drop method. There is a significant change in the slope of the catalyst plot around pH = 9.8. This suggests that the catalyst shows a greater rate enhancement at richer loadings, which is ideal for the CC process.

Effect of flue gas contaminants on the activity of the catalyst C7z and C8z:

Coal-derived flue gas contains impurities such as NOx and SOx gas, which produce a variety of contaminants when in contact with amine-based carbon capture solvents such as nitrates and sulfates. The activity, and robustness, of our CAER catalysts C7 and C8 were tested in the presence of these potential harsh contaminants (Figure 4.3.1 and 4.3.2). A variety and mixtures of the potential end species derived from NOx and SOx gas in amine-based solvents were added to the catalyst solutions and pH-drop methods were utilized to verify the effects. There appears to be a negligible effect of the flue gas contaminants, alone or combined, on the catalyst activity. This is a positive result because the flue gas contains SO_x and NO_x which can affect the process of carbon capture. If the catalyst made at CAER were also affected by the SO_x and NO_x, the operational cost will also increase.

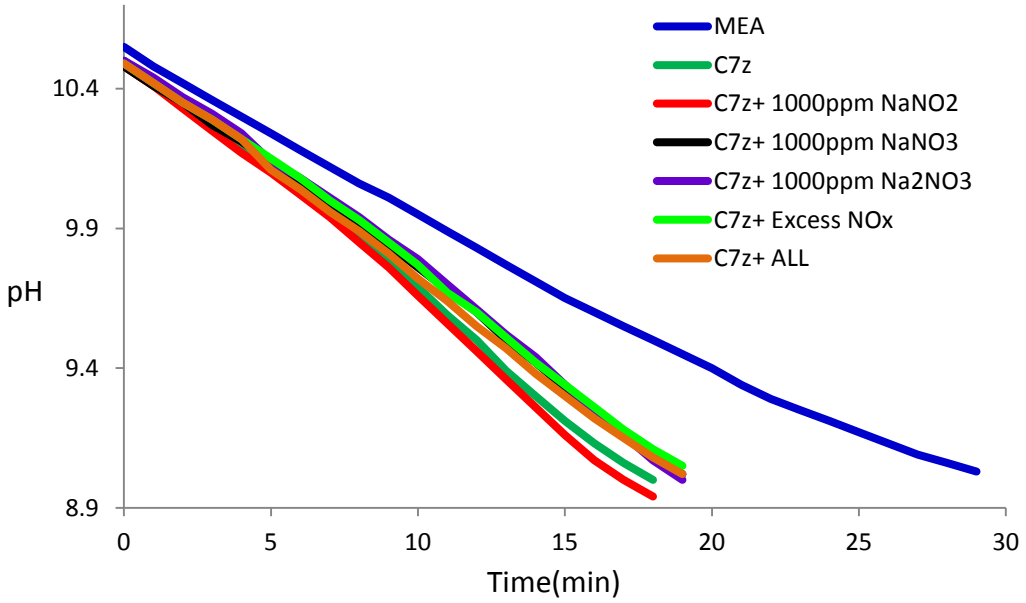

Figure 4.3.1: Effect of SO_x and NO_x gases on the activity of C7z catalyst in 5M MEA.

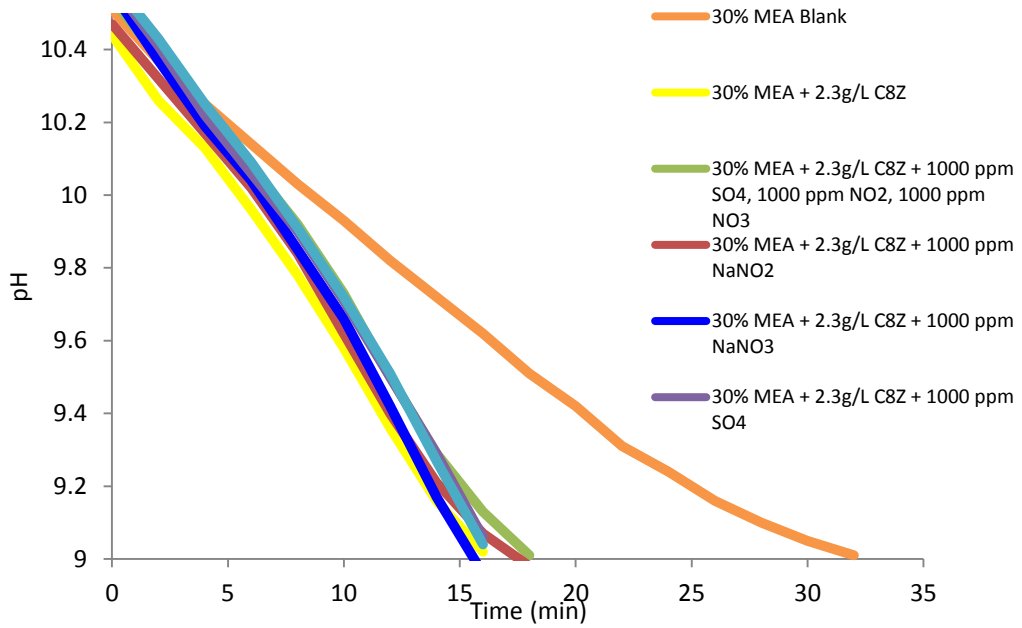

Figure 4.3.2: Effect of SO_x and NO_x gases on the activity of C8z catalyst in 5M MEA.

Fundamental Kinetic Studies of CO_2 Hydration in Amine-Based Solvent Systems (Supported by DOE U.S.–China CERC)

We have been developing a methodology for conducting fundamental studies on the kinetics of CO_2 hydration utilizing stopped-flow UV-vis spectroscopy. Through these studies we aim to obtain rate constants for the individual elementary reactions that govern the overall chemistry of the amine-based CO_2 scrubbing process. By better understanding the individual catalyzed, as well as uncatalyzed, reactions we can gain insight into the kinetics that govern the performance of our solvents and catalysts. We are still in the process of perfecting our method for these experiments, and we am currently attempting to reproduce rate constants published in the literature. Significant progress has been made toward understanding the limitations of buffer/indicator systems, how to collect and process the necessary data, and how to manipulate dissolved gas solutions. We will be receiving a CO_2 probe shortly, at which time we will be better able to quantify the concentration of dissolved CO_2, which significantly affects the experimental rate constants and the consistency of the acquired data.

Several test experiments have been conducted to reproduce literature rate constants, and some of these are shown below. Figure 4.3.3 shows the obtained second order rate constant for CO_2 capture in 2.5 mM 1A2P with 2.5×10^{-5} M thymol blue as the pH indicator. The experimental rate constant, $k = 4079\ M^{-1}s^{-1}$, is reasonably close to the reported value of $5300\ M^{-1}s^{-1}$ considering we do not yet have the capability to measure the actual CO_2 concentration in solution.

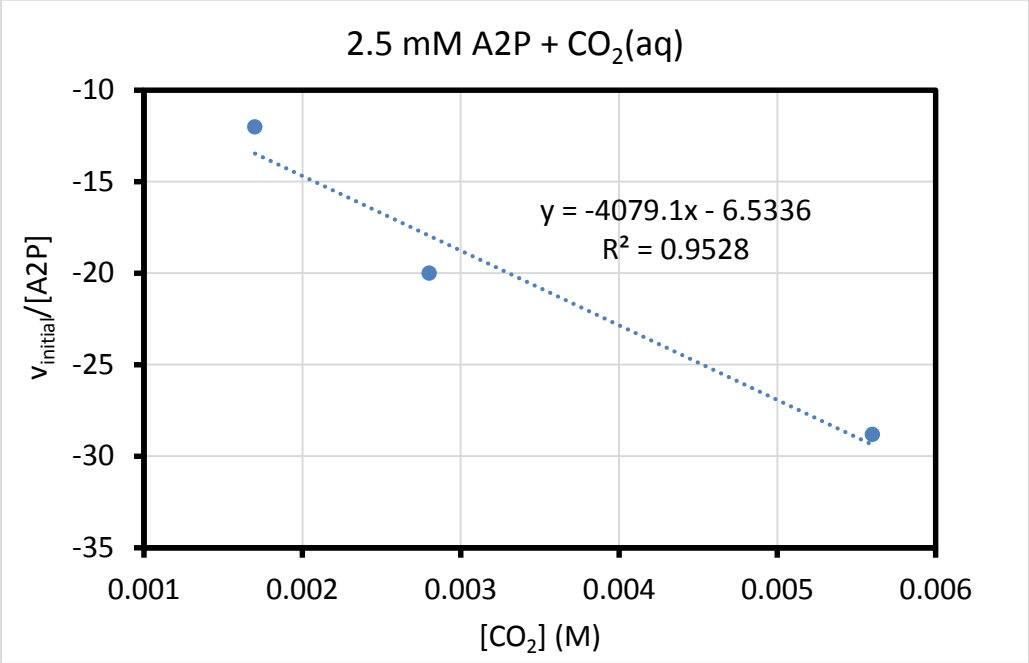

Figure 4.3.3. Stop-flow kinetic analysis of 1A2P.

Another example is shown in Figure 4.3.4, where we applied our kinetic method to determine the hydration rate for AMP, and alternative amine solvent that does not have a reported rate in the literature. The obtained rate constant, k = 1474 $M^{-1}s^{-1}$ is close to what would be expected for this amine, since a close structural analogue (2AP) has a reported rate of 1000 $M^{-1}s^{-1}$.

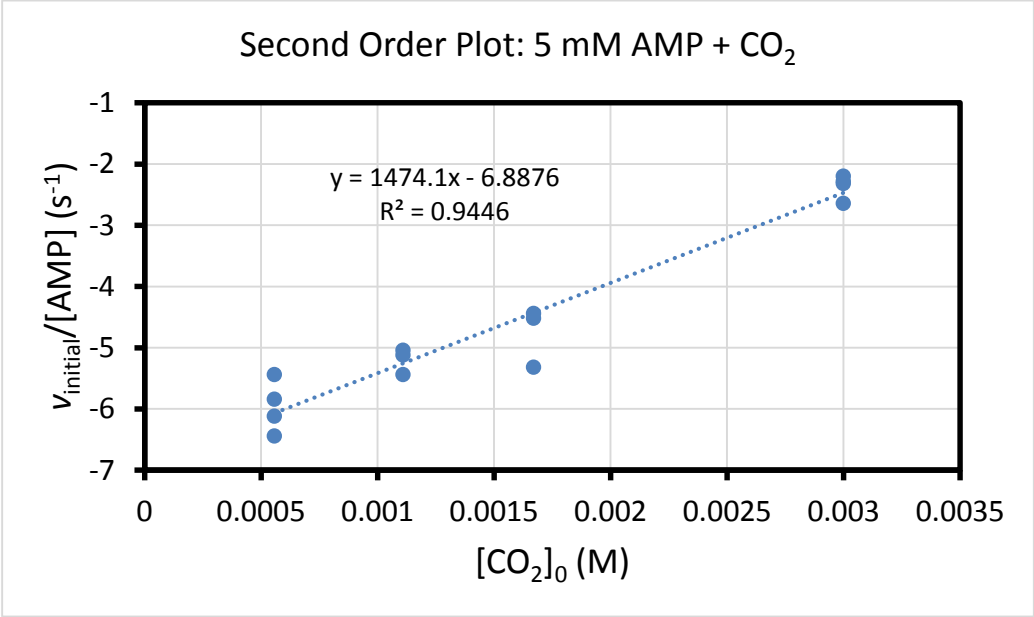

Figure 4.3.4. Stop-flow kinetic analysis of AMP.

We are still addressing several problems with these studies, such as large variability in the data, as well as determining the influence of other factors (i.e. ionic strength) on the overall rates. Additionally, for many of the faster amines, we are limited by the speed of our instrument (12

ms/data point) and are only getting limited data points. Smaller data sets lead to increased error, and slower amines or more dilute solutions may have to be used in the future.

Conclusion

We have prepared, tested, and verified activity of a new catalyst in 30% MEA. A homogeneous catalyst has also been immobilized onto a solid support and shows a small enhancement in CO_2 absorption. Thermal stability test for catalyst C8z shows that it is thermally robust compared to earlier reported zinc catalysts which saw no drop in activity after 92 hours of heating at 145 ^{o}C. Flue gas contaminants were also found to have no effect on the catalytic activity of the catalysts C7z and C8z in 30% MEA. Finally, a kinetics methodology has been developed based on literature methods to obtain quantitative rates and rate constants for reaction of amines and/or catalysts with CO_2.

Plans for Upcoming Quarter

Work in the following quarter will focus on expanding our catalyst library and immobilizing select catalysts onto solid supports, with the intention of discovering a suitable catalyst to function in non-MEA solvents.

Subtask 4.4. – Membrane Development for CO2 Separation from Utility Flue Gas Stream

Approach

Realization of high permeance membranes (>3,000 GPU) would be a transformational achievement resulting in a membrane based separation technology for post combustion CO_2 capture that would exceed the current DOE targets ($20-25 per ton of CO_2; <35 % increase in COE). This subtask effort utilizes both development of advanced materials and membrane manufacturing methods with the goal of achieving a high permeance membrane platform with the required stability and durability characteristics for CO_2 capture from PC derived flue gas. Our approach is: to design and synthesize high CO_2 permselective polymer/RTIL-based hybrid membrane materials; to develop novel methods based on ultrasonically assisted deposition techniques to fabricate ultra-thin composite membranes with unprecedented high CO_2 permeances on commercially attractive support platforms; and to demonstrate these developed materials and methods via evaluations under industrially relevant conditions.

Results and Discussion

Task is Complete

Plans for Upcoming Quarters

Task is Complete

Subtask 4.5. – Post CO_2 Scrubber Solvent Enrichment

Approach

Capacitive deionization (CDI), described in previous reports, is being utilized here in an effort to decrease the amount of carbon-rich MEA solution (mainly water) that needs to be processed during the solvent regeneration step. To accomplish this, carbon-rich MEA ions will be concentrated using the CDI process with porous carbon materials. This work aims to examine specifically carbon xerogel-type (CX) electrode materials. Factors such as pore size, porosity,

surface area, wettability and conductivity are all important for ion capture among others such as electrochemical properties.

This past quarter has been spent examining long-term enrichment of carbon-loaded piperazine with a flow-through CDI cell. Degradation in the separation ability (similar previous results) was seen as well as changes in the pH of the system. However, long-term separation ability can still be maintained with proper applied potentials and tracking of the potential of zero charge (PZC). Energy recovery was also examined with the use of a new dc-dc converter capable of integrating CDI cells together to lower the overall cost of the separation.

Experimental

SiO_2 was deposited on the carbon xerogel surface through TEOS treatments. The modification procedure includes (1) TEOS (Sigma-Aldrich, >99%), ethanol, and HNO_3 were mixed at a volume ratio of 1:20:1, and the mixture was stirred vigorously for 1 h, (2) the CX sheets were dipped into the mixture for 3 min, and dried in an oven at 100 °C for 30 min, and (3) the samples were further heated at 300 °C in the oven for another 12 h. It should be mentioned that procedure (2) was repeated for several times (X = 1, 5, and 10) to increase the amount of SiO_2 loading on the carbon xerogel surface, and the resulting samples were denoted CX-SiO_2-X in the text and figures. As-deposited silica-coated carbon xerogel electrodes were then examined by BET/BJH N_2 adsorption isotherm analysis, SEM/EDS, FTIR, and electrochemical methods.

CDI tests were performed in a flow-through cell assembled with the CX electrodes adjacent to titanium current collectors. The electrodes were separated by a 1.5 mm thick silicon rubber. Adsorption-desorption cycles were performed at 1.2 V and the short-circuit potential, respectively, for a total of 15 combined cycles. The CX electrodes had a total mass of ~0.8 g (~42 cm^2). During system operation, 500 ml of ~4 mM NaCl solution was continuously purged with wetted N_2 in the solution reservoir, and circulated using a peristaltic pump (Masterflex) at 27.2 mL min^{-1}. A conductivity meter (Cole-Parmer 19500-45) at the cell outlet was installed to calculate the electrosorption capacity (Γ).

$$\Gamma = (\Delta\sigma M_w V)/(mc) \qquad (1)$$

where Δσ is the conductivity difference between the adsorption-desorption steps at steady state (last 100 s), M_w is the molar mass of NaCl, V is the volume of the salt solution, m is the mass of the carbon used, and c equals 112.77 determined from the slope of conductivity as a function of NaCl concentration. The current efficiency and charge efficiency were calculated using equations 2 and 3, repectively

$$\text{Current Efficiency} = \frac{\text{Charge}_{\text{Desorption}}}{\text{Charge}_{\text{Adsorption}}} \qquad (2)$$

$$\Lambda = (\Gamma F/M_w)/(Q_{ad}) \times 100 \qquad (3)$$

where Λ is the charge efficiency, Γ is the electrosorption capacity, F is Faraday's constant, MW is the molecular weight, and Q_{ad} is the charge used during adsorption.

Results and Discussion

<u>Adsorption-Desorption Cycling of Carbon-Loaded Piperazine</u>

The CDI cell was operated with an applied potential of 1.2 V for adsorption and short-circuit potential for desorption. However, to the best of our knowledge, the size of the ions in carbon-loaded piperazine (C-PZ) is much larger than Na^+ and Cl^-. Therefore, in order to see a clear

separation profile, 16 pairs of CX electrodes were added into the cell. In addition, during operation, N_2 was not used as a purge gas to prevent the loss of CO_2 from solution. The C-PZ solution was prepared by diluting 5 molarity (M) of C-PZ with deionized H_2O at a weight ratio of 1 (C-PZ) to 1000 (H_2O.) At this dilution ratio, the resulting conductivity of the solution was ~240 $\mu S\ cm^{-1}$.

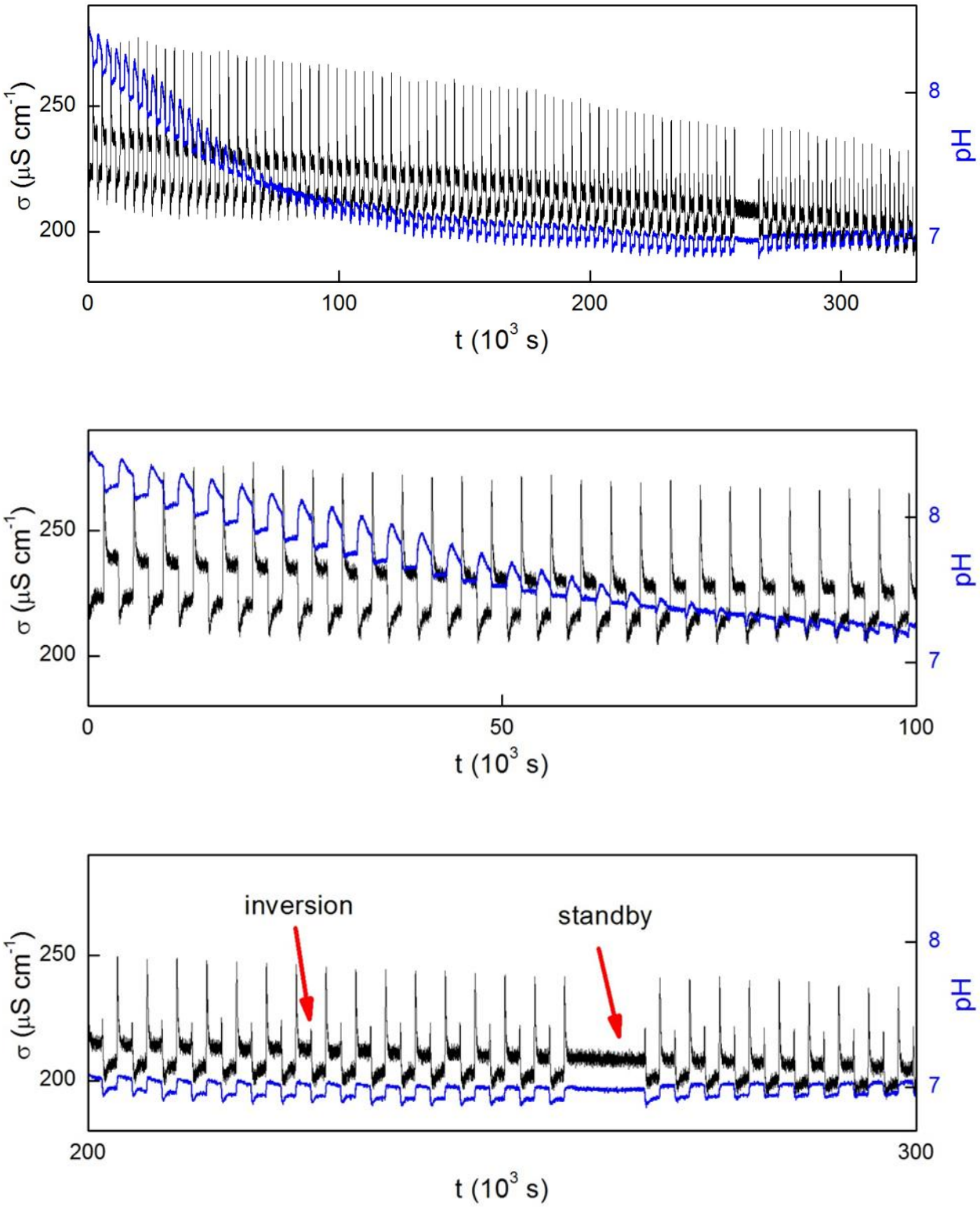

Figure 4.5.1. A plot of overall conductivity profile (top), a plot of conductivity profile between 1 and 100×103 s (middle) and a plot of conductivity profile between 200×103 and 300×103 s (bottom).

Figure 4.5.1 shows the plot of overall conductivity profile received from the C-PZ test. Since we gained much experience from the study of the performance using NaCl. By comparison, it is found in the overall profile (Figure 4.5.1) that the height between the peak and the trough deceases similar to the performance observed when NaCl solution was studied. This decrease is most likely due to shifting of the PZC area for the electrode. This conclusion can be emphasized by looking at the bottom plot, where inversion peaks are formed at the beginning of the adsorption step. It is also found that the conductivity level of C-PZ cannot be stabilized, which is very different from the NaCl study. This observation may imply that PZ is degraded at the electrode. Surely, the decrease in the conductivity indicates that the number of mobile ions is reduced. Liquid samples have been submitted for LC/MS analysis to determine any loss of PZ in solution. At ~270×10^3 s, the power supply was turned off. It can be seen that the conductivity of the C-PZ is still decreasing. Overall, it is considered that C-PZ may not be chemically stable at these concentration for long-term CDI operation. Some chemicals at the carbon surface may catalyze a degradation reaction even without applying potential.

Fig. 4.5.1 also shows the pH values along with the process. It can be seen that the pH value is functionally a wave so as to balance electro-neutrality in the CDI cell. This conclusion was deduced by a previous study in NaCl solution. It is clear to see in the middle plot that the pH value is quite flat, which suggests that the PZC location for both the electrodes are almost located at the short-circuit potential of the CDI cell. Before and after this stable pH area, the variation of the pH value is inverted, e.g., at the beginning of the operation (top plot), the pH increases during adsorption while at the end of the operation (bottom plot), the pH decreases during adsorption. This suggests that at the initial stage, that the cell is limited by the cathodic performance, and at the end of operation, the cell is regulated by the anodic performance.

Energy Recovery with Integrated CDI Cells

Research work continued on the recovery of energy from discharging CDI cells via interfacing with a multi-input bi-directional dc-dc converter towards achieving lower energy requirements. The converter controls energy input from the power supply and the transfer of energy from a discharging cell to one that is charging. Results from the dc-dc converter were compared to direct cell to cell recovery experiments without a converter or power supply utilized during the energy recovery process. Recovery and performance were examined as functions of recovery time and initial potential drop.

Figure 4.5.2 shows the voltage (a), power (b), and conductivity (c) profiles during direct energy recovery from a discharging CDI cell to one that is charging without the power supply or dc-dc converter. Salt solution was continuously circulated at ~30 ml/min through both cells, and no inert gas purging was done. In the direct cell-cell experiments, cell 1 was initially charged at 1.2 V, then directly connected to cell 2. In addition, both cells were completely isolated from the power supply. After approximately 600 s of operation, both cells expectedly achieved the same potential (Figure 4.5.2a), albeit smaller than the theoretical value of 0.6 V due to self-discharge and ohmic losses.

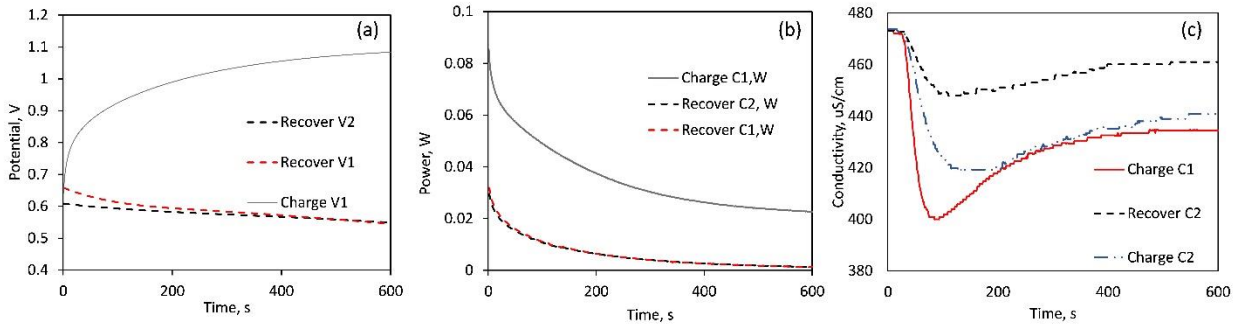

Figure 4.5.2. Voltage, power and conductivity profiles during direct cell to cell energy recovery. Cell 1 was originally charged at 1.2 V with a power supply which was removed when Cells 1 and 2 were connected.

The power curves (Figure 4.5.2b) were obtained via multiplication of the voltage and current at the same time. Integration of the power curves for the cells gives their respective energy. As shown, and expected, only a fractional amount of the energy from cell 1 (~ 17%) was recovered for use by cell 2 after 600 s of operation. This again is due to ohmic contributions, but also to charge leakage during cell 1 charging which cannot be recovered. The conductivity drops were 38 and 13 µS/cm for cells 1 and 2 respectively. Charging cell 2 at 1.2 V gives a conductivity drop of ~33 µS/cm, which implies that ~ 38% conductivity drop was achieved with the recovered energy.

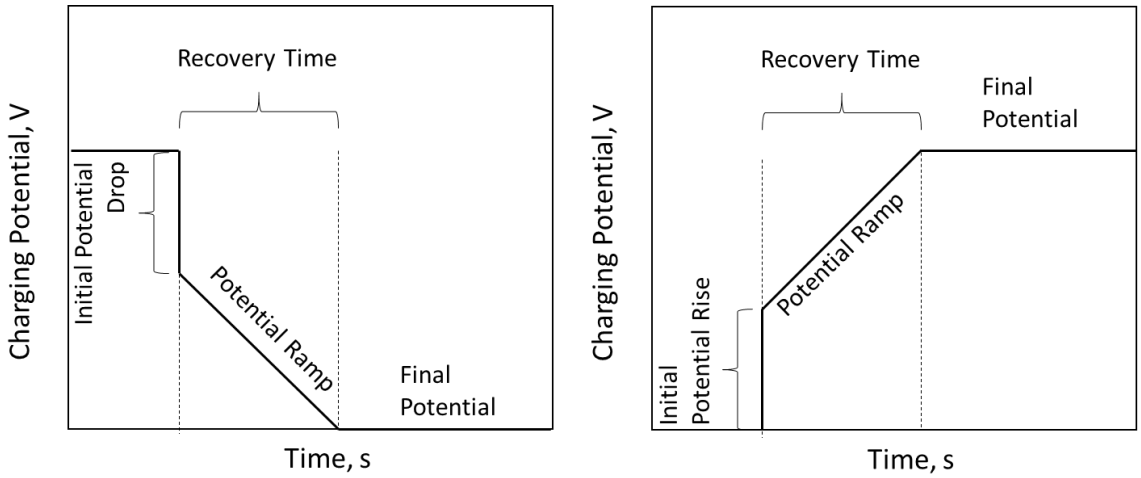

Figure 4.5.3. Potential profiles for the discharging and charging cells during dc-dc converter energy recovery experiments.

For experiments involving the dc-dc converter, the experiments proceeded in several stages. (1) potential drop, (2) potential ramp, and the (3) final potential. This is illustrated in Figure 4.5.3. The converter controls the initial drop and the recovery time. Figure 4.5.4 shows the potential, conductivity, power, and efficiency profiles during a recovery process from discharging cell 1 to charging cell 2. The initial potential drop was ~0.3 V from 1.2 V (C1,V), followed by linear voltage ramping over 300 s of recovery time. The reverse is seen for cell 2 (C2, V). During operation, the converter tries to discharge cell 1 completely in 300 s, after which cell 2 is completely powered by the power supply.

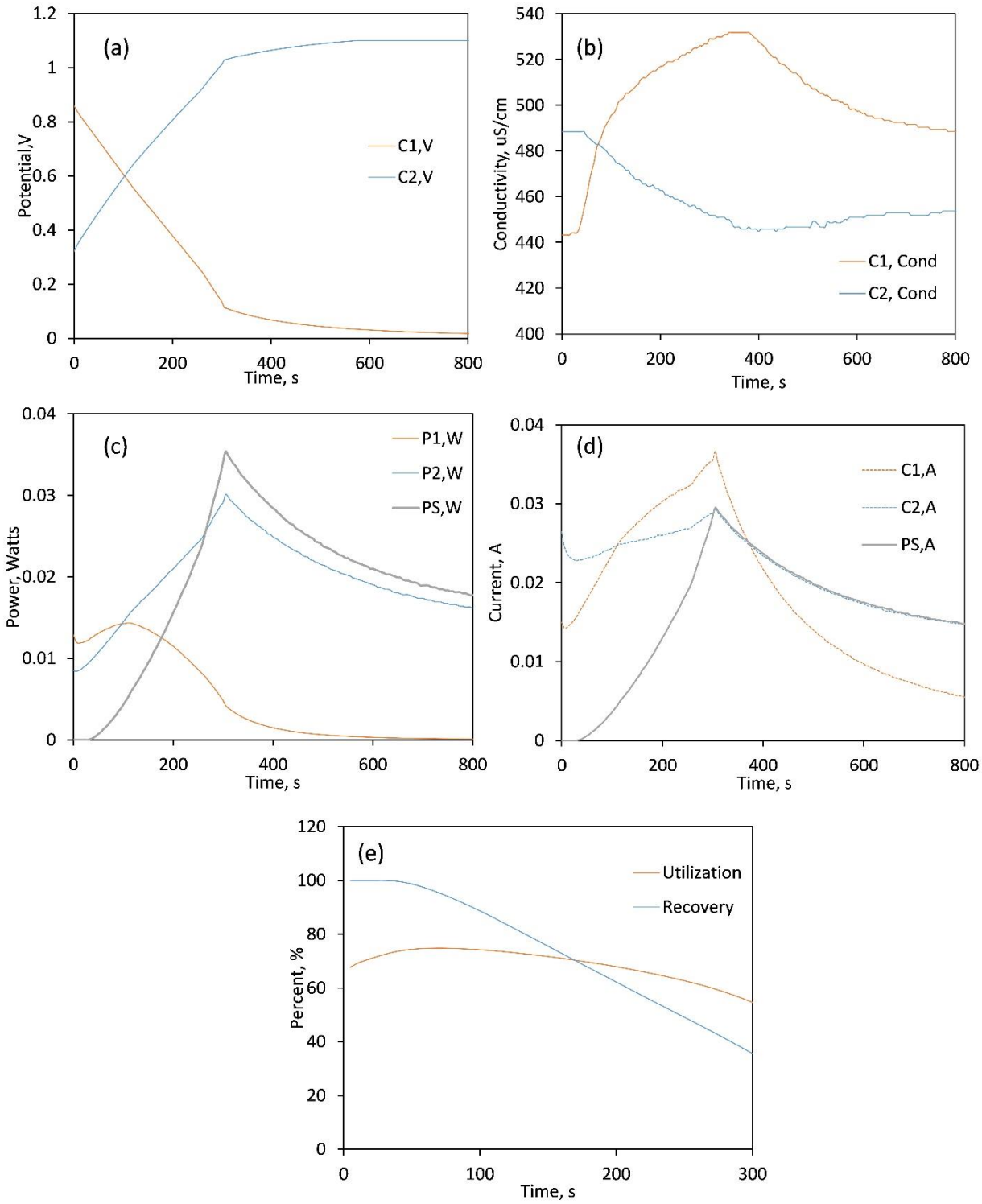

Figure 4.5.4. Potential (a), conductivity (b), power (c), current (d), and efficiency (e) profiles during energy recovery with a DC/DC converter.

Figure 4.5.4b shows the conductivity profiles for the charging and discharging cells. A conductivity drop of ~35 µS/cm at 600 seconds was achieved for cell 2. This result is similar to those of Figure 4.5.2c, where cell 2 was charged at a constant 1.2 V. Figure 4.5.4c shows the power profiles. At ~275 s into recovery, the power from the power supply (PS,W) becomes larger than the power used by the cell (P2,W). Given that the current density from the power

source (PS, A), and cell 2 (C2, A) become equal as shown in Figure 4.5.4d, this mathematically results from the inequality in potential/voltage. The recovery and utilization data are presented in Figure 4.5.4e. Recovery (R) is the fraction of energy used by cell 2 for desalination that does not come from the power supply, while utilization (U) is the fraction of energy used by cell 2 from cell 1. The two terms are mathematically described below.

$$R = \frac{E_2 - E_{PS}}{E_2} \times 100 \quad (2)$$

$$U = \frac{E_2 - E_{PS}}{E_1} \times 100 \quad (3)$$

Figure 4.5.4e shows that the recovery and utilization ratios decrease over time as the input from the power supply continues to increase. So far, we have been able to achieve a recovery of 34 % and utilization of over 54 % in the 300 s window. Recovery and utilization are further explored as functions of converter control parameters which include recovery time and initial drop. For the initial drop experiments, the recovery time was maintained at 300 s, while for the recovery time experiments, the potential drop was maintained at 0.6 V.

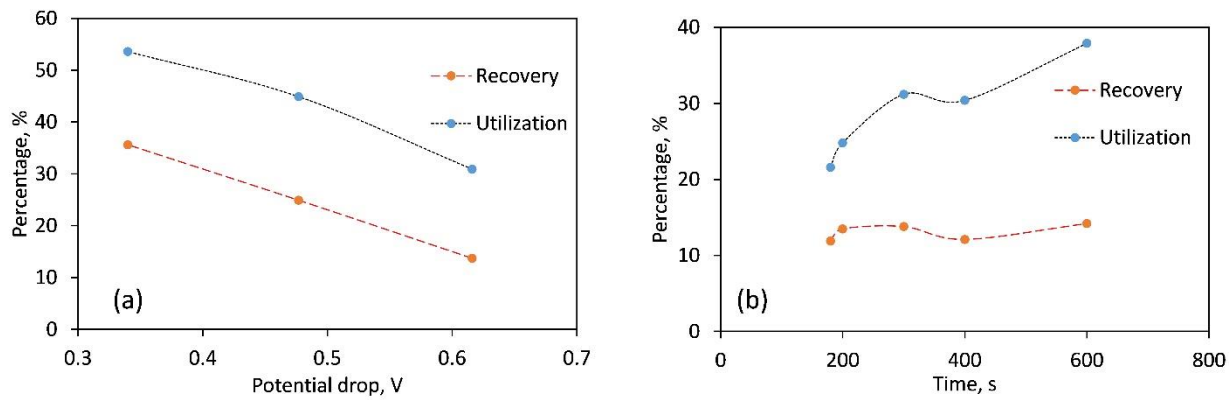

Figure 4.5.5. Utilization and recovery as a function of potential drop (left) and ramping time period (right) with the dc-dc converter.

As shown in Figure 4.5.5 (left), both the recovery and utilization decrease with increasing potential drop. Figure 4.5.5 right shows that the utilization increases with recovery time, while the recovery is almost constant.

Plans for Upcoming Quarter

We will further examine C-PZ solutions before and after a CDI operation in order to understand why the level of conductivity drops over the period of time of the experiment. We will also use N_2 adsorption-desorption measurements for the carbon electrodes used in the PZ test to determine any change in the pore structure and FTIR to examine surface group changes. A study of the pH line during CDI operation in these solutions will be used to determine the effect of pH on separation ability. For energy recovery investigations with the dc-dc converter, a second generation device is currently under development which will include higher efficiencies due to better sensing components. This new converter will be initially assembled on a bread board and subsequently tested as a printed circuit board. Integrated CDI cell operation will take place to determine levels of energy recovery beyond 34% (as shown this quarter).

Theme 5 – Oxy-Combustion Research, Development, and Demonstration of Oxy-Firing Combustion

The goals for theme 5 activities are defined as following:

- Accelerate the development and testing of oxy-coal combustion technologies suitable for Chinese coals.
- Establish a working relationship between the leading oxy-coal combustion development institutes in US and China

Subtask 5.1. – Fuel Characterization and Emissions Study Under Oxyfuel Conditions

Approach

The proposed bilateral joint project will study the fundamental and pilot-scale combustion and emission characteristics of indigenous Chinese and US coals of different ranks under oxyfuel conditions.

- Identify Chinese and US coals, one of each, for benchmark comparison of test data.
- Evaluate and exchange test data, including fuel analysis, devolatilization and char oxidation test results from the bench-scale facilities at both HUST and B&W.
- Validate reaction sub-models in the CFD codes (HUST's FURN and B&W's COMO) using the aforementioned experimental data. The model parameters will be reviewed and revised when necessary.

Results and Discussion

Task is complete at this time.

Plans for Upcoming Quarter

Task is complete at this time.

Subtask 5.2. – Pilot-Scale Oxyfuel Combustion Evaluation and Optimization

Approach

Work will create a model for burner design for oxy-combustion conditions, pilot-scale oxy-combustion evaluation and optimization.

- Evaluate designs of B&W's SBS and HUST's FCS. Exchange furnace and setup CFD models for each facility.
- Define a reference burner for both furnace geometries and perform CFD simulations. Compare the simulation results (flame quality, flow patterns, temperature profiles, heat transfer, emissions, etc.) to identify model deficiencies for improvements. Comparison to existing SBS test data will be made when available.
- In the long-term, develop new burner design and test it using indigenous coals for oxy-combustion applications.

Results and Discussion

Task is complete at this time.

Plans for Upcoming Quarter

Task is complete at this time.

Subtask 5.3. – Steady-State and Dynamic Process Modeling Simulations

Approach

Work will setup steady-state and dynamic process models using Aspen and analyze simulation results for the pilot-scale FCS and SBS.

- Set up Aspen steady-state and dynamic simulation models for both facilities on each side.
- Compare the modeling results to identify oxy-specific process modeling issues and resolve any discrepancies.
- Perform preliminary model validation with existing data from previous SBS oxy-combustion test programs.

Results and Discussion

Task is complete at this time.

Plans for Upcoming Quarter

Task is complete at this time.

Subtask 5.4. – Feasibility Study for Large Scale Deployment

Approach

Conduct a commercial-scale engineering feasibility study for an oxyfuel –combustion reference plant.

- Conduct the technical and economic feasibility study of 1 million tons / year CO_2 capture system
- Obtain the capabilities of optimization and engineering design for post-combustion CO_2 capture system.

Results and Discussion

Task is complete at this time.

Plans for Upcoming Quarter

Task is complete at this time.

Subtask 5.5 Evaluate novel staged oxy-combustion concept:

Approach

In this new subtask, the project team will evaluate novel staged oxy-combustion concept by

- Conducting small pilot testing (100-500 kW) under reduced flue gas recycle (increased oxygen concentration) conditions
- Obtaining experimental data set for CFD model validation
- Studying fly ash and deposition characteristics

Results and Discussion

The major project objective is to study pulverized coal combustion in atmospheres of high oxygen concentration (above 50% O_2), in order to simulate conditions in the early stages of the staged combustion process. In these early stages, the stoichiometric ratio is much greater than one. During this quarter, a WUSTL graduate student was able to visit the University of Stuttgart, where he performed experiments to understand the effect of high stoichiometric ratio on fly ash properties and the slagging/fouling behavior. Experiments were conducted in an electrically heated atmospheric pressure combustor at constant wall temperature. The coal was combusted in an O_2/CO_2 mixture at two stoichiometric ratios – 1.2 & 2.3 Ash deposits were collected on an oil-cooled sampling probe and have been prepared for analysis. The ash and deposit samples are currently being investigated, though visually the deposits seem similar at both stoichiometries. Furthermore, thermodynamic calculations using the FACTSage software were performed to predict the ash mineral composition, structure, and slagging point. The slagging tendency was found not to be strongly dependent upon stoichiometric ration in the range of 1.2 - 2.3.

Modifications to the Advanced Coal & Energy Research Facility continued last quarter. These system modifications included the installation of a new coal delivery pipe and the modification/testing of the existing burner to include an oxygen lance for improved flame stabilization. These modifications were found to be necessary in order operate the system at high oxygen concentration and high stoichiometric ratio, and to obtain a flame of suitable length without flame impingement on the furnace walls.

Experimental results from this project were presented at the Clearwater Coal Conferece:

Dhungel, B, Xia F, Kumfer BM, Axelbaum RL. Investigation of oxygen enriched combustion for application to a novel fuel-staged pressurized oxy-combustion (SPOC) process. The 39th International Technical Conference on Clean Coal & Fuel Systems , Clearwater, FL, Jun. 1-5, 2014.

Plans for Upcoming Quarter

Research: The aim for the next quarter is to measure the heat flux profile under combustion conditions that are similar to Stage 2 of the staged oxy-combustion process: 60% O_2 with stoichiometric ratio = approx. 3. These results will be compared against CFD simulations to validate the radiation model.

US-China Collaboration: A delegation from Huazhong University of Science and Technology (HUST) will be visiting WUSTL during the week of July 27. This group, including Dr. Jun Xiang, Professor, Deputy Director of the State Key Laboratory for Coal Combustion, will be giving giving a seminar on various aspects of oxy-combustion. This will be followed by meetings to discuss opportunities and plans for future collaborations. Prof. Axelbaum will attend the US-China CERC meeting in Hangzhou in Sept. and meet with the Chinese oxy-combustion (Task 5) group.

Theme 6 – Sequestration capacity and near-term opportunities

Subtask 6.1. – Saline Formations at the Basin Scale

Approach

The goal of subtask 6.1 is to build the scientific, technological, and engineering framework necessary for safe, permanent storage of large quantities of anthropogenic CO_2 in the sedimentary basins of the Shaanxi Province and the State of Wyoming through 1) determining the distribution of potential sealing formations and appropriate geological structure; 2) assessing the potential storage capacity of major saline aquifers in the Ordos Basin and Wyoming Laramide Basins; 3) constructing a 3-D geological model of the storage domain for selected storage sites; and 4) completing performance assessments for a variety of injection/storage scenarios at targeted sites using numerical simulations.

Working closely with partners at the Shaanxi Provincial Institute of Energy Resources and Chemical Engineering (SPIERCE), Northwest University (NWU), Yanchang Petroleum Company (YPC), and Institute of Rock and Soil Mechanics of Chinese Academy of Sciences (IRSI), the CERC-ACTC team at the University of Wyoming Carbon Management Institute (CMI) continues to collect and analyze the geologic, geophysical, geochemical, petrophysical, and petrographic data available for the Ordos Basin and Wyoming Laramide Basins, apply these data to generate the site specific geological and property models, conduct numerical CO_2 injection simulations, and assess the challenges associated with commercial scale geological CO_2 storage projects.

Results and Discussion

At present, research scientists from CMI, SPIERCE, and NWU are working on the following assignments: 1) reprocess and analyze data regarding the regional geology, structural/stratigraphic framework, and thermal/burial history of the Ordos; 2) update the inventory for the distribution of energy resources in the Ordos Basin, including oil, gas, coal, and other natural resources; 3) delineate potential CO_2 sources and sinks in the Ordos Basin; 4) refine the regional 3-D geological model for the Ordos Basin; and 5) assessing the potential storage capacity of major saline aquifers in the Ordos Basin and Wyoming Laramide Basins. These tasks were carefully outlined in joint meetings with CMI/CERC partners. CMI and its Chinese partners believe accomplishing these five tasks will expedite the establishment of an effective pathway to a better understanding of CCS for both nations.

In this quarter, the research team has made progress in accomplishing the objectives of each of the above tasks. The structural contour maps for the major stratigraphic horizons have been reconstructed based on the newly available public domain data and a 3-D geological structural model is refined. Results suggest that several members in the Yanchang Formation, the Liujiagou Formation, and the Majiagou Limestone are the major potential CO_2 storage reservoirs in the Ordos Basin. The depositional environments, thermal/burial/diagenetic histories of the basin suggest that both of these stratigraphic units have substantial CO_2 storage potential, particularly in the structural unit “Shaanbei Slope” of the Ordos Basin. The reservoir heterogeneities are prominent, both vertically and laterally for all targeted formations. Based on the experience from the WY-CUSP project at the Rock Springs Uplift, Wyoming, these wide ranges of reservoir heterogeneities will have a significant effect on the storage capacity assessment of the targeted storage formations in the Ordos Basin, China.

The UW CMI team attended the CERC-ACTC workshop, which was held at Wuhan, China, in May. At the workshop, CMI presented the research results from both the Wyoming Rock Springs Uplift geological CO_2 storage site characterization project, and the feasibility study of the geological CO_2 storage in the Ordos Basin. Lessons learned and challenges from current CCS projects were exchanged between the USA and Chinese partners. During the workshop, the potential joint demonstration projects were also identified for the CERC-ACTC Phase 2.

Highly productive discussions about information transfer and the design of cooperative projects carried by Wyoming, Shaanxi, and Wuhan IRSM were ongoing this quarter. A major point of these discussions is to improve the understanding of both the Madison Limestone (analog to the Majiagou Limestone in the Ordos Basin), and the Weber Sandstone and Mesaverde Group (analog to the sandstone of the Liujiagou and Yanchang formations). It is apparent that the Lance Formation and Madison Limestone in Wyoming serve as instructive analogs to the Yanchang Formation and Majiagou Limestone in the Ordos Basin. Both CMI and its Chinese partners are enthusiastic about sharing their expertise and experience in characterizing the CCS attributes of the most promising CO_2 storage sites in Wyoming and Shaanxi.

Storage Capacity Assessment of the Majiagou Formation in the Ordos Basin Based on the Volumetric Approach

The geological CO_2 storage capacity of the Majiagou Formation in the Ordos basin is assessed using the USGS volumetric approach. Burrus et al. (2009) presented a method for estimating CO_2 storage capacity, the total known volume (TKV), based on the volume of pore space in a reservoir. The storage capacity in tonnes (STKV) of a reservoir is given by:

$$STKV = Ta \times Ti \times Ntp \times Ø \times Ce \times Cf \times \rho CO_2,$$

where Ta is the trap area [m2]; Ti is the interval thickness of the storage formation

[m]; Ntp is the fraction of Ti occupied by the reservoir interval [decimal fraction]; Ø is the porosity [decimal fraction]; Ce is the storage efficiency factor (the fraction of the pore space that can be occupied by CO_2) [decimal fraction]; Cf is a unit conversion factor (here, Cf = 1); and ρCO_2 is the density of CO_2 [t/m3].

In order to use above equation to calculate the CO_2 storage capacity of the Majiagou Formation, the trap area (Ta) must first be defined. In other words, we must determine the upper and lower depth limit of the targeted reservoir. The pressure and temperature required for CO_2 to be a stable supercritical fluid (31 °C and 7.4 MPa) are typically met at depths greater than 800 m (2600 ft) under a normal hydrostatic pressure gradient. Considering the lower pressure gradient in the basin, and to reduce the chance that the CO_2 would migrate to pressure and temperature conditions where it would change from the supercritical phase to liquid and vapor, a minimum storage depth of 1000 m (3,280 ft) was chosen for these estimates. The minimum storage depth sets the upper depth limit of a potential CO_2 reservoir. The choice of the lower depth limit for CO_2 storage is more arbitrary than that of the upper depth limit. It is based on the conclusion that if the CO_2 pressure at the wellhead is 15 MPa (2,175 psi) and the CO_2 supercritical density is 0.65 g/cm3, the CO_2 pressure will be 41 MPa (6000 psi) at the bottom of a 4000-m-deep (13,120 ft) well. Therefore, CO_2 injected at this depth will displace normally pressured formation water without additional compression. In the present study, 4 km (13,120 ft) is chosen for the maximum storage depth. On the assumption that 25% of the formation thickness is available for storage, the total volume of rock for CO_2 storage $Ta \times Ti \times Ntp$) was determined from the geologic structure model of the Majiagou Formation in the Ordos Basin to be 14,500 km3. A lognormal porosity distribution with a mean of 0.085, a standard deviation of 0.02, and a

skewness of 0.44 was determined from all available Majiagou porosity measured data. For a saline aquifer, the upper limit on the storage efficiency factor *Ce* is related to the irreducible water saturation of the trap with CO_2 present. Values for irreducible water saturation in petroleum reservoirs are not well known, but probably range from a minimum of about 0.2 in gas reservoirs to about 0.6 in oil reservoirs. The results of the CO_2 injection simulation using FEHM show that most CO_2 saturation values range between 0.1 and 0.6. We chose a storage efficiency factor *Ce* for these simulations of 0.1 and 0.6.

A Monte Carlo simulation from Goldsim software with 10,000 realizations using the volume, porosity, and storage parameters described above was set up for the Majiagou Formation between depths of 1000 and 4000 m in the Shaanbei Slope of the Ordos Basin. **Figure 1** shows the probability density of the CO_2 storage capacity of the Majiagou Formation in the Ordos Basin: ranges from 60 to 700 Gt, with a mean of 287 Gt. Currently, there are approximately 410 Mt emitted from 67 large stationary point sources, which emit more than 100,000 tonnes of CO_2 per year in the Ordos Basin. Even with the minimum storage capacity, the Majiagou Formation has sufficient storage capacity to accommodate over 100 years of CO_2 emissions generated by the coal industry in the Ordos Basin.

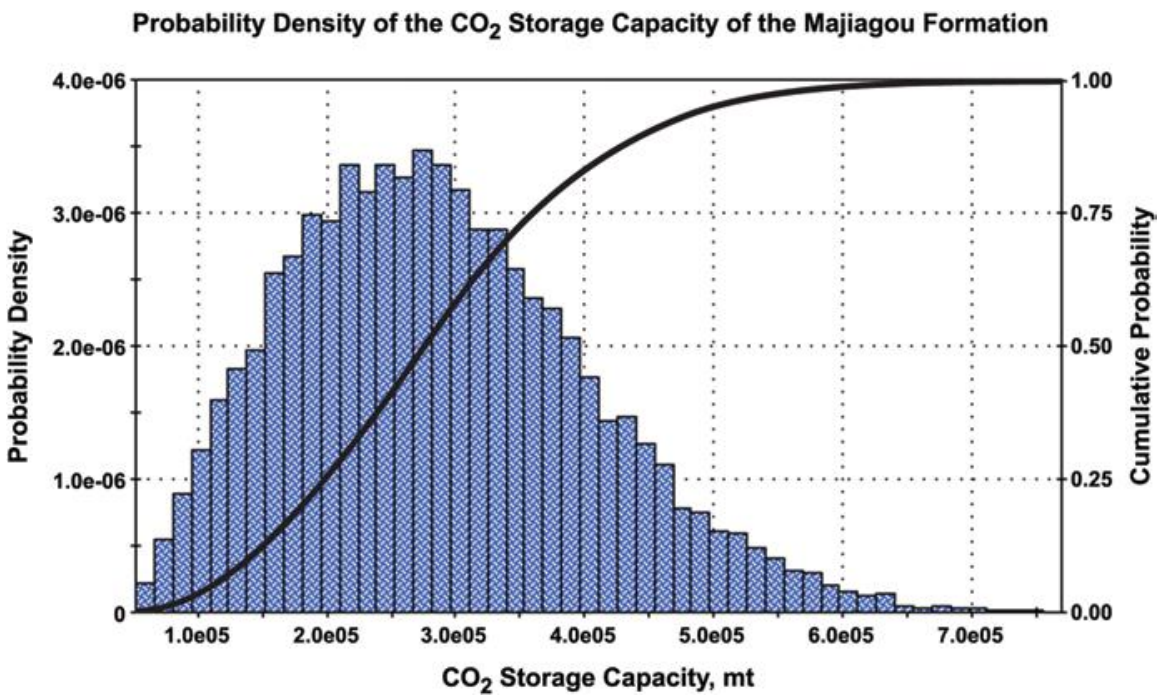

Figure 6.1.1: Probability density of the CO_2 storage capacity in the Majiagou Formation, Ordos Basin. A cumulative probability of 25% yields a value of 200 Gt; this indicates that for this particular distribution, we have a 25% chance of storing 200 Gt of CO_2 or less. In other words, this indicates that we have a 75% chance of storing at least 200 Gt CO_2 in the Majiagou Formation in the Ordos Basin.

In addition, the WVU team has registered domain names to use for a CO2 storage resource viewer for China and the US modeled on NatCarb viewer (http://www.natcarbviewer.org/beta/). The following domain names were registered for a US-China viewer – www.usccerc.com, .net, and .org. We have located a number of national GIS layers for China (CO2 Sources, pipelines, basins, etc.), and these national layers will be integrated with regional geodatabases from Ordos, Shanxi, Tainjin on saline, oil&gas and coal.

Plans for Upcoming Quarter

1) Update inventory results of the distribution of major stationary anthropogenic CO_2 emission sources, including the volumes of captured/vented CO_2.
2) Assemble the reservoir property data for the targeted geological CO_2 storage reservoirs in the Ordos Basin.
3) Select the storage site for a detailed geological structure and property modeling.
4) Analyze the results from the CERC-ACTC phase I studies.

Subtask 6.2: Geologic storage and EOR

Approach

The goal of Subtask 6.2 is to build the scientific, technological, and engineering framework necessary for CO_2 utilization via enhanced oil recovery (EOR) in conjunction with safe, permanent storage of large quantities of anthropogenic CO_2 in the Ordos Basin. The subtask goals will be achieved by accomplishing the following tasks:

- Evaluating the geological characteristics of potential CO_2-EOR reservoirs in the Shaanbei Slope, Ordos Basin;
- Comparing the Ordos reservoir characteristics of mutual oil fields with Wyoming CO_2-EOR fields;
- Constructing detailed 3-D geological models of the targeted oil fields;
- Numerically simulating CO_2-EOR performance for a variety of EOR scenarios at the selected depleted oil fields;
- Evaluating the feasibility of combining CO_2-EOR with CO_2 storage; and
- Planning a CO_2-EOR demonstration project for one selected reservoir in the Ordos Basin.

The University of Wyoming Carbon Management Institute (CMI) team will work closely with researchers from Shaanxi Provincial Institute of Energy Resources and Chemical Engineering (SPIERCE) and Yanchang Oil Company (YOC) to develop an integrated energy/environmental expansion strategy for the energy rich basins such as the Ordos Basin and Wyoming Laramide basins. This integrated energy/environmental expansion strategy will include co-exploration, development of oil, gas, and coal resources, petrochemical and coal chemical industry, water resource management, CO_2 emission control, CO_2 utilization, and geological CO_2 stage.

In this quarter, the University of Wyoming Carbon Management Institute (CMI) team has worked closely with researchers from the Shaanxi Provincial Institute of Energy Resources and Chemical Engineering (SPIERCE) and the Yanchang Oil Company (YOC) to evaluate the geological, petrophysical, petrographic, and petroleum-engineering data available for the EOR/storage project.

Results and discussion

At present, CMI is assisting both YPC and SPIERCE in screening and prioritizing mature oil fields in the Ordos Basin with respect to their potential for using CO_2-flooding techniques. The Wyoming CMI team, working with Chinese partners (YPC and SPIERCE) has developed an assessment strategy, including screening criteria for the Ordos Basin oil fields. CMI is assisting YPC to select one depleted oil field for CO_2-EOR demonstration in the Ordos Basin. The fields under consideration typically are located less than 200 km from major anthropogenic sources of CO_2, such as YPC's Jingbian and Yulin petro/coal chemical industry parks, that presently

capture and vent 5 Mt of CO_2 (> 95% pure) annually (**Figure 6.2.1**). The CO_2 capture facility of 50,000 tonnes has been installed in the Yuheng methanol plant. A 340,000 tonnes capture facility in the Jingbian Petro/Coal Chemical Industry Park is currently under construction and will be completed in the fourth quarter of this year. The capture facility with the coal-to-chemical plant will secure the CO_2 source for the CO_2-EOR demonstration project in the Ordos Basin.

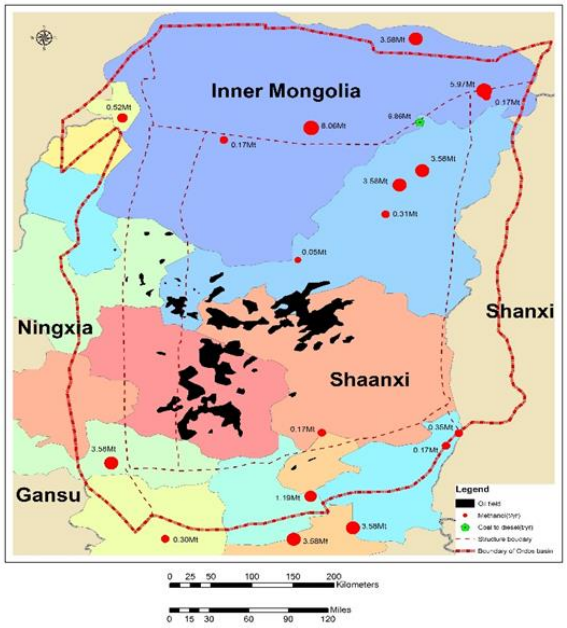

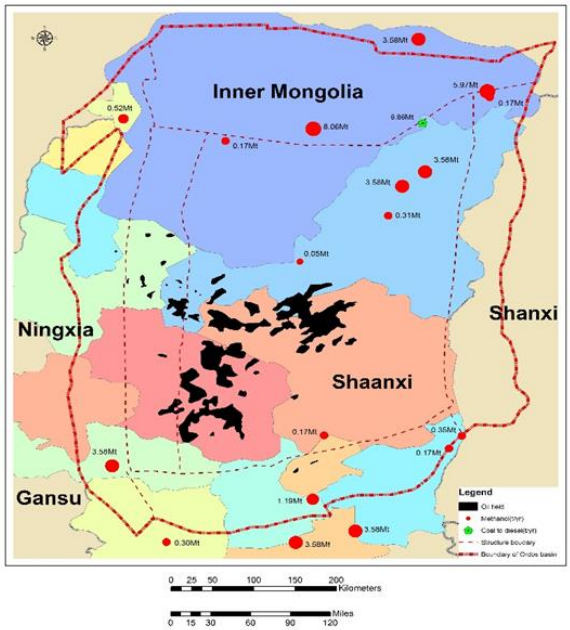

Figure 6.2.1. Map of the Ordos Basin showing geospatial districts, location of gas and oil accumulations, and location of stationary CO_2 emission sources. The total annual CO_2 emissions in the Ordos Basin are approximately 410 Mt.

CMI, YPC, and SPIERCE have agreed to share the information required to screen, characterize, model, design, and implement an enhanced oil recovery and CO_2 storage demonstration project on the Shaanbei Slope in the Ordos Basin. CMI and YPC have prepared a cooperative agreement to achieve Subtask 6.2 objectives. Work plans for years four and five of Subtask 6.2 have been finalized with CMI's Chinese partners and submitted to the CERC-ACT manager.

CMI, YPC, and SPIERCE are collaborating on the investigation of the geologic resources, energy resources, and CO_2 sources and sinks in the Ordos Basin. In addition, the researches study how U.S. EOR experiences and expertise can be applied to depleted oil reservoirs in the Ordos Basin.

An Integrated Energy/CCUS Development Strategy for the Energy Rich Basins

The Carbon Management Institute at the University of Wyoming has outlined an integrated energy/CCUS development strategy to systematically and concurrently develop the coal mining and coal conversion industries, coalbed methane (CBM) production, CO_2 enhanced oil recovery, and CO_2 storage in the Powder River Basin,

Wyoming (**Figure 6.2.2**). The Ordos Basin geologic setting and energy resources profile are very similar to those of the Powder River Basin. The concurrent development of new coal conversion industries and oil-and-gas industries in the Ordos Basin offers the opportunity for applying the integrated strategy developed in Wyoming: the integration of geologic CO_2 storage, and CO_2-EOR. The coal conversion industries (coal to methanol, coal to olefins, etc.) provide affordable, capture-ready CO_2 sources for large-scale CO_2-EOR and storage projects in the Ordos Basin. The ability to use CO_2 emitted by the coal-conversion industries for CO_2-EOR and geologic CO_2 storage will make these projects in the Ordos Basin cost-effective and technologically efficient.

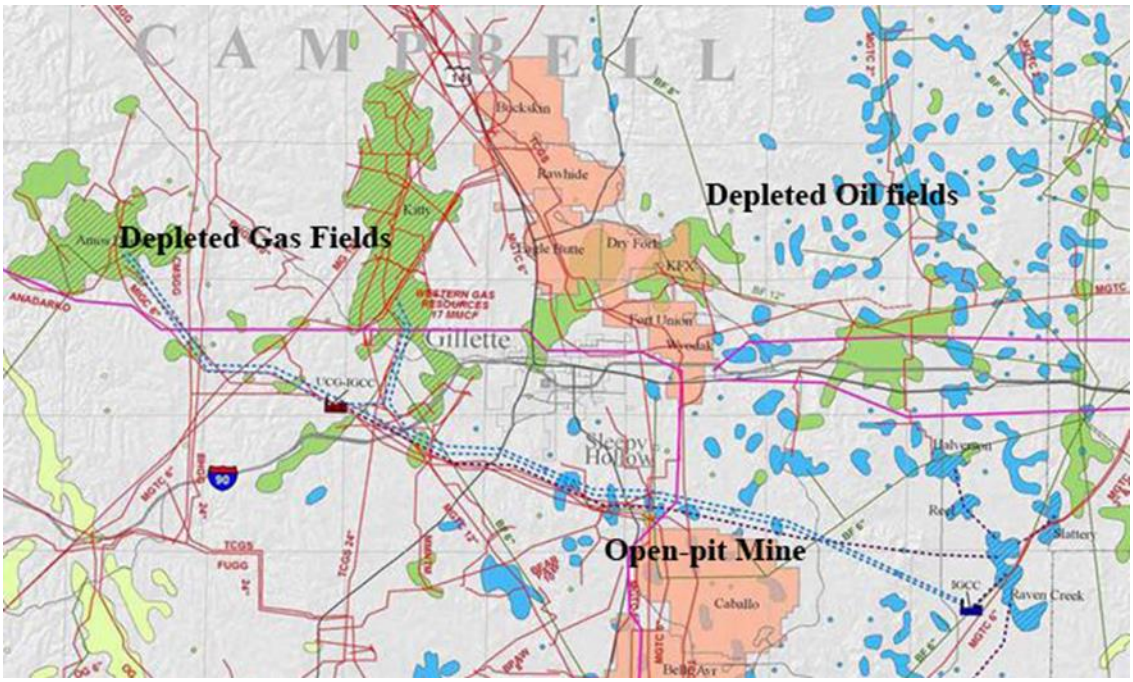

Figure 6.2.2. Map showing the distribution of open-pit mines, depleted gas fields, and depleted oil fields near the Gillette, Powder River Basin, Wyoming.

An integrated energy development strategy has been developed for the Shaanbei National Energy Base. This integrated energy development strategy aims to synchronously, synergistically develop coal mining, the coal conversion industry, coalbed methane production (CBM), CO_2 enhanced oil recovery, and CO_2 storage in the Shaanbei National Energy Base. First, coal mining would continue using existing extractive technology or improved technology. Second, the new coal-to-chemicals facilities would be located as close to the coal mines as possible. In the Ordos Basin, recently constructed coal-to- chemicals plants are sited over underground coal mines (Shenmu Jinjie Industry Park and Yanchang Jinbian Industry Park). Third, coalbed-methane produced water would best support these coal conversion facilities. The volume of water required to supply the plants will vary. In the Ordos Basin, coal-to-methanol plant design is based on a 6:1 ratio of water to product. A 0.6-Mt methanol plant in the Ordos Basin annually uses 1.8 Mt of coal and 6.0 Mt of water, and emits 4.0 Mt of CO_2. A 7-million-barrels-per-year diesel plant annually uses 3.5 Mt of coal and approximately 56 Mt of water, and emits 2 Mt of CO_2. At present, the coal conversion industry in the Ordos Basin would generate 9.24 Mt of methanol and 0.78 Mt of diesel annually, and would emit 50.88 Mt of CO_2 in total. This readily captured, highly concentrated CO_2 would be stored in the adjacent depleted oil and gas fields or saline aquifers, such as Majiagou reservoirs, which have a tremendous CO_2 storage capacity.

Furthermore, Liao et al. (2012) have assessed the CO_2 storage capacities of 14 depleted oil fields in the Ordos Basin at 100 Mt. These depleted oil fields are ideal 1) for storage of CO_2 emitted by coal conversion facilities and 2) as sources of CO_2 for EOR projects in adjacent depleted Yanchang reservoirs. More than 40 mature Yanchang oil fields with EOR potential are located near coal mining/conversion resource confluences, and are eligible for tertiary recovery via CO_2 flooding. Many have gone through the secondary recovery water flooding stage and appear ideal for CO_2 miscible flooding. These Yanchang oil fields together contained 2 Gt of original oil in place (OOIP) (Wang et al. 2007). Typically, CO_2 flooding could recover at least 10% additional production in the Yanchang oil fields, 200 Mt of oil. Recovering the stranded oil via CO_2 flooding would require 700 Mt of CO_2 (3.5 t per tonne of incremental oil recovered). For a 30-year EOR project, about 23 Mt of CO_2 would be required annually. Current coal conversion facilities envisioned 50.88 Mt of CO_2 emitted annually could more than adequately support theses EOR activities. A conservative estimate suggests that the CO_2 would be worth $40/t, or US$28 billion. Therefore, the CO_2 typically regarded as a problem with respect to sequestration would be worth approximately US$28 billion in this scenario. Moreover, the Yanchang reservoirs from which the stranded oil is recovered could be converted to permanent storage sites for CO_2, doubling the CO_2 storage capacity available to the coal conversion facilities.

Plans for the upcoming quarter

In the upcoming quarter, scientists from SPIERCE—in cooperation with CMI—will continue to make improvements in the Ordos Basin and selected CO2 EOR field database. The process and analyses of valuable sources of information regarding Ordos Basin geology, CO2 availability, and enhanced hydrocarbon production will be continued. The petrographic observation of the targeted reservoirs (i.e., Yanchang Formation and Majiagou formation) will be conducted with the samples collected from the Ordos Basin. CMI personnel will visit SPIERCE, NWU, and YPC in the later summer of 2014 to continue the inventory, selection, characterization, and performance assessments for the targeted CO2-EOR reservoirs.

The University of Wyoming Carbon Management Institute (CMI) team will work closely with researchers from SPIERCE and YPC to improve integrated energy/environmental strategy for the energy rich basins such as the Ordos Basin and Wyoming Laramide basins. The detailed 3-D

geological models of the targeted oil fields is refined with more available data; Numerically simulating CO2-EOR performance for a variety of EOR scenarios at the selected depleted oil field will be carried out.

Subtask 6.3. – Geological Storage and Enhanced Coal-Bed Methane (ECBM) Recovery

Approach

Results and Discussion

No input.

Plans for Upcoming Quarter

No input.

Subtask 6.4.a – Simulation and Modeling - LLNL

Approach

Under the simulation task, advanced subsurface modeling tools and approaches are being applied to CO_2 storage projects in the U.S. and China and new simulation approaches and tools are being developed to address the issue of parameter uncertainty. Modeling tools are being used to assess a number of key performance questions as well as to provide quantitative insights that feed into risk characterization, including:

- Quantification of injection mass fluxes and pressures
- Mapping of potential fluid pressure and CO_2 saturation distributions throughout the target reservoir
- CO_2 storage capacity
- Evaluation of leakage pathways for injected CO_2
- Assessment of effective stress on nearby faults
- Gauging the induced seismicity potential
- Quantifying CCS efficacy when used in conjunction with enhanced oil recovery

U.S. and Chinese scientist involved in the subsurface simulation task met in Wuhan, China in March 2012 to develop a detailed work plan and schedule over deliverables over the next year of the project. These are summarized in a set of ten-point plans, to be submitted separately to DOE. In summary, the overarching goals of the simulation task are to develop templates and protocols for demonstration project evaluation, model development, and larger scale injection predictions; assemble a catalog of models and techniques and apply to site data sets, as warranted; compare results and summarize general findings; understand similarities and differences of CCS and CCUS risk assessment methods, needs, and goals between the U.S. and Chinese teams; identify key sites and specific hazards (including economic issues); develop abstractions of subsurface simulations to inform risk calculations; and calculate risk profiles for selected projects and use demonstration scale data to predict larger scale system behavior. These goals are to be addressed using sites in both the U.S. in China as example application, including:

- Ordos Basin, China: saline aquifer geologic storage in Paleozoic units
- Wyoming, USA: saline aquifer geologic storage in the Madison and/or Weber Formations

- Illinois Basin, USA: Saline aquifer geologic storage in the Wabash Valley in the Mount Simon Formation. Of particular interest to the simulation task is the planned injection of CO_2 at the Gibson-3 coal-fired power plant unit in Indiana, where a partnership between Duke Energy and China Huaneng Group to collaborate on CO_2 capture is in place. The simulation task will focus particular effort on this site, since clear synergies exist between the CO_2 capture and storage efforts (e.g., determining the optimal CO_2 flux for capture and subsequent storage) and the interests of the Chinese and U.S. partners directly converge.

Results and Discussion

No Activity This Quarter

Plans for Upcoming Quarter

No Input

Subtask 6.4.b – Simulation and Modeling - LANL

Approach

LANL is tasked with leading efforts into risk analysis for subsurface carbon storage. The risk component of the CERC work relies heavily on input from both characterization (original Project Task 1, new Themes 6.1) and simulation (original Project Task 2, new Theme 6.4). The original work plan for risk (Project Task 3) was written in a way that included multiple aspects of risk. Two primary risk components include subsurface risks for individual injection sites (Pawar et al., 2013) and risks associated with regional systems of multiple sources of CO_2 connected to multiple subsurface sinks (Keating et al., 2011a,b). Economic concerns were included in both components. Target sites for analysis of subsurface risk were chosen in each country including the Rock Springs Uplift (RSU) in Wyoming, the Ordos Basin in China, and the Gibson injection site in southern Indiana. Although LANL is leading the risk effort, researchers at LLNL (Lawrence Livermore National Laboratory), UWY (University of Wyoming), and LANL are working together to produce the large number of related simulations needed to answer questions covering both subsurface and total storage system performance and risk for the chosen sites and their regions.

Subsurface Injection Site Performance and Risk

Methods for calculating CO_2 subsurface storage site performance and leakage risks are currently being developed by several teams around the world (Stauffer et al., 2009a; Oldenburg et al., 2009; Pawar et al., 2013; Stauffer et al., 2013). The state of the art in such modeling involves gathering detailed site specific data that are then used to create numerical models of plume injection and migration including time dependent pressure and saturation predictions. The plume estimates are next used to calculate potential leakage through wellbores, faults, and overlying caprock (Viswanathan et al., 2008). Finally, impacts are calculated on receptors such as drinking water aquifers or releases to the atmosphere that could change near surface concentrations of CO_2. A final step in a risk analysis is to assign consequence values to impacts so that a true risk value can be calculated as risk = probability*consequence. Currently all CERC work is focused on understanding the interplay between probabilities of events, how uncertainties in these events can be reduced through either data collection or engineering, and finally how costs relate to this interplay.

The reservoir simulations supporting the CERC risk work are being run using both the LANL developed porous flow software, FEHM (Zyvoloski 2007; Deng et al., 2012), and the LLNL developed simulator, NUFT. A second component of subsurface risk, seismic potential, is being explored using the same numerical meshes but with the fully coupled stress/flow capabilities of FEHM and through a hybrid stress code coupled to NUFT. Finally, economic considerations including costs associated with brine treatment (as part of a comprehensive reservoir pressure management scheme) are included as part of each individual storage site performance assessment (Sullivan et al. 2012a,b; Surdam et al., 2009; Surdam et al., 2011).

Regional Scale Source to Sink Performance and Risk

Methods employed in a comprehensive regional storage analysis include coupling impacts related to the reality of multiple sources linked to multiple possible sinks including all relevant sources of uncertainty (Middleton et al., 2012a). Such regional studies allow intelligent development of both capture systems and storage sites based on evolving CO_2 capture goals. Algorithms developed at LANL over the past several years are being driven by detailed data on CO_2 sources, surface features (mountains, rivers, cities tec.), and estimates of both storage capacity and injectivity for specific reservoirs (Middleton et al., 2012b). We are using the approaches developed in our previous work with new modifications to tackle ECBM/Shale Gas/ EOR/Saline CO_2 storage questions associated with the Gibson/southern Indiana region and plan to teach/demonstrate the same techniques to our collaborators from the Chinese Academy of Science and Northwestern University.

Results and Discussion

B.1 Quarterly Task 1 Results

Quarterly Task 1 involves collaboration between LANL and the Indiana Geological Survey (IGS) to create a system model for CCUS around Duke Energy's Gibson power plant in southern Indiana. A set of 15 nodes within an 80 km circle around Gibson were chosen. These 15 nodes represent a range of both shallow resources (ECBM, EOR, and shale gas) and deeper saline formations (St. Peter, Knox, and Mount Simon). IGS has extended their earlier characterization work in the Gibson area (Ellett et al., 2013) and completed regional-scale analysis of saline formations and utilization components including ECBM, Shale gas, and EOR. Figures below show the 15 nodes, resources, and analysis of the saline formations. Following the data are results from a presentation made to Duke Energy in June of 2014.

St Peter reservoir (a) top structure, (b) thickness (note Mount Simon max is 10X larger and Knox Group max is 30X larger), and (c) background storage resource model (note porosity meter scale is order of magnitude less than MTSMN or KNOX)

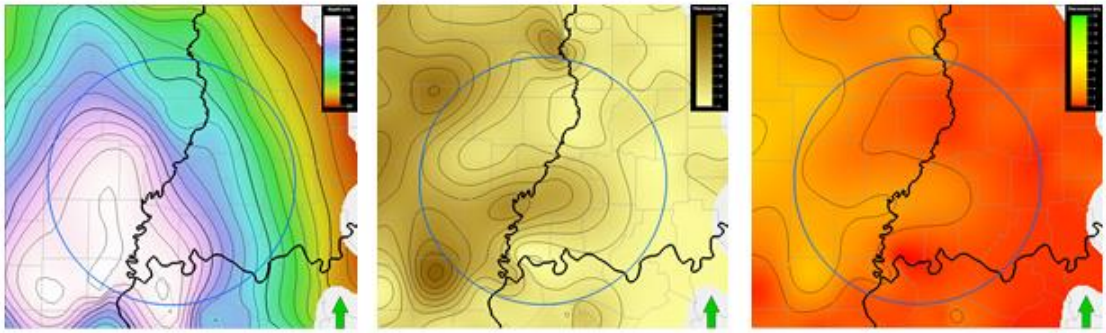

Figure 6.4B.1-1 St. Peter saline storage analysis in the Gibson region

Porosity-permeability transform equations

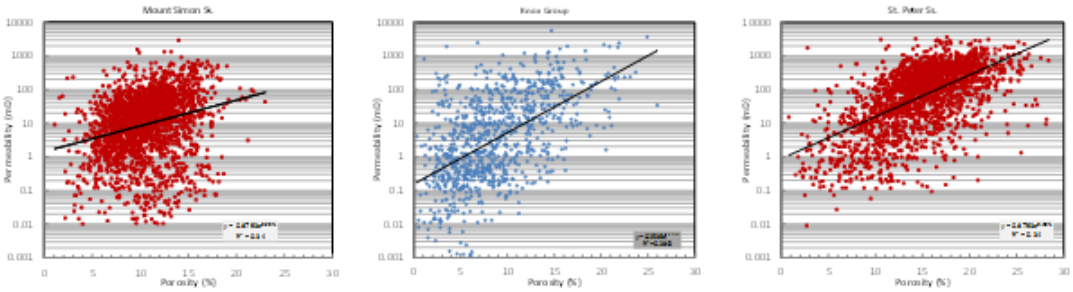

Figure 6.4B.1-2 Porosity-permeability data for the saline formations of interest

Selection of nodal locations for integrated system modeling with stacked reservoirs/utilization resources (saline formations, EOR, ECBM, EGR)

Node	location	utmX	utmY	SF-MTSMN	SF-KNOX	SF-STPTR	EOR/O&G	ECBM/UC	EGR/NAS
1	On site at Gibson Station	433093	4247026	10	6	26	10	0.4	
2	Clay, IL	384900	4276700	13	6	26	109	1	
3	Tri County	454500	4306500	9	8	54	2	0.2	
4	Lawrence, IL	435800	4283800	10	7	45	48	1	
5	Crawford, IL	432700	4310500	9	8	37	64	0.5	
6	White, IL	410400	4225000	12	5	23	51	1	
7	Pike, IN	463000	4258500	9	7	35	15		
8	Knox, IN	473500	4298500	8	7	43			16
9	Sullivan, IN	460600	4318900	8	8	45		0.25	12
10	Clay-Sailor, IL	378900	4295500	12	6	23	18	1	
11	Wabash, IL	422600	4248700	11	6	26	43	1	
12	Hamilton, IL	365800	4209500	18	5	21	28	0.4	
13	Posey, IN	418500	4214000	11	5	32	3	0.5	
14	Henderson, KY	440600	4168800	13	5	45	12	0.25	
15	Davies, KY	476600	4182500	12	5	51	2		

Color codes: relative resource level– high resource med resource low resource

SF number is the estimated radius of idealized CO2 plume (km) for 90 million tonne injection using P_{50} estimate of storage resource (tonnes/km^2)

EOR/O&G number is low range estimate of EOR (million stb) for fields in vicinity of node (<5 km). Note that this is larger than the hard dip radius value in Ellett et al., 2013, CERC-JM poster

ECBM/UC number is low range estimate of ECBM (million scf/acre) for unmineable coals in vicinity of node

EGR/NAS number is estimate of gas production (Bcf) assuming huff-n-puff scenario from Liu et al. (260 MMscf cum production and 40 MMscf CO2 storage) with existing NAS horizontal wells in Knox and Sullivan fields

Figure 6.4B.1-3 15 nodes located within an 80 km radius of Gibson showing relative saline storage and utilization potential calculated from static geological models.

Map showing selection of nodal locations for system modeling (red stars with 5km radius) along with estimated EOR potential of oil fields and existing horizontal well infrastructure in the New Albany Shale play (blue circles)

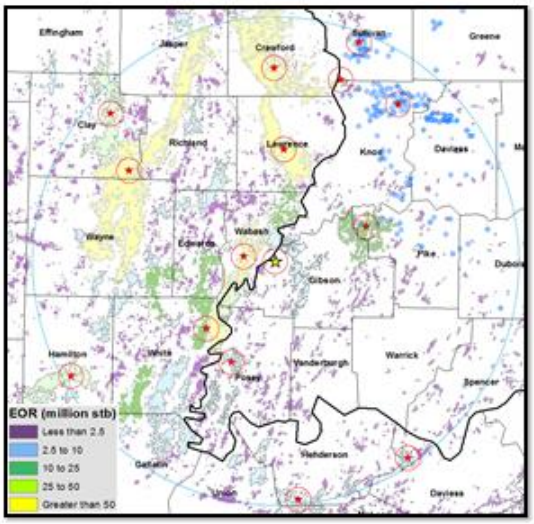

Figure 6.4B.1-4 Map view of the 15 nodes located within an 80 km radius of Gibson.

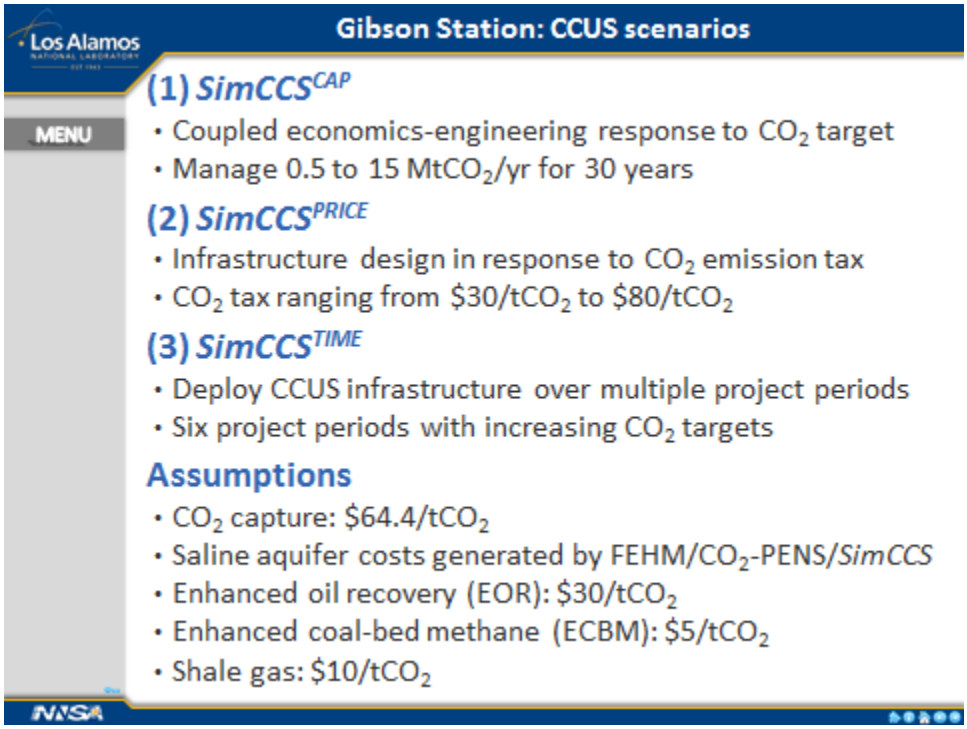

Figure 6.4B.1-5 CCUS scenarios presented to Duke Energy

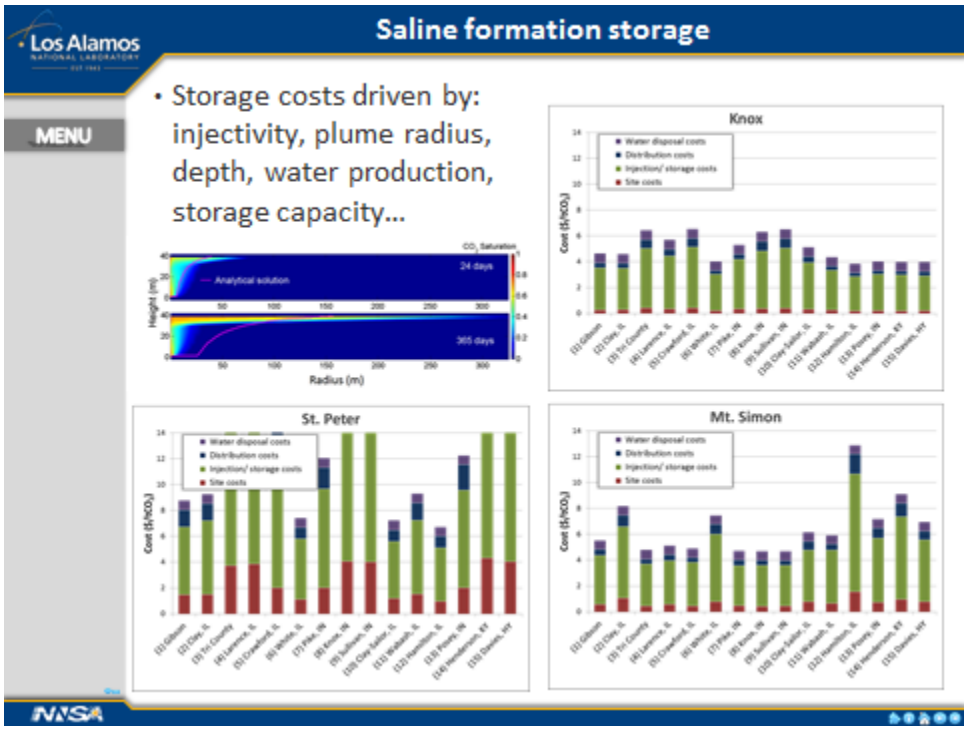

Figure 6.4B.1-6 Distribution of costs for each reservoir for each of the 15 locations.

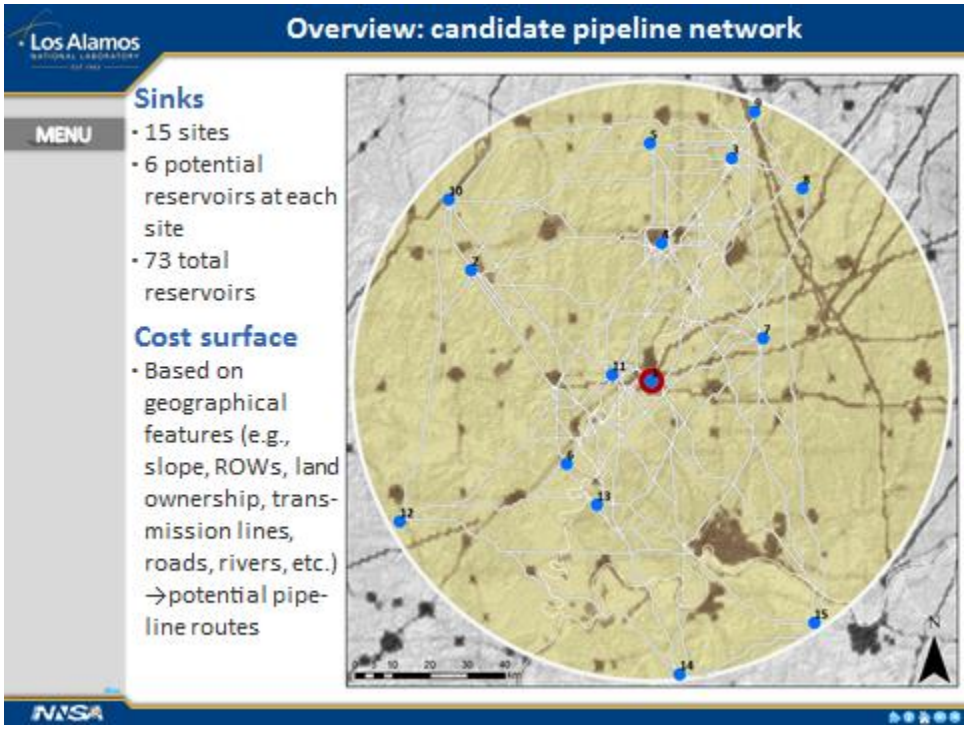

Figure 6.4B.1-7 Candidate pipeline networks for the Gibson area linking the power plant at the center to the 15 potential sinks within 80 km.

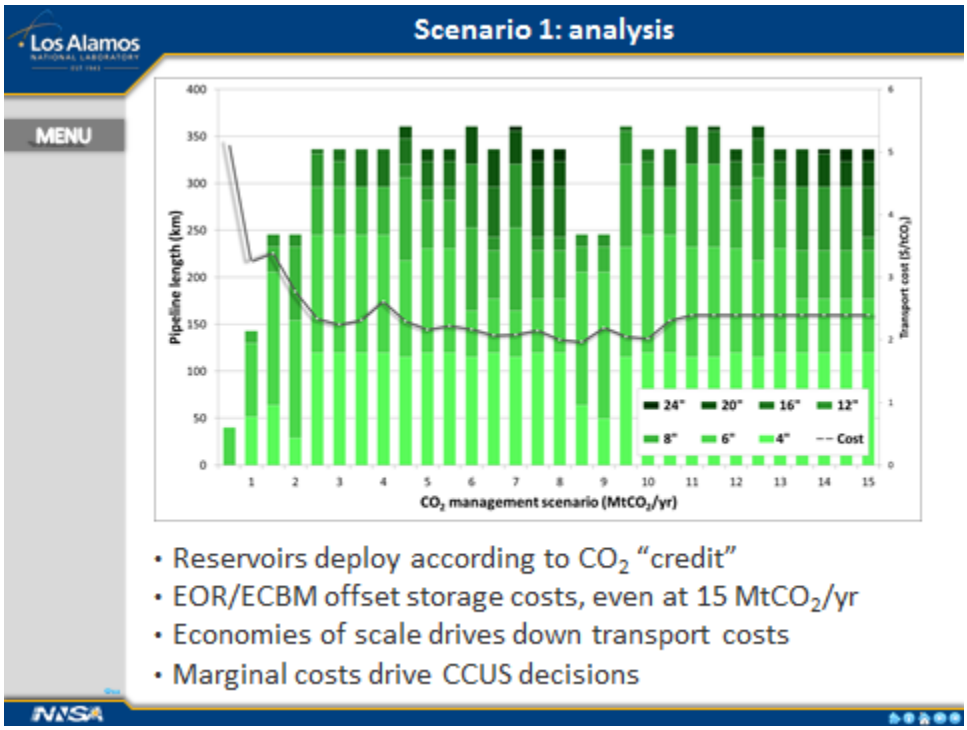

Figure 6.4B.1-8 Analysis of pipeline costs and lengths for different capture scenarios (1-15 MT/yr).

Summary of accomplishments

This quarter, LANL and IGS have worked closely together on two CERC projects:

1) Quarterly Task 1 involves collaboration between LANL and the Indiana Geological Survey (IGS) to create a system model for CCUS around Duke Energy's Gibson power plant in southern Indiana. IGS and LANL have had many telecons and data exchanges related to planning the simulation effort. Particularly, a set of 15 nodes within an 80 km circle around Gibson were chosen. These 15 nodes represent a range of both shallow utilization and storage resources (EOR and storage in oil and gas reservoirs, ECBM and storage in unmineable coal seams, and EGR and storage in the New Albany Shale) and deeper storage resources in saline formations (St. Peter Sandstone, Knox Group dolomites and Mount Simon Sandstone). IGS has completed regional-scale characterization of the saline formations and has calculated estimates of CO2 utilization resources (EOR, ECBM and EGR) from static geological models in the region around Duke Energy's Gibson Station.

John Rupp, Kevin Elliot, and Richard Middleton met with Duke Energy in late June 2014 to present the results of this study. Duke has requested a report summarizing the work. The feeling from the meeting is that there is some interest in the system analysis approach but that more communication between Duke and CERC will lead to a better product. Results of this work are presented in Section B.1.

2) Quarterly Task 2 involved planning and execution of a workshop in Wuhan with our Theme 6 Chinese collaborators from both the Chinese Academy of Sciences and the Northwest University. At this meeting we brought together the Ordos Basin characterization efforts of two Chinese teams (Northwest University and CAS) through an example of characterization and simulation for the Gibson region of the Illinois basin (Quarterly Task 1 above). A major outcome of this meeting was the realization that there are three distinct Ordos basin models that need to be brought into a common model space. It was agreed that Zhou Lifa and John Jiao would oversee data quality for the effort. CAS agreed to work with Lifa to incorporate public domain data into a PETREL model for the Ordos basin.

The workshop in Wuhan was also very important in planning the last 1.5 years of the project including tight collaboration between the international teams. The Chinese are very interested in LANLs coupled system modeling of CO2 injection with brine production tied to resource utilization. Additionally, the Chinese side shared plans for a second 5 year collaboration (CERC 2.0) and we worked together to ensure that their proposals include strong links to capabilities and interests on the US side.

CERC-ACTC Theme 6 at the Three Gorges Dam. Workshop attendees from the US include: Jeff Wagoner (LLNL), John Rupp and Kevin Elliot (IGS), Phil Stauffer and Richard Middleton (LANL), and Sarah Forbes (WRI). Bai Bing and Wei Ning (CAS) hosted this team building trip.

3) Quarterly Task 3 is a new CERC task to address a prefeasibility study at the Tianjin GreenGen power plant. Huaneng Power has asked CERC to generate this study to explore the possibility of using CO2 to extract brackish water for industrial, heating, or agricultural uses. LANL helped write the proposal for this work in late June 2014. The proposal is included in Section B.2.

4) Quarterly Task 4 is the creation of a presentation for the high visibility DOE CCUS conference in Pittsburgh. This truly collaborative effort involves Theme 6 researchers from the US and China. Sarah Forbes presented this work titled:

Linking CO2 Sources, Sinks, and Infrastructure for the Ordos Basin, China. Sarah Forbes4, Philip Stauffer1 Richard Middleton1 Bai Bing2 Kevin Ellett3 John Rupp3 LiXiaochun2 1Los Alamos National Laboratory 2Chinese Academy of Sciences 3Indiana Geological Survey 4World Resources Institute

5) Quarterly Task 5 is another high visibility presentation given at the DOE CCUS conference in Pittsburgh.(May 2014). This presentation builds on analysis into using high value chemical production streams as a relatively low percentage cost CO2 source for a large scale demonstration of CCUS in the US. Many of the economics of the system will translate to China where coal to liquids plants could prove extremely useful in generating CO2 for large scale demonstrations of CCUS.

The Price must be Right: a new pathway to jumpstarting CCUS. Richard Middleton, Jonathan Levine, Jeff Bielicki, Philip Stauffer.

Plans for Upcoming Quarter

Theme 6 plans for the future are ambitious and will depend on sufficient funding being made available to the participants by the CERC. This would to allow both LANL and IGS to expand the initial collaborations with both Duke Energy and the Chinese Academy of Sciences in

Wuhan. Similarly, the Carbon Management Institute at the University of Wyoming will be moving to a more advanced stage of simulation and modeling including EOR simulations covering parts of the Ordos Basin that could be made more valuable by enhanced funding. Expanded collaboration will require more intensive data analysis and increasingly complex numerical simulations. Ideally, Theme 6 will have enough resources to create more detailed and accurate simulations of geological sequestration that would include incorporating reservoir heterogeneities and site specific structures for both the Ordos and Illinois basins. Additional simulations would also include conceptualizing "carbon utilization" strategies such as advanced EOR and shale gas simulations which would leverage faculty at the Indiana Geological Survey, Indiana University and University of Wyoming.

1) The team will continue work on the Gibson region in collaboration with the Indiana Geological Survey and LLNL. An interesting discussion from this collaboration concerns the use of enhanced coal bed methane and/or deep shale as potential sinks for CO_2 in the southern Indiana region. Even preliminary work in this area would greatly assist in the development of Theme 6.3 (ECBM). At the beginning of July, 2013, IGS provided LANL with data on the New Albany Shale, a development that improves our changes of incorporating shale gas production coupled to CO_2 storage into our techno-economic analysis of the Gibson area. We will continue to work with Duke to generate a detailed report of the presentation materials.

2) LANL will work during the upcoming quarter to generate preliminary analysis of Enhanced Water Recovery at the Huaneng GreenGen site. This work has excellent ties into the possible CERC2.0 through the utilization component as well as through the focus on younger rocks in the Bohai basin.

3) LANL will work with the University of Wyoming (J. Jaio) to set up simulations of CO_2 injection related to sites in the Ordos Basin. The work will begin with CO_2/brine but migrate to inclusion of an oil phase toward the end of Q4 or the beginning of FY15. Development of the oil phase in FEHM is not being paid for by CERC and we thus do not control the schedule of oil phase completion in the code. The oil phase simulations in FEHM may not be ready until FY15. In the interim, we have been using commercial codes to generate results for EOR fields (Quarterly Task 2 Q3FY13). These results are being extracted and built into a reduced order model for risk analysis.

4) LANL plans to write papers summarizing the results of the US China collaboration on the Ordos Basin geological sequestration assessment for both the GHGT-12 meeting and a future journal submission. At GHGT-12 we will present a paper on the Ordos Basin system modeling.

<u>Subtask 6.5. – International Standards for Geologic Storage (ISO TC265)</u>

Approach

WRI is engaged as a liaison to the development of international standards for CCS (ISO TC265). Sarah Forbes is also a member of the US Technical Advisory Group (US TAG) and has been appointed to Workging Group 5 (WG5), Cross Cutting Issues. The ISO TC 265 is chaired by

Canada with China as the mirror chair.

Results and Discussion

- A proposal for a technical report addressing the overall risks associated with CCS projects has been co-developed by Li Xiaochun (CAS-WHRSM) and Sarah Forbes (WRI). During this quarter, the proposal was formally submitted to WG5 and then to the the ISO TC265 Secretariat. Following approval, the proposal will be voted on by the entire TC265. Initial discussions with the US National Risk Assessment Program (NRAP) manager regarding the issue were held in May 2014.

Plans for Upcoming Quarter

- The next ISO TC265 meeting has been scheduled for January 2015 in Birmingham, Alabama.

Subtask 6.6. – Pre-feasibility Study for Active Aquifer Management

Approach

Quarterly Task 3 is a new CERC task to address a prefeasibility study at the Tianjin GreenGen powerplant. Huaneng Power has asked CERC to generate this study to explore the possibility of using CO2 to extract brackish water for industrial, heating, or agricultural uses. LANL helped write the following proposal for this work in late June 2014.

Project Proposal: Pre-feasibility Study to identify opportunities for increasing CO_2 storage in deep,

saline aquifers by active aquifer management and treatment of produced water

Participants: CERC/ACTC

Project term: 1 July14 to 31 Aug 14

Injection of CO_2 into the subsurface creates high pressure regions around injection wells. Storage capacity is partly controlled by pressure buildup in the area around the injection wells. Pressure build-up is generally not permitted to rise above hydrofracture pressure to ensure the integrity of the sealing rocks. Pressure build-up is a function of injection rate, fluid properties, rock porosity, rock permeability to both water and CO_2, and the connectivity of permeability at the kilometer scale.

There are two options for management of pressures within the target reservoir: passive and active. Under passive management, CO_2 displaces groundwater (brine) and the resulting plume moves in response to uncontrolled pressure gradients in the reservoir rock. In active management, brine is withdrawn (produced). Brine production serves two primary purposes. First, brine production provides pressure relief and allows CO_2 to flow toward the lower pressures regions. Second, brine production opens pore volume for CO_2 migration, thus increasing the storage capacity of the reservoir. Active management can also be used to create preferential zones for CO_2 migration and can help to control the CO_2 distribution throughout the reservoir.

In active management, produced brines are brought to the surface and treated to supplement agricultural, human use, or industrial process water. Significant volumes of treated water may be made available. For example, Huaneng's Tianjin IGCC power project captures 100,000 t

CO_2/year which could displace 125,000 m^3 of groundwater (238 L/min). Treatment of brines to industrial, agricultural, or human use standards is well understood, though the optimal treatment train for a specific brine and its associated cost should be based on the logistics and chemistry of a specific saline aquifer. Another important factor in the system level cost calculations is to include the use and disposal of treatment byproducts (e.g., salt cakes, brine concentrates, thermal energy, and mineral resources). Members of our team have done preliminary work on the cost/benefit analysis for low temperature geothermal energy extraction coupled with aqueous phase Lithium mining and CO_2 injection (Figure 01). By keeping track of all costs and returns, total project profit/loss parameters can be better estimated.

Huaneng's Tianjin CCS Project

Huaneng is operating an IGCC unit near Tianjin PRC that is currently capturing about 100,000 t of CO_2 per year. Huaneng's project plans call for injection of captured CO_2 into a deep, saline reservoir for permanent storage. The target injection reservoir is at a depth of about 3,000 m and is saturated with saline groundwater (brine).

We propose that to more effectively use the pore space within the storage reservoir and to control the migration of CO_2, saline water should be produced as part of an active pressure management system. Desalination of the produced water has the potential to supplement the region's limited water supply. Thermal energy from deep brines and aqueous phase mining of dissolved minerals could both be important contributions to overall project profitability.

<u>Treatment</u>

Two Phase Study

Evaluation of this opportunity will involve a two phase project. With this proposal, we are proposing initiation of the phase 1, pre-feasibility study. Success would lead to consideration of a detailed feasibility study in phase 2:

Phase 1.Pre-feasibility study to determine whether the concept has merit and adds value to Huaneng and to CERC-ACTC.

Phase 2. Detailed feasibility study to identify reservoir management and water treatment options for a full scale operation.

This project will evaluate the feasibility of withdrawing water in order to increase storage reservoir capacity, decrease leakage risks, and provide a water source through desalination of produced water. Additional benefit may be gained by extraction of mineral resources (e.g., lithium) from the produced water. Specific objectives include:

- Development of an active reservoir management scheme including production of deep saline water that will

1) Optimize storage of the CO_2 generated by the Tianjin IGCC unit
2) Maximize reservoir storage capacity
3) Reduce reservoir overpressure and related leakage risks
4) Combine modeling strengths from LANL and LLNL (Figure 02)

- Identification of treatment strategies to gain useable water from produced brine (Table 01)
- Use of heat from produced water in desalination or mineral extraction processes
- Develop beneficial uses for byproduct brines/salts

- Combine the results into a system analysis that will explore uncertainty (risk) in both physical processes and economic feasibility.

Phase 1. Pre-feasibility Study

An eight week pre-feasibility study is proposed to address key unknown factors and make a preliminary analysis of the reservoir management and water treatment opportunities. In phase 1 we will work with our Chinese colleagues at CAS and with published literature to address the following critical unknowns:

Critical unknowns

- Brine chemical composition-both produced and treatment reject brines. The latter will be estimated based on produced brine chemistry and treatment method.
    1) Build on existing knowledge and data bases from LLNL, WVU, UWY, and LANL for desalination costs built from interaction with industrial contacts.
    2) Work with Chinese CERC collaborators to generate costs for systems in China
- Hydraulic conductivity of the target reservoir rock
    1) Leverage existing CERC relationships to gain access to porosity, permeability, and facies data from the GreenGen subsurface (Chinese Academy of Science, Yangchang Oil, Northwest University, Tshingua U.).
    2) Estimate CO_2 injection rates and groundwater withdrawal rates to avoid development of excessive pressure gradients
    3) Suggest modeling strategies that use the best of our existing capabilities (LLNL, WVU).
    4) Use coupled economic/technical models to simultaneously optimize well spacing, pumping rates, storage capacity, and extracted resources.
- Chemical interactions between injected CO_2, reject brines and formation brines at prevailing pressures/temperatures.
    - Use geochemistry codes (PFLOTRAN/FEHM/NUFT) and knowledge gained from prior simulations and field experiments of CO_2 injection (In Salah, Sleipner, Cranfield) to guide Phase 2 plans.

Tasks:

- Address critical unknowns (above) (During Phase I we will formulate a plan for gaining access to the necessary data including literature review and suggestions for new data collection (e.g., 3-D Seismic at the target drill site, test wells, pump tests, etc.). **LEAD-Carr**
- Develop cost/performance model (Phase I will base the costs on US research and suggest ways to bring in China costs for Phase II). **LEAD-Stauffer**
- Evaluate reservoir management/brine treatment options. (Phase I will do limited new simulations and focus mainly on summarizing existing research on reservoir management). **LEAD-Bourcier**
- Develop a reservoir management strategy (Maybe say we will suggest paths forward for the next generation of reservoir management calculations). **LEAD-Jiao?**

- Identify a brine treatment, handling strategy (Again, suggest a path forward but leave the selection of site specific plans for Phase 2 since we have such limited data for Phase I). **LEAD-Lin**
- Develop strategy for the Phase 2 study. **LEAD-Stauffer**
- Write final report. **LEAD-Ziemkiewicz**

Phase 1 Schedule:

Phase 1 will extend from early July to the end of August. Table 02 outlines the project schedule.

Phase 1 project team:

Paul Ziemkiewicz, PhD, Director of the West Virginia University Water Research Institute, will serve as the project principal investigator. Other lead researchers will include:

Los Alamos National Laboratory

Philip Stauffer, PhD, Senior Hydrogeologist

Earth and environmental sciences

Lawrence Livermore National Laboratory

Bill Bourcier, PhD

West Virginia University

Lance Lin, PhD, Civil and Environmental Engineering

Joseph Donovan, PhD, Geochemist, Geology and Geography

Timothy Carr, PhD, Petroleum Geologist, Geology and Geograph

Results

A report will be prepared that will include description of reservoir management and brine treatment options. The report will then describe the technical and cost implications of each option resulting in recommendation of a strategy for managing reservoir CO_2 injection rates and capacities and whether brine withdrawal is a viable strategy for enhancing reservoir capacity.

<u>Value Proposition</u>

Huaneng anticipates developing a carbon storage strategy at its operating IGCC in Tianjin. Evaluation of storage options will require appropriate reservoir conditions and the assurance that CO_2 storage volumes and injection rates meet expectations. Several fundamental assumptions are involved:

- Reservoir capacity
- Adequate hydraulic conductivity throughout the reservoir
- CO_2, formation brines and reject brines will not form scale/precipitates and interfere with reservoir conductivity
- Withdrawal of formation brines will increase effective CO_2 storage capacity
- The selected brine treatment strategy will meet technical and financial expectations

Failure to meet any of these assumptions may have serious financial implications for the project and require major additional investment/corrective measures after the project has gone on line. The value of this project is to provide the company with a comprehensive evaluation of the

reservoir management and brine treatment options to lessen uncertainty prior to finalizing project designs.

Deliverables

Theme 7 – CO_2 Algae BioFixation and Use

Subtask 7.1. – Screening of Algae Strains

Approach

Identifying a strain of algae that will endure, and indeed thrive when fed with flue gas is an important aspect of this project. The ability of algae to grow robustly and quickly will define CO_2 uptake rates while the strain used will also play a role in determining the optimum approach for utilization of the biomass. Hence, this subtask focuses on identifying and culturing optimal summer and winter algae strains to be used in the CO_2 mitigation system.

Results and Discussion

In the last quarter protein and glucose analyses were performed on our preferred summer and winter algae strains. The average protein content of snow algae *Chloromonas rosae var. psychrophila* was determined to be 53%, compared to the 31% found for the summer strain, *Scenedesmus acutus* (Figure 7.1.1). The relatively high protein concentration of *Chloromonas* makes it an ideal additive to increase the nutritional value of animal feed. The carbohydrate analysis shows *Chloromonas* has an average of 8.5% glucose while *Scenedesmus* has an average of 5.7% (East Bend photobioreactor) and 9.6% (airlift photobioreactors at UK) glucose (Figure 7.1.2).

Analysis of the lipids in *Chloromonas* was also conducted. Two methods were applied: in the first, the oil in *Chloromonas* was extracted using a standard procedure (Bligh-Dyer method), subjected to transesterification with methanol and analyzed by GC. In the second, a recent literature procedure was followed, involving *in situ* transesterification of the lipids, followed by GC analysis. As shown in Figure 7.1.3, three main fatty acids chains are present, corresponding to palmitic, oleic and linolenic, albeit that the two analyses show different proprtions of these chains. This may be related to the fact that different batches of algae were used for the two analyses. Overall, these results indicate that while the lipids in *Chloromonas* are well suited for the production of biodiesel (or indeed, for conversion to a hydrocarbon-type fuel), the nutritional value of the oil is low (since there are no ω-3 unsaturated fatty acids present).

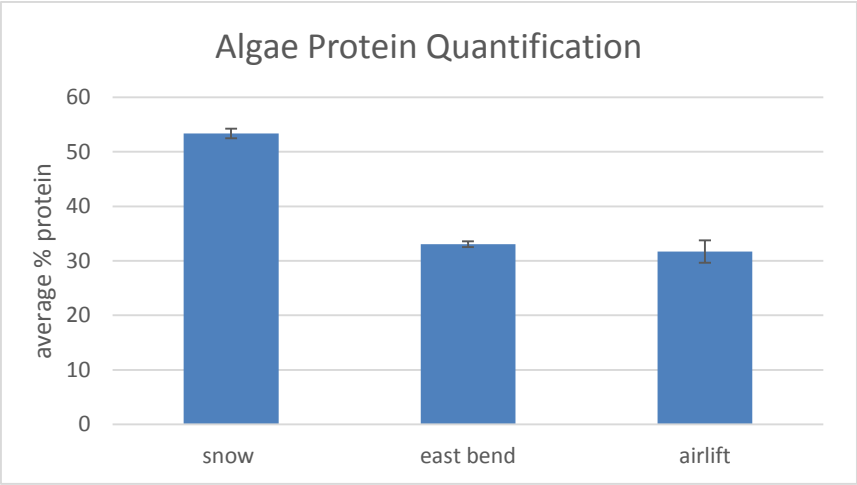

Figure 7.1.4. Protein concentration of *Chloromonas* (snow algae, cultured in airlift reactors) and *Scenedesmus* (cultured in East Bend reactor and UK airlift reactors).

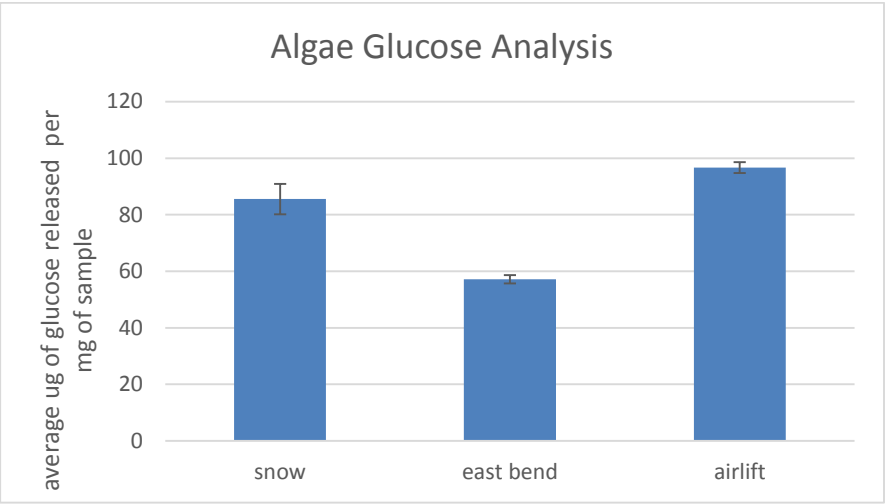

Figure 7.1.5. Glucose concentration of *Chloromonas* (snow algae, cultured in airlift reactors) and *Scenedesmus* (cultured in East Bend reactor and UK airlift reactors).

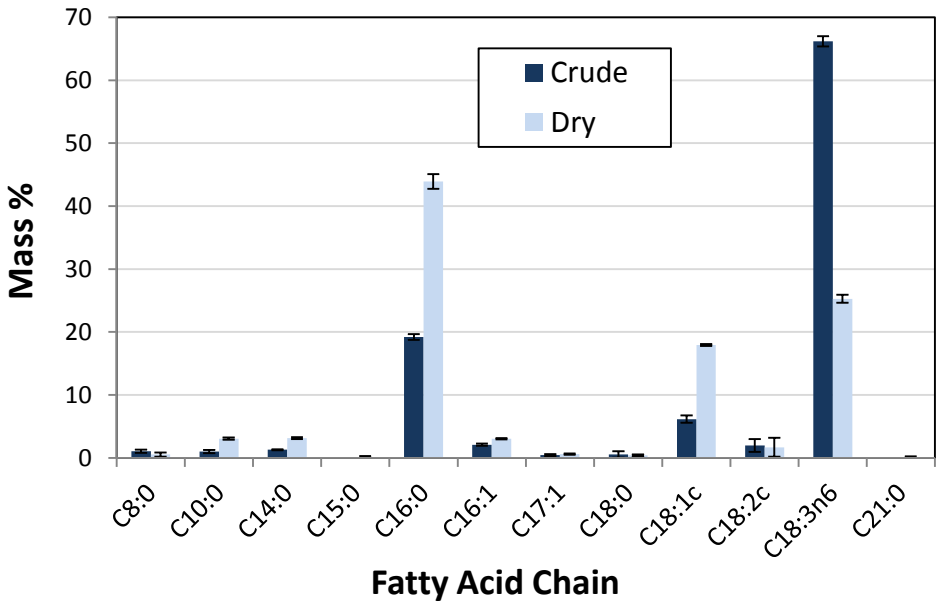

Figure 7.1.3. Lipid profile of algae *Chloromonas rosae var. psychrophila* (cultured in airlift reactors). Crude: analysis of crude (extracted) oil; Dry: *in situ* analysis of lipid contained in dried algae.

Plans for Upcoming Quarter

Work on *Chloromonas* will focus on optimizing its growth medium (i.e., to achieve maximum growth rates at minimum nutrient cost).

<u>Subtask 7.2. – Growth System Optimization</u>

Approach

Optimize culturing process and technology; this should include a demonstration of algae cultivation at pilot-plant scale under summer and winter conditions, incorporating optimized nutrient and water recycling. Specific actions will include working with Duke Energy to identify a site for the pilot-scale demonstration, operation of the demonstration plant using optimal summer and winter microalgae, examining the feasibility of recycling nutrients derived from the

anaerobic digestion of algae, and examining the effect of recycle water (derived from harvesting) on algal growth.

Results and Discussion

With the help of a Mechanical Engineering senior design team, a new low cost frame was developed to support the new 'cyclic flow' reactor (Figure 7.2.1). This frame represents a substantial cost reduction over the old frame (ca. 70% cheaper). The frame was subsequently installed at Duke Energy's East Bend Station, ahead of the arrival of the new reactor.

Figure 7.2.1. Low cost frame prototype and ME seniors.

Meanwhile, an Electrical Engineering senior design team completed a working prototype of a low cost control system. This microcontroller-based system uses the pH, dissolved oxygen concentration, conductivity and temperature as inputs, and can control the introduction of gas based on the pH and dissolved oxygen settings. All of the process data are stored and can be accessed via an intranet set up for downloading and graphing. Figure 7.2.2 shows the control system prototype.

Figure 7.2.2. Control system prototype.

In tandem, the cyclic flow prototype photobioreactor was completed (Figure 7.2.3). Two 5-foot sections were plumbed together with a tank and pump system. Solenoid valves were installed to control the flow and integrated with a National Instruments Labview controller. In order to prevent biofilm accumulation, pipe pigs were installed in each tube. The pig design incorporates rubber gasket material that contacts the inner surface of the tube and cleans the tube as the reactor bodies fill and drain.

Figure 7.2.3. Chemical Engineering students Chase Cecil (r) and Travis Jarrells trouble shooting the cyclic flow reactor

Based on the satisfactory functioning of the prototype reactor at the UK CAER, work was started on installing the new reactor geometry at East Bend Station. All 72 tubes were assembled and installed on the low cost frame built by the Mechanical Engineering students. Figures 7.2.4 and 7.2.5 show the tubes in place.

Figure 7.2.4. 72-Tube cyclic flow reactor, with biofilm cleaning pigs installed

The automatic valves, pump, and tank were plumbed together and the electrical control system was put in place. One benefit of this reactor geometry is that the entire system can be placed on a flat surface and doesn't require the tank to be situated below the tube array.

Figure 7.2.5. Side view of reactor showing effective surface for harvesting photons

Plans for Upcoming Quarter

The reactor will be mechanically finished and tested. Once the operational parameters are set, the reactor will be inoculated from algae grown in the CAER greenhouse.

Subtask 7.3. – Algae Post Processing

Approach

When using microalgae to biologically fix CO_2 contained in flue gas (in essence, enabling the CO_2 to be recycled), there is the potential to obtain valuable biomass-derived products which can

help to off-set the high costs of algae cultivation and processing. To this end, this subtask aims to assess the various products (and their corresponding value) which can be derived from algal biomass.

Results and Discussion

Work in the last quarter focused on the extraction and purification of algal lipids. A simple method was developed to remove chlorophyll from lipids extracted from *Scenedesmus* algae (based on adsorption onto activated carbon or K10 montmorillonite). Initial results suggest that this method is also successful in removing phospholipids, the purified lipid extract consisting of triglycerides, fatty acids and traces of sterols. The removal of phosphorus-containing compounds is particularly significant given that these can act as poisons for many types of heterogeneous catalyst. The purified extract was subsequently subjected to Ni-catalyzed deoxygenation to obtain diesel range hydrocarbons. The latter work is being performed as part of a separate project at the UK CAER concerned with catalytic processing of waste/inedible lipid feedstocks to liquid transportation fuels.

Plans for Upcoming Quarter

The lipid extraction/purification work will be completed and written up for publication.

Subtask 7.4. – Techno-economic Analysis

Approach

We plan to leverage the expertise of the US and Chinese project partners to conduct a detailed techno-economic assessment of the potential of algae for CO_2 utilization. Working with Duke Energy, biological CO_2 fixation at a coal-fired power plant will be demonstrated, the resulting data functioning as inputs for the techno-economic model. In this manner, we aim to arrive at rational and detailed cost estimates for CO_2 fixation and utilization.

Results and Discussion

No work was performed on this task in the last quarter.

Plans for Upcoming Quarter

Work will begin on a lifecycle analysis of CO_2 capture and recycling using algae, incorporating the improvements made in the refined photobioreactor design.

Theme 8 – Integrated Industrial Process Modeling and Additional Topics

Subtask 8.1: Power Plant Cycling and Load-Following Operations (NEW)

Approach

Coal-fired power plants are experiencing increased cycling and load-following operation for several reasons: demand for electricity from the grid fluctuates over time; natural gas plants supply more baseload power; and, variable renewable and intermittent power generation (e.g., wind, solar) grows more rapidly in the modern grid era.

Many coal-fired plants were not designed to operate with large variations in power output, but must now cope with wide changes in power demand, often on an hourly basis. This increased cycling and load-following operation will degrade plant performance, e.g., increased derates and emissions. In addition, plant stress and equipment damage via thermo-mechanical fatigue will be accelerated and plant operation and maintenance costs will increase.

The purpose of this new, DOE-NETL-lead project will be to investigate the effect of repeated cycling of coal-fired plants by integrating the AVESTAR high-fidelity, real-time dynamic simulators to Intertek's COSTCOM® for use in computing damage accumulation rates and dollar costs for cycling operation and determining the cost impacts of increasing ramp rates, MW load transient ranges, and shortened startup times.The results of this work will improve cycling and ramping strategies to minimize thermal and pressure gradients, reduce costs, minimize damage accumulation rates, and improve control of load transients.

Results and Discussion

No Activity This Quarter

Plans for Upcoming Quarter

No Activity This Quarter

Subtask 8.2: Systems Modeling of Post-Combustion Capture Technology

Approach

Before introducing disturbance to the 550MWe supercritical pulverized coal power plant dynamic model, a 50% coal feed turn down test run was carried out to investigate the system's robustness and stability. Based on this test run, a modification was made to the low pressure turbines to enable the model running smoothly while ramping down the coal feed. Flooding is the condition at which liquid holdup in the tower becomes excessive and the separation deteriorates with a subsequent sharp increase in pressure drop. An accurate pressure drop model is required for a high fidelity column simulation because the distribution of the gas to the multiple parallel absorber trains will be affected significantly when the pressure drops across the absorbers vary. It was found that Aspen Plus and Aspen Plus Dynamics use different pressure drop models and that Aspen Plus's model is more rigorous. Therefore, a pressure drop model based on a specific packing was developed

Results and Discussion

Modification to the Low Pressure Turbines

Before introducing disturbances into the integrated dynamic model and controllers, it is necessary to investigate the system robustness and stability under off-design conditions. The

existing supercritical pulverized coal power plant can usually operate down to 50% of design capacity when power demand is low. Therefore, the dynamic power plant model would be expected to run smoothly when the coal feed is cut off by 50%. The original 550MWe supercritical pulverized coal power plant's low pressure turbine has five stages. The pressure at each stage outlet is given in the DOE report (Cost and Performance Baseline for Fossil Energy Plants Volume 1: Bituminous Coal and Natural Gas to Electricity - Cases 11 and 12, Revision 2, November 2010, DOE/NETL-2010/1397). At the design point, a mixed pahse (vapor-liquid condition) exists at the outlets of the third, fourth and fifth stages. As the coal feed continues to ramp down, a mixed phase begins to appear at the second stages outlet. An integrator error is seen to occur due to the phase calculation for this stage and it stops the dynamic run. However, this problem cannot be fixed by switching the phase calculation option from "Vapor-Only" to "Vapor-Liquid". Performance curves for low pressure turbines are at their default values since no other information is available for these turbines. Therefore, the last four stages of low pressure turbines, as well as the extraction points and feed water heaters, were combined together (Figure 1 and 2).

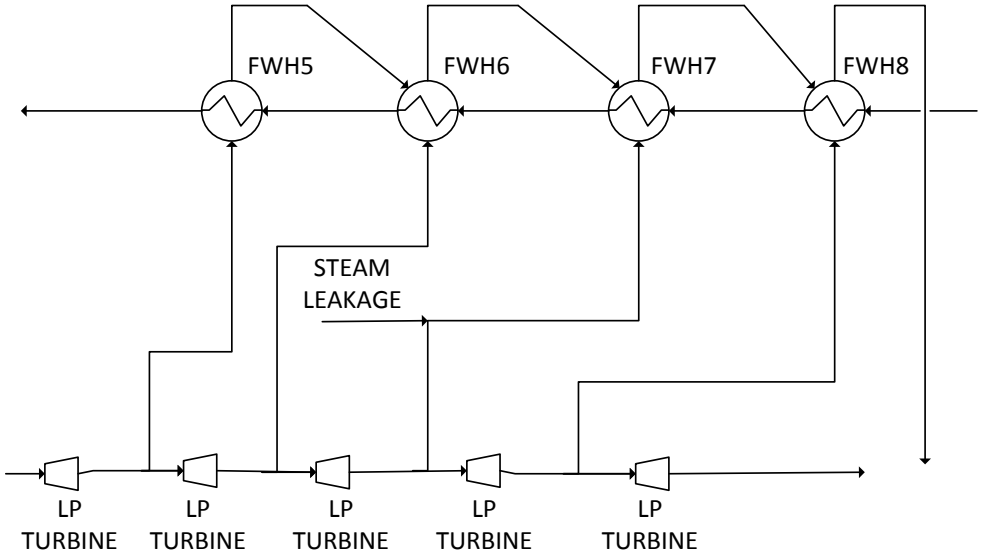

Figure 8.2.1: Low pressure turbines configuration in original model

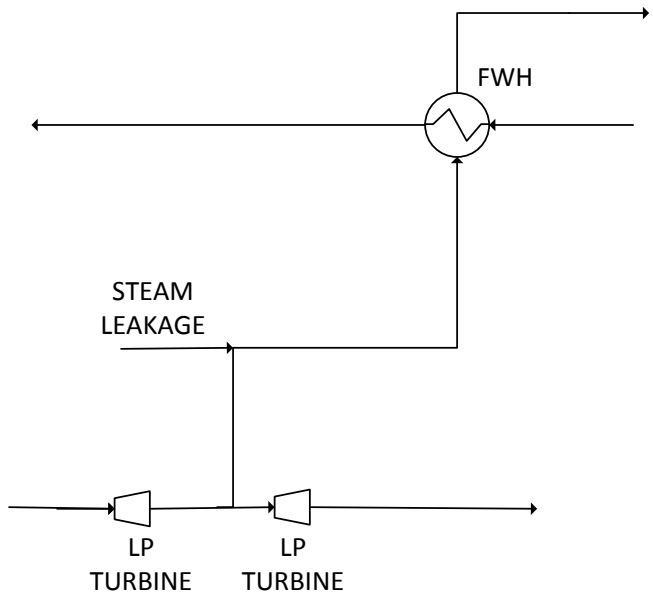

Figure 8.2.2: Low pressure turbines configuration in modified model

The net power output of plant with the CO_2 striper reboiler at steady state for the modified model is 491MWe, compared with 488MWe in the original model. The difference in net power output is about 0.6% (3MWe). After applying this modification, the power plant dynamic simulation was stable below 50% operating capacity without any issue.

Flooding Model

Since the steady state model is developed using the rate-based separation option, a rigorous model of pressure drop, interfacial area, liquid holdup and mass transfer coefficients are available for the non-equilibrium stage calculations. The pressure drop would increase significantly when the column is close to the flooding point. However, the columns in the dynamic model are all simulated using equilibrium stage calculations. To capture the effect of flooding on separation in the dynamic equilibrium model, only pressure drop and Murphree efficiency can be used as the tuning parameters to match the dynamic results with the steady state model. Murphree efficiency is difficult to predict but can be correlated with process variables using the steady state results above the flooding point. The determination of the flooding point depends on the packing type. For IMTP, the random packing used in this work, the approach to flooding can be found in the manufacturer's brochure. Efficient capacity C_{SC}, which is the flooding point, is shown as Equation (8.1).

$$C_{sc} = C_o \left[\frac{\sigma}{20}\right]^{0.16} \left[\frac{\mu}{0.2}\right]^{-0.11} \tag{8.1}$$

Where C_O is the velocity factor correlated with flow parameter, σ is the surface tension and μ is the liquid viscosity. Flow parameter X is shown as Equation (8.2).

$$X = \frac{L}{G}\sqrt{\frac{\rho_G}{\rho_L}} \tag{8.2}$$

Where L, G are liquid and gas mass rate, respectively. ρ_L, ρ_G are liquid and gas density, respectively. The approach to flooding is then defined as C_S/C_{SC}. Capacity factor C_s is shown as Equation (8.3).

$$C_S = V\sqrt{\frac{\rho_G}{\rho_L - \rho_G}} \tag{8.3}$$

Where V is the superficial gas velocity.

It was also found that Aspen Plus Dynamics uses a different pressure drop model from Aspen Plus. The pressure drop model correlated to IMTP packing size and vapor-liquid phase property is based on air-water systems. Pressure drop across dry column ΔP_o is given in Equation (8.4)

$$\Delta P_o = \frac{2a\left(\frac{s}{d_n}\right)^b H\rho_G\left(\frac{V}{\varepsilon}\right)^2}{d_h} \tag{8.4}$$

Where a,b are the constant need to be determined. $d_n, d_h, s\ and\ \varepsilon$ are packing characteristics. H is the packing height. Pressure drop across the wetted column (ΔP) is shown in Equation (8.5).

$$\Delta P = \frac{\Delta P_o}{(1 - A_O - \Delta A)^3} \tag{8.5}$$

$$A_o = cRe_L^d Fr_L^e Eo^f \tag{8.6}$$

$$\Delta A = gFr_L^h \left(\frac{L\rho_L}{V\rho_G}\right)^i Eo^j \tag{8.7}$$

The term of $(1 - A_O - \Delta A)^3$ accounts for the effect of liquid holdup. $Re_L, Fr_L\ and\ Eo$ are the liquid Reynolds number, liquid Froude number and Eotvos number, respectively. L is the liquid superficial velocity. *c, d, e, f, g, h, i, j* are constants needed to be determined for the system of interested and are given in Table 8.1.

Table 8.2.1: Constants for Direct Contact Cooling, Absorber and MEA Wash

	Direct Contact Cooling	Absorber	MEA Wash
a	0.96	0.9	0.9
b	0.27	0.32	0.27
c	2.5	2.6	2.6
d	-0.1	-0.04	-0.05
e	0.44	0.43	0.43
f	0.21	0.21	0.21
g	7.0×10^{-4}	7.0×10^{-4}	7.0×10^{-4}
h	-0.16	-0.16	-0.16
i	1.02	1.02	1.02
j	0.14	0.14	0.14

By applying the data in Table 8.1 to the Direct Contact Cooling section, Absorber and the MEA Wash section, the predicted pressure drops can be matched to the values from Aspen Plus steady

state model at the design points except for the top stage of the Absorber and the MEA Wash section. However, the differences are small, 14 Pa and 5 Pa, respectively. The predicted and simulated results for the different approaches described here are shown in Figures 8.3 - 8.5.

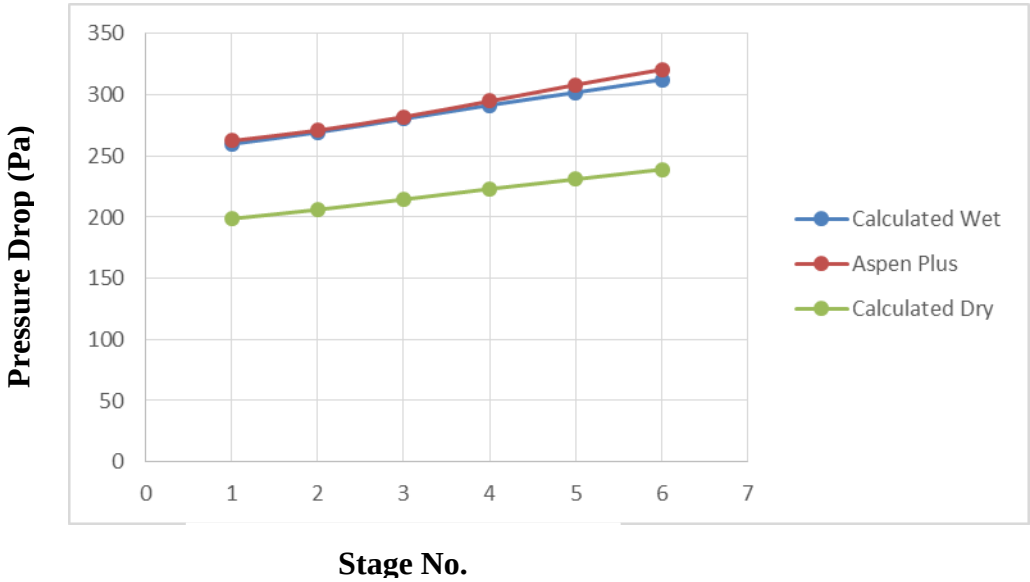

Figure 8.2.3: Comparisons of pressure drop within Direct Contact Cooling section

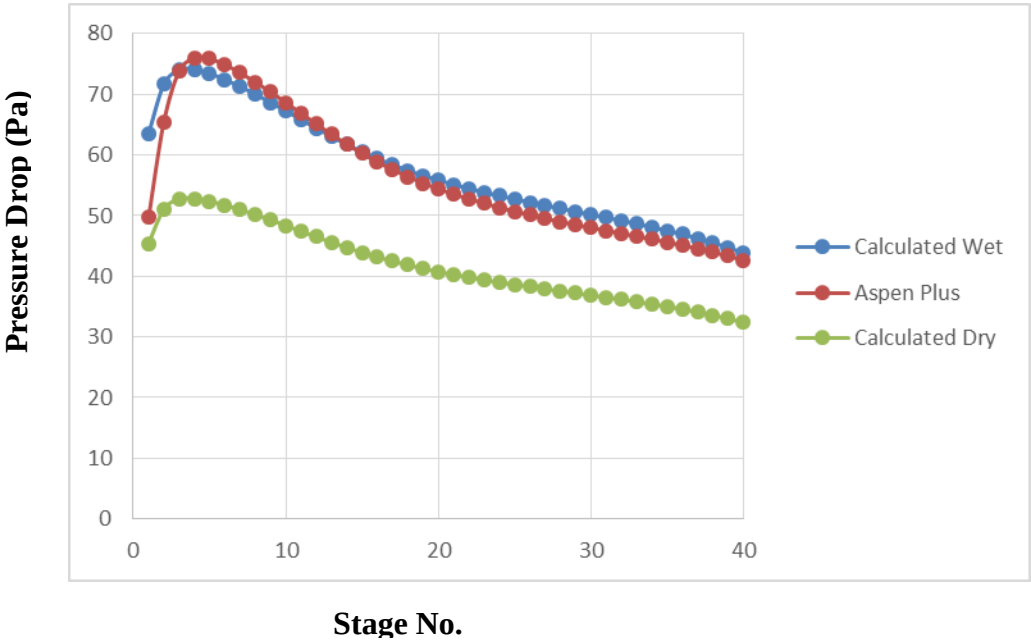

Figure 8.2.4: Comparisons of pressure drop within Absorber

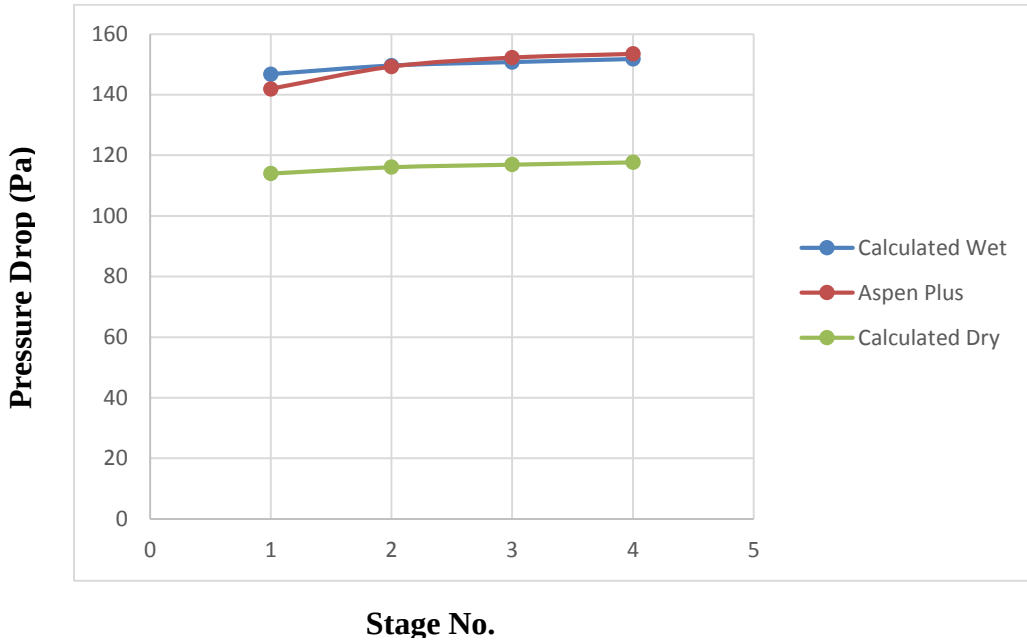

Figure 8.2.5: Comparisons of pressure drop within MEA wash section

Plans for Upcoming Quarter

- Develop the pressure drop model that can fit Aspen Plus results for off-design points, especially close to/and above theflooding point.
- Develop the Murphree efficiency model close and/or above flooding point.
- Integrate the modified power plant dynamic model with the CO_2 capture process and apply MPC to the integrated model.

<u>Subtask 8.3: Initialization of Dynamic Model with Immersive Visualization</u>

Approach

Initialization and augmentation of a dynamic model with immersive visualization capability for a generic IGCC system with gas turbine and steam bottoming cycle is addressed in this subtask. NETL and WVU have dynamic models and an operator training facility for a generic IGCC coal-fed power plant and the implementation of a 3D immersive training system (ITS) is planned. We propose to offer training to our Chinese collaborators through the CERC project and funds to cover this training are included in the WVU budget.

Results and Discussion

Plans to upgrade the hardware for the Immersive Training System were discussed with Invensys. This upgrade will allow the latest version of EYESIM (the simulation platform used in the ITS) to be implemented and run. This will significantly increase the speed to start up the system and the overall system performance.

A workshop on the IGCC OTS and ITS was held June 9-14 with 4 researchers from Huaneng Clean Energy Research Institute (Shi Shaoping, Yan Shu, Fang Fang, and Zhou Xian) and

particpants from WVU (Richard Turton, Fernando Lima, and Zhang Qiang) and DOE NETL (Steve Zitney, Eric Liese, Priyadarshi Mahapatra, and Jinliang Ma).

Plans for Upcoming Quarter

- Hardware updates will be implemented for the ITS
- Software updates for EYESIM are scheduled for August.

Subtask 8.4: Static and dynamic modeling of post combustion carbon capture plant; tools for training and visualization

Approach

Static and dynamic modeling of post combustion carbon capture plant; tools for training and visualization.

China Supported Task Only. Does not include DOE or Cost Shared Support. Any technical data or results provided to the US CERC-ACTC Team will be included in project reporting. Task is included for completeness and clarity.

Results and Discussion

No Input This Quarter

Plans for Upcoming Quarter

No Input This Quarter

Subtask 8.5: Modeling of pre-combustion process and IGCC commercial knowledge exchange

Approach

Modeling of pre-combustion process, IGCC commercial knowledge exchange; solvent-based commercial assessment; static modeling of new technologies; static modeling of pulverized coal boiler power plants with carbon capture; tools for training and visualization.

China Supported Task Only. Does not include DOE or Cost Shared Support. Any technical data or results provided to the US CERC-ACTC Team will be included in project reporting. Task is included for completeness and clarity.

Results and Discussion

No Input This Quarter

Plans for Upcoming Quarter

No Input This Quarter

Subtask 8.6: Life-cycle analysis of coal-to-chemical systems with pre-combustion capture. **(**Shenhua group**)**

Approach

China Supported Task Only. Does not include DOE or Cost Shared Support. Any technical data or results provided to the US CERC-ACTC Team will be included in project reporting. Task is included for completeness and clarity.

Results and Discussion

No Input This Quarter

Plans for Upcoming Quarter

No Input This Quarter

Theme 9 – Communication, Integration, and Intellectual Property Rights Management

Subtask 9.1. – International communications and integration support.

Approach

The CERC ACTC strives to operate as an integrated bilateral team working together on research designed to benefit both countries. The complexity naturally rising from the multi-partner and multitask effort makes it necessary to have efficient and effective communication among the teams and tasks to promote successful collaboration and integrate the research progress of different tasks. The primary goals of the theme are three-fold:

- Ensure effective sharing of information and facilities.
- Facilitate personnel exchanges among the different teams of the two countries and the different tasks of the consortium.
- Establish a communication network inside the US-China consortium to maximize the achievements of the cooperation. This includes integration other technical tasks within each national team as well as international coordination.

Results and Discussion

During this reporting period, the following significant actions were taken towards supporting international communications and integration:

- Jerry Fletcher and Sarah Forbes testified before the Sentate's US-China Economic and Energy Security Review Commission on April 25, 2014. Sarah's testimony was summarized on WRI Insights and picked up in a May 16, 2014 China Daily article.
- Public presentations regarding research results were given at various meetings, including the Annual CCS conference in Pittsburgh, PA in May 2014.
- Facilitated continued communications between the US and Chinese ACTC Leadership teams and theme leaders to further develop plans for CERC 2.0 collaboration
- Facilitated regular dialogues within the US leadership team, Theme Leads, and Private Sector Advisory board.
- Preparation for the bilateral CERC Directors presenation during the US-Strategic and Economic Dialogue in July 2014
- Preparation and coordination for the annual CERC-ACTC meeting in Hangzhou in September 2014
- Participated in ACTC Sequestration Bilateral Workshop in Wuhan, May 4-10, 2014 which resulted in the following bilateral input for upcoming discussions about future research directions:

CERC 2.0 THEME 6 TOPICS

Theme 6 Geological Storage (Aquifer, EOR, EWR)	Topic	Leaders and Participants CAS-WHRSM/LANL-WY
1	Improve the feasibility of commercial-scale CO_2 utilization via CO_2 flooding	UWY(L), Yanchang(L), SPIERCE, NWU, LLNL
2	Reservoir Characterization and Assessment	SPERCE(L), UWY(L), Yangchang, NWU, (Shengli?), IGS
3	Subsurface Simulation of CO_2 injection and Coupled Processes	Tshinghua(L), CUMT-Xuzhou, LANL(L), LLNL, IGS, UWY
4	Monitoring, Risk Assessment and Hazard Management	SPIERCE(L),Yangchang, WHRSM, Shenhua, Shengli, LANL(L)
5	CO_2 hydro-fracking of shale, coalbed and HDR	CUMT-B, Tshinghua WHRSM,CUMT-B+X, Yangchang(L), SPER, LANL

CERC 2.0 THEME 7 TOPICS

Theme 7 Utlization and novelties	Topic	Leaders and participants
1	Improve the feasibility of commercial-scale CO_2 utilization via microalgae by increasing biomass yield and the value of algal products	Xinao(L), Zhejiang U, Chinese Academy of Agricultural Sciences Feed Research Institute, Institute of Hydrobiology, DUST, KY
2	Brine water treatment and system optimization for EWR	Huaneng(L),UWY(L), Shenhua, WHRSM, SARI, LLNL, LANL,
3	Source-sink matching and standardization	WHRSM(L), Shenhua, Shengli, UWY, SPIERCE, NWU, CAS, IGS, LANL, WRI

WORLD RESOURCES INSTITUTE

Plans for Upcoming Quarter

- WRI Insights blog post regarding Strategic and Economic Dialogue Announcements
- Public presentations on CERC-ACTC during Strategic and Economic Dialogue
- Public presentations on CERC-ACTC for the U.S. Energy Association
- CERC 2.0 Leadership discussions (US-July and Bilateral Leadership-August)
- Annual meeting in Hangzhou, China in September

The US-China teams

The current membership of the ACTC teams in the US and China are summarized in Tables 9.1.1 and 9.1.2. Members include research institutions, universities, national labs, NGO, and companies with long and successful partnerships working with both sides.

Table 9.1.1. The US-ACTC CERC team

Consortium Director: Dr. Jerald J. Fletcher, West Virginia University			
Technical Program Lead: TBD (In process now)			
Universities and Geological Surveys	**National Labs**	**Non-governmental organizations**	**US Companies**
West Virginia U.	Lawrence Livermore Natl. Lab	US-China Clean Energy Forum	LP Amina
U. of Wyoming	Los Alamos Natl. Lab	World Resource Inst.	Duke Energy, Inc.
U. of Kentucky	National Energy Tech. Lab		
Indiana Geol. Survey			
Washington University at St. Louis			

Table 9.1.2. The China-ACTC CERC team

Consortium Director: Dr. Zheng Chuguang, Huazhong University of Science and Technology Dr. Xu Shisen, Huaneng Clean Energy Research Institute		
Chief Scientist: Yao Qiang		
Research Institutions	**Universities**	**China Companies**
Huaneng Clean Energy Research Institute	Huazhong U. of Science and Technology	China Huaneng Group
Research Center for Clean Energy and Power, Chinese Academy of Sciences	Tsinghua U.	Shenhua Group
Institute of Rock and Soil Mechanics, Chinese Academy of Science	Zhejiang U.	ENN
Shaanxi Provincial Institute of Energy Resources and Chemical Engineering	China U. of Mining and Technology	China Power Investment Corp. Group
Northwest University	Shanghai Jiao Tong U.	China Power Engineering Consulting Corp.
	Harbin Institute of Technology	Shaanxi Yanchang Petroleum (Group) Co., LTD.
	Northwest U.	Gemeng ** (Pending)

Summary

Figure 9.1.1 provides a summary of the specific research projects being conducted under each research theme and indicates the nature of the collaboration on that project. In total the CERC ACTC includes 38 projects, 32 of which are joint, 5 of which are crosscutting and 6 of which are conducted by either the US or China to compliment CERC ACTC research.

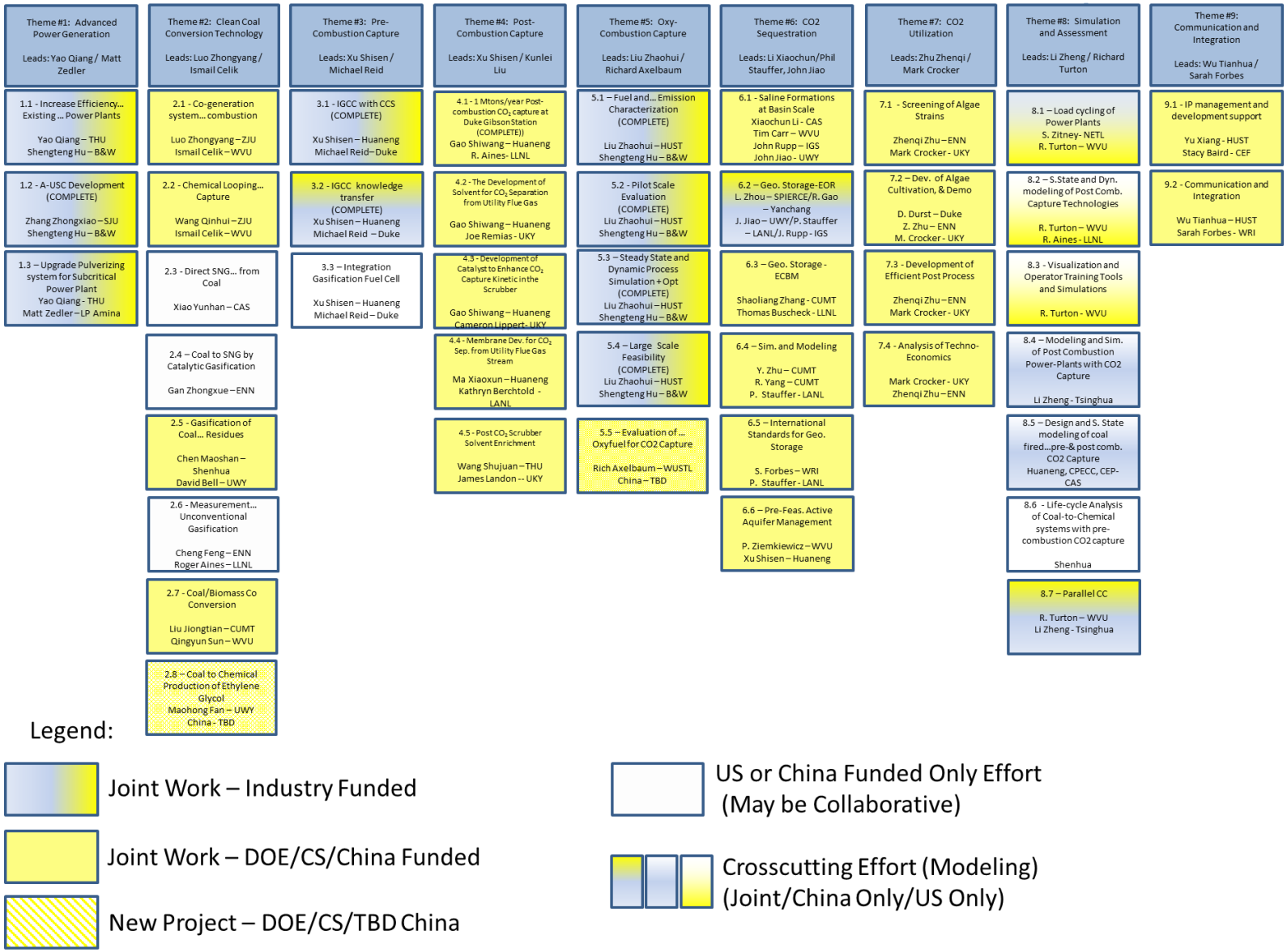

Figure 9.1.1. CERC-ACTC Project Listing

Subtask 9.2. – IP Management and Development Support

Subtask 9.2 – Intellectual Property Management and Support

Approach

The US-China Clean Energy Forum (CEF) recognized a "toolbox" of resources should be developed to help researchers implement the IP aspects of the CERC Protocol, its IP Annex and the Technology Management Plans (TMPs). This "toolbox," would include several guidance and instructional documents which we have described in previous quarterly reports. CERC leadership also recognized the value of an IP Workshop to educate participants with regard to CERC IP, the TMP and applicable laws of each country. IP is a central area of interest and concern for CERC Participants. For this reason, CERC leadership established an IP Experts Working Group to address IP issues going forward. In its initial conception, along with the other two consortia, CERC ACTC would provide expertise and support for the working group.

Results and Discussion

Building on the CERC-wide IP Experts Working Group's first formal meeting at the ACTC Jackson, Wyoming meetings, IP leadership from the US and China have been exchanging ideas with regard to a work plan for the next year.

Plans for Upcoming Quarter

During the next ACTC meeting, scheduled for May 24-26, in Wuhan, China, the CERC IP Experts group will convene to outline that work plan.

Subtask 9.2.1 – Intellectual Property Workshops

Approach

Following the success of the first IP Workshop held in Hainan, China in March, 2012, the second workshop took place February 26-27, 2013 at Stanford Law School in Palo Alto, California. CEF was responsible for organizing the Workshop for the US.

Results and Discussion

There have been no activities related to IP Workshops this past quarter.

Plans for Upcoming Quarter

CEF is in the process of planning an IP Summit in China and will continue that planning in the quarter, with the Summit to take place the following quarter. In the next year, ACTC will participate in the CERC IP Experts Working Group meetings in the US and China, the first to be scheduled for the July, 2014, to coincide with CERC and ACTC meetings in Beijing, China. At least two IP Experts groups meetings per year, with additional 'virtual' meetings as needed will take place and planning for those events will be ongoing through this quarter.

Subtask 9.2.2 – Technical Assistance and Guidance Documents

Approach

As an outcome of the first IP Workshop, CEF has taken the lead in developing support materials and continue to provide Participants general technical support with regard to intellectual property issues arising with regard to CERC projects and in CERC-related contract negotiations.

Results and Discussion

A major focus for this quarter was to populate the CEF IP website, ipknowledge.org, with information particularly of interest and use to researchers desiring a better understanding of the patent system. A new section was added to provide links to external patenting resources, including instructional materials, forms and patent-search databases. Significant news and opinion publications were also distributed via the website. Going forward, CERC is expanding the scope of the technical assistance and guidance materials available to ACTC participants. CEF and its Chinese counterparts are currently exchanging and evaluating ideas to meet the needs of CERC Participants in this area.

Plans for Upcoming Quarter

CEF has undertaken a major planning exercise for IP-related activities for CERC over the next two years. Included for the upcoming quarter in that effort will be a survey of all CERC participants to better assess what technical assistance and guidance documents will be of greatest value. The ACTC has been an effective leader in this area and CEF expects that leadership to continue.

Subtask 9.2.3 – Bilateral Intellectual Property Working Group

Approach

From the initial observations that IP was of central concern and interest for CERC Participants, interest grew among all CERC consortia to establish an IP Working Group. Last quarter, US and China's CERC leadership agreed to establish a joint US-China Intellectual Property Experts Group to identify and implement approaches to enhance innovation, utilization, protection and management of intellectual property, for CERC and oversee the provision of technical assistance with regard to IP for CERC Participants.

The US-China CERC IP Experts Group will explore such ideas as new approaches to dispute resolution to minimize litigation risk and reduce the cost of disputes, such as alternative dispute resolution undertaken in a third-party country, under internationally accepted rules and enforced by both the U.S. and China, mechanisms to establish damages awards or injunctive relief, intellectual property risk insurance and other approaches to clarify legal relations of IP ownership and sharing between the project partners, to safeguard the legitimate interests of the partners, and to promote research and development and commercialization.

The Experts Group will oversee other initiatives to provide IP related services to CERC participants which could include executive training, researcher education on IP or consulting or negotiation facilitation services to CERC projects.

Results and Discussion

The ACTC IP leadership from each side, CEF for the U.S. and HUST experts for China, have been designated as the leadership for the CERC IP Experts Working Group. These leaders have been exchanging ideas on which issues to address in the context of the CERC IP Experts Working.

Plans for Upcoming Quarter

CEF is working with its Chinese counterparts to undertake significant activity this coming quarter, including the Participants survey previously described herein and a meeting in Wuhan, China during the ACTC meetings scheduled for July during which the work plan for the CERC IP Experts Working Group undertakings will be drawn.

Subtask 9.2.4 – Consistent and Transparent Process to Bring New Participants into CERC

Approach

CEF identified a need to ensure there is a clear pathway and transparent uniform process to bring new business, industrial and non-governmental entities into one or more of the CERC consortia as participants. It was determined by CERC leadership that there would be an agreement between DOE and MOST that would describe the basic requirements and process for consortia inviting an entity to join CERC.

Results and Discussion

New members were admitted to the CERC ACTC under the new process.

Plans for Upcoming Quarter

There are significant ongoing efforts to engage and enroll new members into the CERC ACTC under the new process and requirement.

Theme 0 – Project Management Activities

Subtask 0.1. – Hold relevant meetings and teleconferences

Approach

Results and Discussion

During the current reporting quarter, the CERC-ACTC team worked to synchronize and implement recommendations from the China ACTC leadership meeting, Wuhan, March 1, 2014, to develop the Guidelines for Joint Research Projects for a Potential Phase II Renewal Application, and to respond to US Department of Energy (DOE) inquiries in support of a potential CERC 2.0 continuation request. Also, the continuation for the 5th year of the current ACTC project was submitted to DOE on June 30, 2014.

A joint US DOE and MOST steering committee meeting of senior DOE personnel and staff from each of the 3 US-China CERCs is scheduled for Beijing in July, 2014. The US ACTC team will support development of materials for these meetings in conjunction with the Chinese ACTC team, for joint presentation at these meetings.

Other activities included the finalization and submission of the Joint U.S.-China CERC-ACTC annual technical report to DOE. The team has begun to co-organize the next US-China Joint meeting, scheduled for Hangzhou, China, on September 18-19, 2014.

James Wood, former deputy assistant secretary for clean coal in the U.S. Department of Energy, has joined West Virginia University Research Corporation as Director of the U.S.-ACTC of the CERC, effective May 15, while Dr. Jerald Fletcher has maintained the role of Founding Director and continues as the Principal Investigator for the U.S.-ACTC activities. Mr. Wood will focus his effort on building stronger ties between industry and academia to advance global clean coal technologies.

Plans for Upcoming Quarter

Subtask 0.2. – Appoint and Manage Private Sector and Technical Advisory Boards

Approach

The initial Private Sector Advisory Board (PSAB) was composed of industrial partners identified in the original proposal.

Results and Discussion

With the addition of Mr. Wood, the ACTC has increased our outreach activities to relevant Private Sector entities. Mr. Wood has engaged with AEP, Alstom, B&W, Duke Energy, GE, LP Amina, Southern, and Summit Energy, and will continue to aggressively pursue industry partnerships. Other avenues are being investigated for potential partnerships with Arch Coal, Peabody Energy, and Ameren.

Plans for Upcoming Quarter

Continue to outreach to private sector entities, with a renewed focus on US industrial partners.

Subtask 0.3. – Create a commercialization plan

Approach

A Technology Management Plan (TMP) will be created to manage intellectual property provisions and sharing for organizations partnered under the CERC-ACTC.

Results and Discussion

No Activity this Quarter

Plans for Upcoming Quarter

No Input.

Subtask 0.4. – Manage and update Web site

Approach

A SharePoint site was developed for effective transfer of information between the internal and external stakeholders.

Results and Discussion

The SharePoint site, while operational, has not proven to be an effective method of information transfer between partners. Access issues from outside of WVU, related to cumbersome User ID and Password schemes has caused issues, and full access issues (white screen) at US DOE and in China have proven problematic. The team is currently investigating other options for the remainder of this project, and possible options in the event of a continuation of the program.

Plans for Upcoming Quarter

No Input.

Subtask 0.5. – Hold end-of-year meeting and publish report

Approach

The Directors of the US ACTC and the China ACTC (approved by Bob Marlay, the US CERC Director) have an agreement to develop a report for joint activities through December 31, 2013.

Results and Discussion

The annual report is complete and has been submitted to DOE. The project report was jointly developed similar to last years report.

Plans for Upcoming Quarter

Continue to support DOE in the production of the Joint CERC report as needed.

Subtask 0.6. – Maintain and update management systems and procedures

Approach

Results and Discussion

No Input

Plans for Upcoming Quarter

No input

Subtask 0.7. – Facilitate Research Exchanges

Approach

Results and Discussion

As outlined in the individual sections of this report, the technical teams continue to host technical exchanges.

Plans for Upcoming Quarter

Theme 6 plans a significant research exchange in July. Plans for the annual Joint ACTC technical meeting, in Hangzhou, China are well underway. Meeting is scheduled for September, 2014.

Subtask 0.8. – Communicate the Outcomes of the Research

Approach

Publish results of research in the peer-reviewed literature and presentations at technical conferences.

Results and Discussion

ACTC has submitted content for the DOE annual report. Other literature is described in the individual technical sections.

Plans for Upcoming Quarter

Cost Status

Project Title:	US-China Clean Energy Research Center Advanced Coal Technology Collaboration
DOE Award Number:	DE-PI0000017

YEARS 1-7 Start: 10/01/10 End: 09/30/2015

Baseline Reporting Quarter	Q1 (12/31/10)	Q2 (3/31/11)	Q3 (6/30/11)	Q4 (9/30/11)	Q5 (12/31/11)
Baseline Cost Plan	(From 424A, Sec. D)				
(from SF-424A)					
Federal Share	2,500,000				5,000,000
Non-Federal Share	2,711,000				5,422,000
Total Planned (Federal and Non-Federal)	5,211,000				10,422,000
Cumulative Baseline Costs					
Actual Incurred Costs					
Federal Share	0.00	366,506.38	460,573.82	677,725.95	516,169.87
Non-Federal Share	0.00	0.00	42,304.06	169,384.07	126,960.28
Total Incurred Costs - Quarterly (Federal and Non-Federal)	0.00	366,506.38	502,877.88	847,110.02	643,130.15
Cumulative Incurred Costs	0.00	366,506.38	869,384.26	1,716,494.28	2,359,624.43
Uncosted					
Federal Share	2,500,000.00	2,133,493.62	1,672,919.80	995,193.85	2,979,023.98
Non-Federal Share	2,711,000.00	2,711,000.00	2,668,695.94	2,499,311.87	5,083,351.59
Total Uncosted - Quarterly (Federal and Non-Federal)	5,211,000.00	4,844,493.62	4,341,615.74	3,494,505.72	8,062,375.57

Cost Status (Continued)

Project Title: US-China Clean Energy Research Center Advanced Coal Technology Collaboration

DOE Award Number: DE-PI0000017

YEARS 1-7 Start: 10/01/10 End: 09/30/2015

Baseline Reporting Quarter	Q6 (3/31/12)	Q7 (6/30/12)	Q8 (9/30/12)	Q9 (12/31/12)	Q10 (3/31/13)
Baseline Cost Plan	(From 424A, Sec. D)				
(from SF-424A)					
Federal Share				7,500,000	
Non-Federal Share				7,922,000	
Total Planned (Federal and Non-Federal)				15,422,000	
Cumulative Baseline Costs					
Actual Incurred Costs					
Federal Share	393,669.67	899,387.50	406,156.70	498,753.07	440,928.74
Non-Federal Share	671,649.51	554,069.94	887,549.37	382,036.74	1,313,008.54
Total Incurred Costs - Quarterly (Federal and Non-Federal)	1,065,319.18	1,453,457.44	1,293,706.07	880,789.81	1,753,937.28
Cumulative Incurred Costs	3,424,943.61	4,878,401.05	6,172,107.12	7,052,896.93	8,806,834.21
Uncosted					
Federal Share	2,585,354.31	1,685,966.81	1,279,810.11	3,281,057.04	2,840,128.30
Non-Federal Share	4,411,702.08	3,857,632.14	2,970,082.77	5,088,046.03	3,775,037.49
Total Uncosted - Quarterly (Federal and Non-Federal)	6,997,056.39	5,543,598.95	4,249,892.88	8,369,103.07	6,615,165.79

Project Title: US-China Clean Energy Research Center Advanced Coal Technology Collaboration

DOE Award Number: DE-PI0000017

YEARS 1-7 Start: 10/01/10 End: 09/30/2015

Baseline Reporting Quarter	Q11 (6/30/13)	Q12 (9/30/13)	Q13 (12/31/13)	Q14 (3/31/14)	Q15 (6/30/14)
Baseline Cost Plan	(From 424A, Sec. D)				
(from SF-424A)					
Federal Share			10,000,000		
Non-Federal Share			10,422,000		
Total Planned (Federal and Non-Federal)			20,422,000		
Cumulative Baseline Costs					
Actual Incurred Costs					
Federal Share	1,157,140.72	225,538.99	161,228	458,760.16	409,648.52
Non-Federal Share	834,266.63	987,612.23	590,907.31	788,934.06	362,364.77
Total Incurred Costs - Quarterly (Federal and Non-Federal)	1,991,407.35	1,213,151.22	752,135.65	1,247,694.22	772,013.29
Cumulative Incurred Costs	10,798,241.56	12,011,392.78	12,763,528.43	14,011,222.65	14,783,235.94
Uncosted					
Federal Share	1,682,987.58	1,457,448.59	3,796,220.25	3,337,460.09	2,927,811.57
Non-Federal Share	2,940,770.86	1,953,158.63	3,862,251.32	3,073,317.26	2,710,952.49
Total Uncosted - Quarterly (Federal and Non-Federal)	4,623,758.44	3,410,607.22	7,658,471.57	6,410,777.35	5,638,764.06

Appendices: